The age and structural setting of limestone and basalt on the main ring fault of south-east Rhum Inner Hebrides Scotland

Smith, Nicholas J.

The Age and Structural Setting of Limestone and Basalt on the Main Ring Fault of south-east Rhum, Inner Hebrides, Scotland.

By

Nicholas J. Smith B.Sc (Hons) Dunelm

Being a thesis submitted for the degree of Master of Science within the University of Durham.

Submitted September 1987.

Contents

	Page
Abstract	v
Declaration	vi
Frontispiece	vii
Preface	viii
Acknowledgements	ix
Chapter 1 Introduction and Previous Research	1
1.a Regional Setting of the Rhum Centre	2
1.b Brief History of the Rhum Pluton	3
1.b.i Stage 1	
1.b.ii Stage 2	
1.b.iii Stage 3	
1.c South-east Rhum - Description of Field Area	5
Figures, Plates and Tables	7
Chapter 2 Lithologies of South-east Rhum	8
2.a Introduction	9
2.b Lewisian Gneiss	9
2.c Torridonian Sediments	11
2.d Mesozoic Sediments	18
2.e Amygdaloidal basalts (sheared within MRF)	19
2.f Porphyritic Felsite and Explosion Breccia	20
2.g Hybrid Rocks	23
2.h Ultrabasics - The Eastern Layered Series	26
Figures, Plates and Tables	28
Chapter 3 The Mesozoic Strata	49
3.a Description of Outcrop	50

3.b Mesozoic Lithologies 51

3.b.i Sandstone
3.b.ii Limestone
3.b.iii Shale

3.c Palaeontology 56

3.d Comparison of Rhum Jurassic rocks to other Hebridean occurrences 58

Figures, Plates and Tables 61

Chapter 4 The Sheared Tertiary Amygdaloidal Basaltic Lavas

4.a Introduction 86

4.b Geological Setting 86

4.c Mineralogy and Geochemistry 88

4.c.i Mineralogy
4.c.ii Geochemistry

4.d Comparison with adjacent areas 92

Figures, Plates and Tables 96

Chapter 5 Structure of the Main Ring Fault (MRF) 116

5.a Introduction 117

5.b The MRF in South-east Rhum 117

5.b.i The Outer Ring Fault (ORF)
5.b.ii The Centre Ring Fault (CRF)
5.b.iii The Inner Ring Fault IRF)

Figures, Plates and Tables 122

Chapter 6

Implications of the MRF in South-east Rhum to the Early Tectonic History of the Volcanic Complex. 127

6.a Introduction 128

6.b The Development of Calderas 129

6.c The formation of the Rhum Caldera 131

6.c.i Phases in the Development of the Rhum Caldera

Figures, Plates and Tables rear pocket

Appendices 145

Appendix 1 - X-ray Analysis Techniques 146

Introduction 147

A1.a Preparation of Samples

A1.a.i Rock Grinding
A1.a.ii Production of Fused Glass Beads
A1.a.iii Production of Pressed Powder Pellets

A1.b Data Reduction Techniques 150

A1.B.i Major Elements
A1.b.ii Trace Elements

Figures, Plates and Tables 154

Appendix 2 CIPW Norm Calculations 172

Figures, Plates and Tables 176

Appendix 3 Paper: 'The Age and Structural Setting of Limestones and Basalts on the Main Ring Fault in South-east Rhum'. Geol. Mag. V. 122. 1985. 177

Appendix 4 Paper: 'The Early Igneous and Tectonic History of the Rhum Tertiary Volcanic Centre'. Geol. Mag. V. 122. 1985. 182

References 187

Tailpiece 198

NOTE.

The text in this thesis is split into chapters, with each chapter also subdivided for ease of reference. Each figure, plate and table is numbered according to chapter ie. Figure 1.1 being the first Figure in Chapter 1. Anything prefixed by the letter 'A' indicates the particular item occurs in the appendix. All figures plates and tables occur at the end of each relevant chapter, EXCEPT Figure 2 and Figure 6.1 which will be found in a pocket on the inside back cover.

N.J.S. Sept. 1987

'The Age and Structural Setting of Limestone and Basalt on the Main Ring Fault in South-east Rhum, Inner Hebrides, Scotland'.

By

Nicholas John Smith B.Sc. Hons. (Dunelm):

Being a thesis submitted for the degree of Master of Science within the University of Durham. September 1987.

ABSTRACT.

In south-east Rhum a Mesozoic/Tertiary sequence is preserved as a fault bounded/rotated wedge. This is juxtaposed between Precambrian rocks (Torridonian sediments and Lewisian Gneiss) and caught up in the complex structure of the Main Ring Fault (MRF). The MRF shows three distinct phases of movement, each one along a different sub-parallel component fracture; i) the Outer Ring Fault (ORF), ii) the Centre Ring Fault (CRF), iii) the Inner Ring Fault (IRF), Smith (1985).

The Mesozoic rocks comprise fossiliferous limestone, sandstone and shale, which show differing degrees of thermal metamorphism depending on their proximity to the Ultrabasic Complex. On a basis of faunal and lithological evidence the Mesozoic sediments have been correlated with the Lower Liassic, 'Broadford Beds', of Skye. The Rhum Jurassic sediments are overlain by a sequence of sheared Tertiary amygdaloidal lavas, the contact between them probably representing the original landscape unconformity. These lavas have been successfully correlated by geochemistry with plateau lavas found on the adjacent island of Eigg, and provide evidence for a once extensive lava field extending over Rhum prior to the emplacement of the postulated Rhum Caldera.

The presence of these fault bounded lithologies provides crucial evidence for a major phase of central subsidence during the early tectonic history of the Rhum Volcanic Centre.

Reference.

Smith N.J. 1985. The Age and Structural setting of Limestones and basalts on the Main Ring Fault in south-east Rhum. Geological Magazine V.122 pages 435 - 439.

Declaration.

The contents of this thesis are the original work of the author, except where other peoples work is acknowledged by reference. This thesis has not been previously submitted for a higher degree at this or any other university.

Nicholas John Smith

September 1987.

Copyright.

Frontispiece

Frontispiece - 'Late evening at Kinloch '

Preface

"Although the rough and dangerous shores, the trackless surface, and the perennial rain of this Island are repulsive to the general traveller, the geologist will here meet with appearances of such interest, as to induce him to brave its tempests and to defy the toil which he must encounter in its investigation...."

John MacCulloch (1819)

From: 'A Description of the Western Isles of Scotland'

Acknowledgements.

Firstly, I would like to acknowledge gratefully the advice, assistance and patience of Dr C.H.Emeleus during the protracted production of this thesis. Also I would like to thank my fellow members of the Geology Department for useful discussions on various aspects of this work notably; Dr D.M. Hirst, Dr. J. Faithful, also my fellow office mates, Mr C.Bradshaw, Mr R.England and Mr N.J.G. Pearce.

For help with geochemistry and XRF analysis my thanks are extended to Dr.J.G. Holland, Mr P.Laverick, and especially Mr R.Hardy. The MANY thin sections were prepared excellently by Mr R. Lambert and Mr. G.Randall, whilst Mr D. 'Fixit' Asbery never once failed to 'procure' obscure items needed to aid production of this thesis.

The much valued financial support of S. Chad's College, in the form of a Scholarship for fieldwork expenses, is also acknowledged.

Lastly my thanks go to the N.C.C. for permission to work on Rhum, especially to Mr L. Johnstone. the Warden, and the Estate Foreman Angus Macintosh, who regretably is no longer with us.

1.a Regional Setting of the Rhum Centre

The Rhum Central Complex lies some 15 km south-west of the Central Complex of Skye and 20 km and 50 km north-west of the Ardnamurchan and Mull Centres respectively. The aforementioned centres all outcrop above sea level, the Blackstones Centre (c.100 km south-east of Rhum) however, is a submarine centre and is described by Durant et al (1976). The Blackstones Centre has the highest Bouguer gravity anomaly of any of the western Scottish Tertiary centres (Figure 1.1). Rhum shows the highest gravity anomaly of the exposed centres. Collectively all the Tertiary centres of western Scotland and Ireland form what is called the British Tertiary Volcanic Province (BTVP).

Rhum lies astride a north-north-east trending ridge of Precambrian strata consisting of a basement of Lewisian Gneiss overlain by Torridonian sediments. To both east and west Rhum is flanked by Mesozoic basins; to the east by the Hebrides basin and to the west by the Minch basin. The Hebrides basin extends under Eigg and Muck and northwards to southern Skye (the Strathaird Peninsula) but is separated from Rhum by the north-north-east - south-south-west trending Camasunary - Skerryvore fault (Binns et al 1974, figure 2) . The Minch basin extends westwards from Rhum (probably under Canna but see Section 3.d) until the Minch fault is encountered. The Minch basin is seen to to just lap onto the the north-western part of Rhum at Monadh Dubh, here a thin Triassic succession (calcretes, grits and sandstone) is draped over Torridonian strata.

By analogy with southern Skye a thin succession of Lower Lias strata (Section 3.d) must have covered Rhum in a similar way to that now seen at Strathaird on Skye (Figure 3.3) and also lying to the west of the Camasunary - Skerryvore fault. Sedimentation in these extensive submarine basins appears controlled by the major north - south trending faults (Minch, Camasunary, and locally on Rhum the Long Loch Fault (LLF)). On Rhum however it was not just sedimentation that was affected by the LLF it may have played a role during emplacement of the later members of the Central Series of the Layered Ultrabasic Complex (McClurg 1982, Volker 1983).

1.b A Brief History of the Rhum Pluton.

The Rhum Volcanic Centre is not totally confined to the Ultrabasic pluton (although these rocks are volumetrically the most important) but has undergone a very complex history. This history has involved an early plateau lava episode, dyke injection, acid and explosive magmatism, emplacement of the Ultrabasic mass, and a final waning stage of basic magmatism. The geological history is summarised by Dunham and Emeleus (1967) and Emeleus and Forster (1979).

The evolution of the Complex can be basically broken down into 3 distinct phases (Emeleus et al. 1985. See Appendix 4) but it is the events of Stage 1 which relate most directly to south-east Rhum, consequently it is with this early history that this thesis is primarily concerned. The most important features of each Stage are laid out below.

1.b.i Stage 1

In essence this involves emplacement of the early acid members, the Western Granophyre and porphyritic felsite, producing doming and the eventual formation of an arcuate ring fracture, the Main Ring Fault (MRF). This was accompanied by de-gassing of acid magma and the formation of a caldera, possibly followed by a period of resurgent uplift. This part of the history is dealt with in detail in Chapter 6.

1.b.ii Stage 2

Stage 2 (Emeleus et al 1985) involves the emplacement of the Ultrabasic magma to the high structural levels it now occupies. Originally Wager and Brown (1968) proposed that the Ultrabasics were emplaced as an essentially solid body, with the margins of the body lubricated by basaltic magma, now the marginal gabbro. It was thought necessary to invoke such a solid emplacement mechanism due to the fact that layering of the body continues almost up to the contact with the country rocks. The idea of emplacing an essentially solid plug of very dense (c.3.0 g/cm^3) rock, which on geophysical evidence (McQuillin and Tuson 1963) probably extends down to 15 km into basement Lewisian Gneiss of density c. 2.8 g/cm^3 (at 11 km) with this Ultrabasic plug moving UPWARDS presented some rather fundamental physical problems.

If on the other hand (as now thought probable - see Chapter 6) the emplaced body was essentially liquid, and derived by say fractionating a model picrite (Cox 1980) or a magnesium rich olivine tholeiite (Thompson 1982) (as has been postulated for generating the ultrabasic mass beneath the Mull Centre - Bott and Tantrigoda, (1987) then the density controls (Figure 6.1) are more than sufficient to allow for emplacement by diapiric uprise of the Ultrabasic mass in the ductile lower crust (>12 km) and by forceful emplacement (fracturing and stoping) in the cooler more brittle upper crust (4 - 12 km).

1.b.iii Stage 3

This involved late emplacement of evolved basic lavas (icelandite, hawaiite and mugearite) in north-west Rhum - Emeleus 1987.

1.c South-east Rhum - Description of Field Area.

The area dealt with in this thesis lies in the south-east corner of the Isle of Rhum and centres around the valley of the Allt nam Bà (NM 406 943). The area (of some 4.5 km^2) extends from the sea cliffs in the east to the summit of Beinn nan Stac in the west; and from Welshman's Rock (NM 417 947) southwards to the Dibidil valley (Figure 2).

The geology of the area described above is dominated by the arcuate bounding Main Ring Fault (MRF) (Bailey 1945). In the south-east the MRF is a series of sub-parallel fractures whereas elsewhere on Rhum it is only a 'simple' single component fracture. For the sake of clarity a new nomenclature for the MRF in south-east Rhum has been proposed (Smith 1985. See Appendix 3). A summary of this terminology is as follows:-

Outer Ring Fault (ORF)	- Eastern-most arcuate fault
Centre Ring fault (CRF)	- Central fault, separating sheared basalts from felsites and Gneiss.

Inner Ring Fault (IRF) - Inner-most low angle reversed fault bringing Torridonian against, and over, Jurassic sediments and sheared lavas.

This new nomenclature will be used throughout this thesis, a more in depth study of the fault itself comprises Chapter 5.

South-east Rhum shows a number of lithologies which are unique on Rhum - the sheared Tertiary lavas and the Mesozoic (Jurassic) sediments.

Prior to this study sheared lavas had been noted (Emeleus and Forster 1979) but their extent has been rather increased during recent mapping (cf Figure 2 with op cit. fig 5). These lavas are dealt with comprehensively in Chapter 4.

The Jurassic sediments were thought to be restricted to highly re-crystallised limestone from immediately south of Allt nam Bà - Duham and Emeleus (1967), and found to be fossiliferous by Dr G. Farrow . Limestone containing the mineral tilleyite was described by Hughes (1960b) also from Allt nam Bà, he did not however discover any fossils and consequently assigned it to the Lewisian (see Chapter 3). Hughes' noted that Geikie (1897) had found limestone 'on the northern slopes of Glen Dibidil' and assumed that his limestone with tilleyite was that of Geikie. However, the author has recently discovered the true 'Geikie limestone'. which is shown on Figure 2, and is indeed on the northern slopes of Glen Dibidil. Figure 2 also shows the extent of two new Jurassic lithologies - fossiliferous sandstone and shale, which have yielded fossil material allowing for dating of the Jurassic sediments to be made (Chapter 3).

Figure 1.1 Bouguer Anomaly Gravity Map

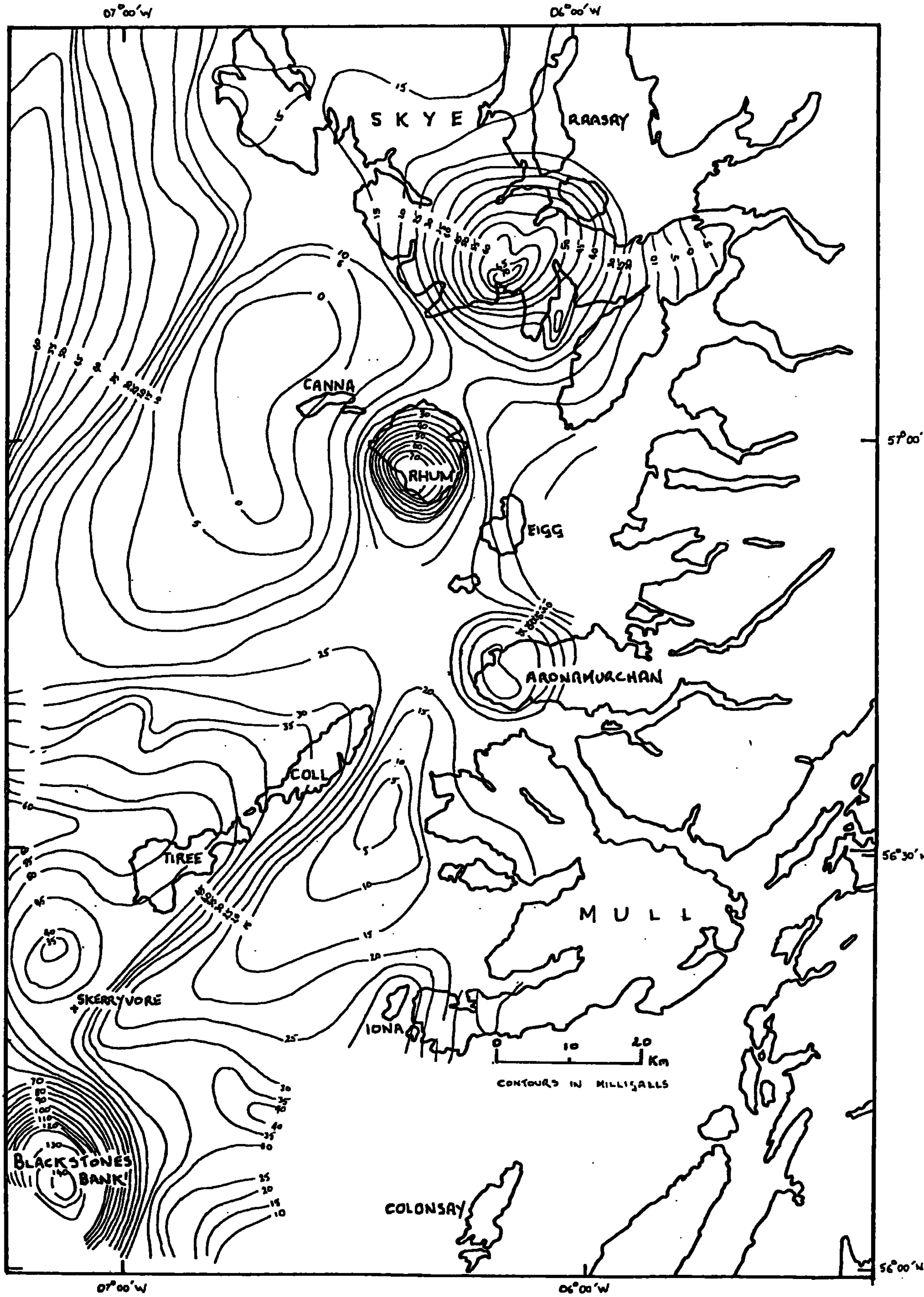

From Binns et.al. 1979

Chapter 2

Lithologies of South-east Rhum

2.a - Introduction.

2.b - Lewisian Gneiss

2.c - Torridonian sediments

2.d - Mesozoic sediments

2.e - Amygdaloidal basalts (Sheared within MRF)

2.f - Porphyritic felsite and explosion breccia

2.g - Hybrid rocks

2.h - Ultrabasics - The Eastern Layered Series (ELS)

Figures, Plates and Tables

2.a Introduction

With the exception of the 'western granophyre' all the major rock types found on Rhum outcrop to some extent in the south-east, (Figure 2.1). These major lithologies are detailed in stratigraphic order in this chapter and shown on (Figure 2.) Only a brief introducion is made to the Mesozoic sediments and sheared Tertiary lavas within the MRF, as these are lithologies unique to south-east Rhum, they are dealt with fully in Chapters 3 and 4 respectively.

2.b Lewisian Gneiss

Harker (1908a), in his memoir on the Small Isles, interpreted all Rhum "gneisses" as 'the invasion of Tertiary ultrabasic and basic rocks by acidic magma'. This interpretation was not, however, widely accepted and Tilley (1944) re-instated Rhum gneisses to the Lewisian.

In the south-east the Lewisian strata are confined to a small "whaleback" like outcrop (NM.404 905) (Plate 2.1 and Figure 2), totally bounded by the Outer and Centre ring faults. This gneiss forms a faulted inlier between younger Torridonian to the east, and Tertiary lava to the west. It is characterised by large scale "gneissic" foliation (Plate 2.1a) which, although showing minor deformation, has a general trend of c. 340^{o}. This gneiss resembles other Lewisian rocks on Rhum, especially those described from the "Southern Mountains Complex" - SMC.

In thin section the gneiss is seen to be composed predominantly of quartz, feldspar, biotite and hornblende in varying proportions, with alternation of felsic and mafic components producing the typically foliated nature exhibited by these rocks.

Both alkali and plagioclase feldspar occur. The alkali felspar is typically microcline exhibiting poor cross-hatched twinning, with the plagioclase the more sodic member albite. Both types of feldspar are extensively altered (predominantly to sericite) although some relict microperthitic structures are still observed.

Quartz remains generally unaltered, but does show some evidence of strained extinction. Relatively unaltered quartz often forms cores to highly sericitized feldspars, as well as forming discrete granular aggregates and crystals. Quartz and feldspar form the leucocratic components of the gneiss. The gneisses show distinct foliations on both a centimetre and metre scale.

The mafic components show very high degrees of alteration, chlorite is the predominant alteration product but patches of oxide minerals (haematite) are also present. Where the original mafic minerals are discernable they are biotite and hornblende. Small high relief, moderate birefringent zircons occur as the only accessory mineral. Plates 2.2 and 2.3 are photomicrographs of typical samples of the Lewisian gneiss.

The extent of alteration in the gneisses is in no small way enhanced by a degree of thermal overprinting. This phenomenon is manifest by somewhat embayed margins to the feldspars and the development of patches of granophyric texture (Plate 2.4) Granophyric texture has been described in gneisses elsewhere on Rhum, Tilley, (1944) in the gneisses capping the summit of Ard Nev in western Rhum. This feature is ascribed by Tilley to melting by underlying granophyre. This may well have been the case for the Ard Nev gneiss, however, other gneisses on Rhum show this texture, and are not associated with underlying granophyre. Lewisian gneiss caught up in otherwise totally unaltered explosion breccia exhibits similar high temperature features (see Emeleus et al 1985). Therefore, it seems necessary to invoke an early high temperature thermal event prior to emplacement of the ultrabasic mass. Implications of this feature are discussed further in Chapter 6.

In conclusion the Lewisian inlier represents the oldest strata caught up in the MRF in south-east Rhum. The structural position it now occupies indicates that upward movement of the order of 2.5 km, on the ORF, is required to bring the gneiss into contact with the Bagh na h-Uamha shale members to the east of the fault. A similar downward displacement (c. 2km) on the CRF is required to juxtapose the gneiss against Tertiary lavas to the west (Figure 2). Detailed descriptions of the faults and fault movements are dealt with in Chapters 5 and 6 (see also Smith (1985), and Emeleus, Wadsworth and Smith. (1985)).

2.c Torridonian sediments

Precambrian (Torridonian) sediments form the country rocks into which the Rhum volcanic centre was emplaced. These sediments have, like the Lewisian gneiss, also become involved in the movements on the bounding ring fractures. For example, in Coire Dubh, on the northern margin of the complex (Figure 2.1), basal Torridonian micro-conglomerate (Basal Grit?) is brought up inside the MRF (Dunham 1962, Emeleus 1980).

In the west and south-west there are no Torridonian rocks outcropping at sea level. Offshore however Torridonian rocks are once again inferred, found margining the submarine portion of the Ultrabasic Complex (Binns et al. 1974, figure 2).

To the north of Kinloch Glen the Torridonian sediments are best exposed, here they are gently dipping (c. 15 to 25 degrees west) and comprise a succession of grits and arkoses which form a distictive bench and scarp topography (Plate 2.5). Working eastwards, because of the regional dip of the rocks, successively older strata are encountered. The basal Torridonian unit outside the MRF is a thick (c. 430m) predominantly shaley unit - the Bagh na Uamha shale. The true basal Torridonian (basal Grit) is only ever found inside the MRF (see Emeleus 1980). The full Rhum Torridonian succession has previously been divided into five units, by Black and Welsh (1961), minimum thicknesses are:-

Local Unit name	Thickness (metres)	Correlation with Skye (Stewart, 1966)
Guirdil Arkose	- 1830	Applecross Group
Loch nan Eala Arkose	- 850	Applecross Group
Rudha na Roinne Grit	- 1220	Applecross Group
Bagh na Uamha Shale	- 430	Diabig Group
Basal Grit	- 90 (430m-Dunham 1962)	Diabig Group
Total thickness	4420	

Table 2.1

Table 2.1 shows the characteristic lithological features of each of the local units.

In south-east Rhum it is the Bagh na Uamha Shale which forms the bulk of the country rock (Figure 2). The shale extends from the sea cliffs of Sgeir a Mhaim Ard and Stac nam Faoileann westwards, almost to the summit of Beinn nan Stac. The above description gives a rather false impression as to the true thickness of the Torridonian strata, the reason is that the MRF intervenes and brings lower Torridonian units to high structural levels to the west of the fault.

Four features of the shale in south-east Rhum are important:

i) Sandstones, which form subordinate layers low in the shale sequence, become predominant as the boundary with the Outer Ring Fault is approached (see Emeleus 1980)

ii) The dip of the bedding steepens markedly towards the MRF (see Smith, 1985, figure 3) from 4^{o} west at sea level to c. 60^{o} west against the ORF.

iii) The degree of induration increases towards the MRF zone.

iv) The Torridonian to the west of the IRF is more highly deformed than that to the east of the fault.

The first point is made to emphasise that stratigrapically high members of the Bagh na Uamha Shale, plus the lower members of the Rudha na Roinne Grit, outcrop to the east of the ORF, whereas to the west of this fault and also the IRF, lower members of the Torridonian are present (including Basal Grit). This must indicate that aggregate displacement within the ring fault was upward.

The second point concerns the dip of the beds to the east of the ORF (see Smith 1985, figure 3). If the aggregate displacement within the Main Ring Fault zone is indeed upward then the dip of these beds to the east of the fault is reversed, i.e. indicative of downward movement. There are two possible explanations of this; that the proven phase of downward movement on the MRF (Smith 1985, and Chapter 5) dragged the Torridonian outside the MRF downwards, or, that it was due to emplacement of the ultrabasic rocks (see later). The former explanation falls down in that the Torridonian is bent downward against faulting where the movement has been upward (eg the southern portion of the ORF) or even where faulting is not observed at all (eg to the east of the Allt Nam Ba waterfall). By far a more reasonable hypothesis is that folding was caused by the hot ultrabasic rocks expanding outward on emplacement ie. making room for themselves, and forcing the country rock to deform (plastically due to the high heat flow from the ultrabasic rocks) into a series of folds parallel to the edge of the intrusion. The resultant downwarping could have been enhanced at a somewhat later date by a process involving the dense ultrabasic rocks gravitationally re-equilibrating with the lighter country rock, and so dragging it downward slightly. The ultrabasic rocks just north of the Allt nam Ba waterfall do themselves dip inwards at angles approaching 30 degrees which gives further credence to this hypothesis. Interestingly though, this re-equilibration, if it did occur, did not do so around the periphery of the whole complex. Country rocks elsewhere (eg the northern margin of the complex, around Coire Dubh) show dips AWAY from the Complex, (indicative of central upward movement) with the ultrabasic rocks showing NO signs of inward dips like those in south-east Rhum.

The cause of increased induration of country rock as the MRF is approached is due to the relative closeness of the underlying ultrabasic rocks as shown by Smith (1985 figure 3), here the margin of the complex is envisaged as dipping almost vertically below the MRF, and at no great depth from it. Induration is extreme where the Torridonian country rocks abut the ultrabasic or gabbroic rocks (Figure 2). In this case either true hybrids are developed (see Section 2.g), or the Torridonian shows evidence of rheomorphism with the development of spheroidal (pseudo-coralline) structures, (Plate 2.6) and dykes becoming back-veined and broken up, (Plate 2.7).

The rheomorphic Torridonian is shown in thin section in Plate 2.8. It is c. 90% quartz and alkali feldspar, with accessories of biotite, epidote, ilmenite, and magnetite. Alteration in the form of sericitisation and chloritisation can be extensive. The important features in thin section are the development of granophyric texture and the presence of small acicular needles of quartz. These needles are thought to represent quartz paramorphs after tridymite (as descibed in section 2.g). Paramorphs after tridymite constitute almost 30% of one section (NJ 83 3-10), PLATE 2.9a but more normally constitute only 4-5%. The presence of tridymite is indicative of high temperature low pressure conditions, (Black, 1954, and Brown, 1963).

In contrast the appearance of unaltered Torridonian Bagh na h-Uamha shale is shown in Plate 2.9. The thin section shows very fine grained sub-angular quartz and alkali feldspar, in approximately equal proportions, set in an argillaceous groundmass. Some epidote and detrital zircon is also present - up to 0.5% modally.

The Rudha na Roinne Grit, the basal part of which is also present in south-east Rhum as a strip c. 100m wide to the east of the MRF (Figure 2, and Emeleus 1980), is shown in thin section in Plate 2.10. The rock is a fine grained arkosic sandstone, with a greenish tinge. The grains are equigranular, sub-angular grains of quartz, plagioclase and alkali feldspar. Grain size is in the range 0.1-0.3mm. Small laths (c.0.2 mm) of biotite and muscovite are also common, (c. 5% modally).

The only other Torridonian in south-east Rhum is a small tract of 'Basal Grit'. This occurs sandwiched between the ORF and CRF, along with Lewisian Gneiss, (see Figure 2). Alteration is extensive (to sericite and chlorite) but the mineralogy is alkali feldspar (65%), quartz (25%) plus biotite and zircon as accessories. The rock has undergone quite extensive thermal metamorphism judging by the strained extinction of the quartz and rather embayed margins of both quartz and feldspar.

The last point to be explained is the rather more deformed nature of the Torridonian Bagh na Uamha Shale to the west of the MRF zone. To the east of the MRF zone the Torridonian is only highly deformed close to the MRF. To the west of the MRF zone signs of extensive alteration are present throughout the whole sequence. The dip and strike of this Torridonian varies greatly (see Figure 2), with no real overall structural picture emerging. It has to be admitted that more detailed work is required on these sediments to unravel the true complexity. In essence though the rocks here dip westwards at angles which can reach 90^{o}, but in general the degree of folding is such that few of the original structures remain. Induration to produce flinty hornfelses is common. Included dykes are often involved in the deformation but some late dykes transgress the whole area relatively undisturbed.

Large dislocations, easily discernible on aerial photographs, are interpreted as low angle thrusts or fault planes, discussed further in Chapters 3 and 6. One of these 'thrusts' is visible in cross section on the northern slopes of Dibidil, where Torridonian rests on Jurassic sandstone and limestone (see Plate 2.18).

Deformation must have taken place with these rocks in a plastic state, judging by the degree of contortion of fine laminations within the shales, (Plate 2.12). The heat source involved is undoubtedly the Ultrabasic Complex. The Ultrabasic Complex lies beneath the Torridonian sediments (see Smith 1985,figure 3,) with the junction dipping gently eastwards. The junction between ultrabasic rocks and Torridonian is generally not very sharp but is more gradational. The sequence of rocks at the junction is; ultrabasic rock (peridotite and allivalite), marginal gabbro, acicular hybrids, indurated Torridonian shale. Where the boundary is somewhat sharper, as often occurs on the southern side of Beinn Nan Stac, the reason is probably that hybrids could migrate from the original site of formation along the boundary of the complex and thereby act as separate intrusive bodies. Hybrids, and their relationships with adjacent rocks, are discussed in Section 2.g.

It appears that the Torridonian of Beinn Nan Stac is roof rock to the original ultrabasic intrusion, hybrids forming in situ (with possible later migration) at the igneous contacts, and with overlying Torridonian shale being baked by heat radiating outwards from the large body of underlying ultrabasic magma. Plate 2.13 shows the present day appearance of Beinn Nan Stac taken looking southwards from Allt nam Bà.

2.d Mesozoic sediments

The Mesozoic rocks only require brief introduction here as they are described at length in Chapter 3. Essentially they are composed of an overturned faulted wedge lying between older Torridonian sediments (see Figure 2).

The lithologies present are; sandstone, sandy limestone, limestone and dark organic rich shale. Outcrop is not extensive, but the areal extent can be established to some extent by the distribution of sink holes.

The Jurassic sediments are all fossiliferous to some degree, although metamorphism, which is extreme in certain outcrops, often precludes precise fossil identification. Where fossils are better preserved a Jurassic, Lower Liassic assemblage is found. Fossils include; Chlamys sp. Passaloteuthis sp. and the scleratinian corals Thecosmilia sp. and Montvaltia sp.

The maximum thickness of the Lower Liassic rocks of Rhum is in the region of 60 m, this thickness is developed just to the south of the Allt Nam Bà waterfall (NM 405 933).

Limestone and sandstone of probable Jurassic age have recently been discovered in Dibidil. It is heavily re-crystallised making direct correlation with the Allt Nam Bà limestone difficult.

2.e The sheared amygdaloidal basalts

Similarly to the Mesozoic sediments, the sheared lavas are an important feature of the MRF in south-east Rhum, consequently they are dealt with comprehensively later (Chapter 4).

The sheared basalts were first recorded by Emeleus and Forster (1979) as a small fault bounded wedge of 'crushed basaltic rocks', (ibid. figure 3 locality II.3). Recent work has enlarged the known outcrop and, by using petrographical and geochemical techniques, shown them to lie in the field of alkali olivine basalts. On the basis of features such as incompatible trace element ratios, correlation has been made with lava flows on the neighbouring island of Eigg, and cobbles found in conglomerates below the lavas in north-west Rhum.

In hand specimen the basalts are fine grained melanocratic rocks, often highly amygdaloidal, with the amygdales generally infilled with green epidote. Occasional phenocrysts of feldspar can also be observed. Extensive shearing is present, the rocks lying as they do between the IRF and the ORF, (Figure 2) and Smith (1985). Where the basalts are not totally fault bounded (as to the north of NM 4032 9370) the contact is against the Mesozoic sediments, with the contact probably representing the original Tertiary landscape unconformity (Chapter 4).

2.f Porphyritic Felsite and Explosion Breccia

Outcrop of these two rock types in south-east Rhum is not extensive but is nonetheless important to the understanding of the tectonic history of the MRF (Chapter 5). Elsewhere on Rhum porphyritic felsite and explosion breccia can form extensive outcrop, and have been described in detail (eg. The Southern Mountains Complex (Hughes 1960a), The Northern Marginal Complex (Dunham 1965, 1968)). In south-east Rhum the outcrop is restricted to two main areas, (Figure 2), firstly as a capping to the summit of Beinn Nan Stac, and secondly, within the MRF zone. It is the association within the MRF zone which is of particular interest to this study. On the ORF, outcrop is restricted to a number of small pockets of explosion breccia, (Plate 2.14) with no felsite in evidence (Figure 2). This explosion breccia is essentially monomict, composed of country rock clasts (c.2 cm) of Torridonian Bagh na Uamha shale but with occasional arkosic fragments. The matrix is composed of similar but highly comminuted country rock . The relationship of this explosion breccia to the ORF represents utilisation of the structural weakness of the fault during a phase of de-gassing of underlying felsitic magma (Emeleus et al 1985, and Chapter 5). The second occurrence of explosion breccia, this time associated with felsite, is to the south of the gneiss 'whaleback' (NM 404 935), along the line of the CRF. The outcrops along the CRF are predominantly of dark porphyritic felsite, explosion breccia is very much subsidiary in volume and is restricted to patches of lightly brecciated country rocks around some of the smaller outcrops of felsite.

Where felsite is in contact with the gneiss in the extensive 'whaleback' at around (NM 4027 9338) felsite interfingers into the gneiss producing veins and stringers of felsite, often many centimetres long. This contrasts sharply with the contacts where the CRF is exploited directly by the felsite. Here the contacts are very sharp (Plate 2.15) against both the gneiss to the east and sheared lavas to the west. The felsite along the CRF is easily distinguished from the surrounding lithologies as it breaks down readily into cm sized blocks producing a very characteristic rubbly weathering (Plate 2.16).

In thin section (Plate 2.17) the felsite shows a flow banded glassy matrix constituting about 60% of the slide, with phenocrysts (often skeletal) of quartz, plagioclase and augite. The feldspar shows some alteration to sericite. Ferromagnesian minerals are totally restricted to a few grains of biotite. Apatite is also occasionally present as small (mm) euhedral grains. Other features of particular interest include glass shards, fiammé and fragments of basaltic material (Plates 2.17c & 2.17d). The presence of glass shards tends to suggest formation of this felsite in a sub-aerial/high level environment, the shards and fiamme produced from underlying volatile rich magma de-gassing on reduction of overburden pressure as the surface was approached. Such de-gassing also explains the close spatial relationships of felsite and explosion breccia. Structures similar to those just described from the south-east Rhum felsite (shards, fiammé, embayed phenocrysts and fragments of country rock, eg basalt) have recently been described by Williams (1985) where certain felsites in and around Cnapan Breaca have been ascribed to a sub-aerial /high level origin. Many of the Cnapan Breaca felsites are in fact re-classified as 'eutax itic textured welded tuffs' or welded ignimbrites (cf Smith 1960). Although it is by no means suggested that the south-east Rhum felsites are welded tuffs the inference is for a fairly high level origin.

The felsite-explosion breccia assemblage along the ORF and CRF is regarded as solidified magma, injected up along the pre-existing faults on collapse of the 'central piston block' of Emeleus et al (1985). Solidification of felsite magma along the CRF must have occured after movement on the fault was finished as no faulting, shearing or deformation is observed within this felsite.

So far no mention has been made of the felsite-explosion-breccia assemblage of Beinn nan Stac. The Beinn nan Stac felsite is separated from the Torridonian country rock (highly indurated Bagh na h-Uamha shales) by a zone of explosion breccia varying in width from approximately a metre to many tens of metres. The contacts with the felsite are gradational, with the number of country rock clasts diminishing over a distance of c.2m.

Similarly to the Cnapan Breaca/Meall Breac felsites and explosion breccias the Ultrabasic Complex underlies the Beinn nan Stac felsite at no great depth. These felsites at both Cnapan Breaca and Beinn nan Stac are in roof like relationships to the ultrabasics, with the contacts dipping outwards, away from the volcanic centre. Interestingly if the contacts are projected upwards they converge on a point not far above the present level of Askival, this may well suggest that the present summit of Askival was not far removed from the actual top of the magma chamber. The overlying roof rocks of Lewisian gneiss, Torridonian sediments, granophyre and early Tertiary plateau lavas having been eroded off, but preserved in part in the conglomerates beneath the north-west lava hills of Fionchra, Bloodstone and Orval, (Emeleus, 1985 and Chapter 5).

2.g Hybrid rocks

Around the margins of the ultrabasic, Eastern Layered Series (ELS) in south-east Rhum, thermal metamorphism of the surrounding country rocks can be so severe as to produce evidence of partial melting (granophyric texture, quartz paramorphs after tridymite and back veined dykes). These features are described in Section 2.a. Occasionally however the fusion has been so complete that hybrids have been produced by mixing of mafic liquids with granitic liquids produced by the anatectic melting of arkosic country rock.

Hybrids often occur as discrete bodies, with sharp contacts between Torridonian country rocks and 'marginal gabbro', eg. to the south of the Allt nam Bà waterfall at (NM 4061 9420) Figure 2. The most extensive hybrids however are those beneath the Torridonian sediments within the ring fault (below the summit of Beinn nan Stac) Figure 2, and Emeleus and Forster (1979) locality II.4, figure 5. Along this contact the transition from 'marginal gabbro' through hybrid to Torridonian sediments is gradational. Such gradational contacts are found right around the contact of ultrabasic and Torridonian rocks below Beinn nan Stac.

The south-east Rhum hybrids seem therefore to exist in two distinct forms, ie those with gradational contacts and those forming discrete bodies. It has been postulated (R.C. Greenwood pers comm) that after the formation of the hybrids the resulting liquids could either act as separate intrusive bodies and migrate along the margins of the intrusion, or, remain in place, as seen beneath Beinn nan Stac. Similarly the 'marginal gabbro', which is probably not so much a gabbro as contaminated marginal members of the Ultrabasic Complex (R.C. Greenwood pers comm, based on Pb and Sr isotope work), could also act as a separate intrusive body migrating along the margins of the intrusion. The fact that below Beinn nan Stac the contacts between ultrabasic rocks and Torridonian appear gradational tends to imply that the Torridonian was in its present position above the ultrabasic rock at the time of intrusion of the main Ultrabasic Complex. ie. that the Torridonian as we now see it on Beinn nan Stac is original roof material (see Plate 2.18). If this is so then igneous layering was able to form to within a few metres of the wall of the intrusion. Plate 2.18, taken from the south side of Dibidil clearly shows the roof like nature of the Beinn nan stac Torridonian with the layering forming to within a metre or so of the contact.

In the field the hybrids are easily distinguished, they are leucocratic fine to medium grained rocks characteristically containing visible (5-10 mm) acicular green amphibole (Plate 2.19). The amphibole appears rather embayed giving it a somewhat 'graptolitic' appearance.

In thin section the most prominent feature is acicular amphibole (Plate 2.19). The amphibole is skeletal in nature varying in length from 0.5-10 mm with a width of 0.005-0.5mm. Pleochroism is pronounced; a=light brown b=red brown, c=dark red brown. The amphibole appears to be an alteration of original ortho-pyroxene (hypersthene), although the possibility also exists that conversion from original titan-augite in the ultrabasic rocks to the titanium amphibole kaersutite has occured. Some of the amphibole in these hybrids does show extinction angles rather less than for hornblende. Kaersutite has been positively identified by electron microprobe micro-analysis of amphibole from similar hybrids from the northern slopes of Beinn nan Stac (R.C Greenwood pers comm.).

Another feature of these rocks are the small (0.1-0.5 mm) radiating clusters of quartz after tridymite (Plate 2.19c). Such features have been described from contacts of basic/ultrabasic rocks with arkoses and sandstones elsewhere in the British Tertiary province; Wager, Weedon and Vincent (1953), Black (1954), Brown, (1963). It is still uncertain as to the precise constraints of pressure and temperature under which such inversion to tridymite occurs, although it is generally accepted (Black. 1954) that it forms under conditions of high temperature but low pressure . This fact is also conducive to prevalent ideas that the ultrabasic series formed in-situ at fairly high crustal levels, (ie low confining pressures; Emeleus et al (1985), Emeleus (1987), and R.C Greenwood (pers comm)).

Granophyric texture is a feature also well developed in the hybrids (Plate 2.19b), rather similar to that developed in the highly indurated Torridonian, ie graphic intergrowths of quartz and alkali feldspar. The rest of the mineralogy in the hybrids is plagioclase felspar (AN 50+) with opaque oxides consisting of ilmenite, magnetite and pyrite. In one section of hybridised gabbro (NJ 83.3-12.) pyrite forms 30% of the slide.

2.h Ultrabasic rocks - The Eastern Layered Series (ELS)

To the north and west of the Allt nam Bà waterfall, (NM 4060 9436) the rocks exposed are those of the Eastern Layered Series (ELS)and are shown on Figure 2. They are comprised of alternating layers of peridotite and allivalite. although higher up in the sequence thin seams of chromite are found. Both the lower ELS (units 1-5 Of Brown,1956) and the upper ELS (units 5-15) have been the subject of much recent study. Far more detailed descriptions of these rocks than is here presented can be found in the following publications; Faithfull (1985) -the Lower ELS, Butcher (1985) -the Upper ELS, Tait (1985) -geochemistry of unit 10, Palacz and Tait (1985) -isotopic study of unit 10. These more recent works supplement the classic studies by; Brown (1956) and Wadsworth (1961).

This study is not really concerned with a detailed analysis of the ultrabasic rocks, although one particular detail of the Lower ELS is unique, and useful in the interpretation of the structural history of the MRF. This feature is the relatively steep dip of unit 1 allivalites and peridotites (30^{o} - 40^{o} westwards), in conjunction with the steep westerly dip of the country rock to the north of Allt nam Bà. As Faithfull (1985) points out this sort of situation is more consistant with central subsidence, rather than uplift as has been previously postulated (Dunham, 1980).

Plates 2.20 and 2.21 show the appearance of the layered series on Rhum.

Figure 2.1

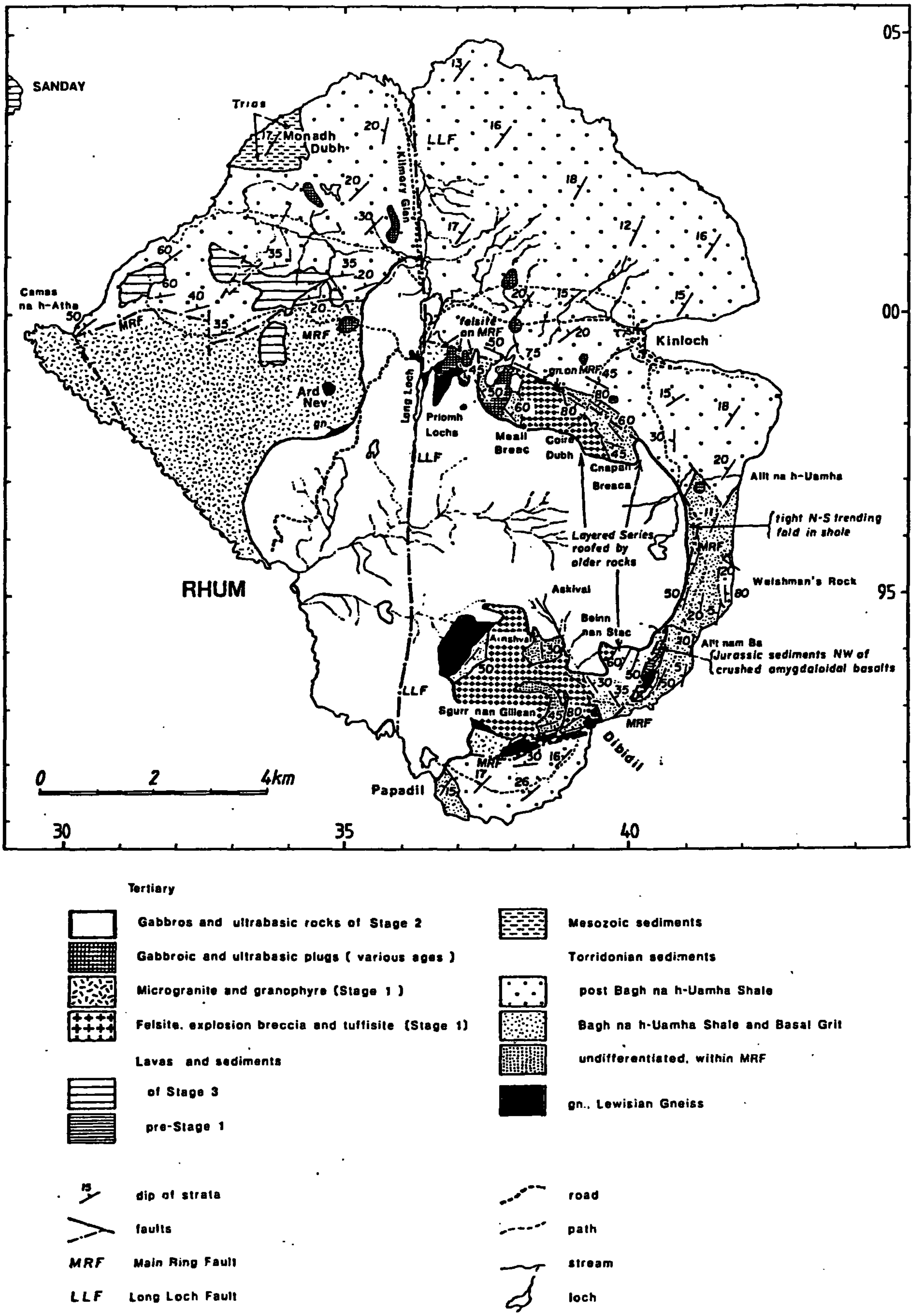

Geological Sketch Map of the Isle of Rhum. (From Emeleus et. al. 1985).


FELSITE
EXPLOITING FAULT
PLANE
LEWISIAN
GNEISS
LINE OF CRF

Plate 2.I Gneiss 'whaleback' and the Trace of the Centre Ring Fault (looking North).

Plate 2.Ia Foliation in the gneiss 'whaleback' (looking south-east).

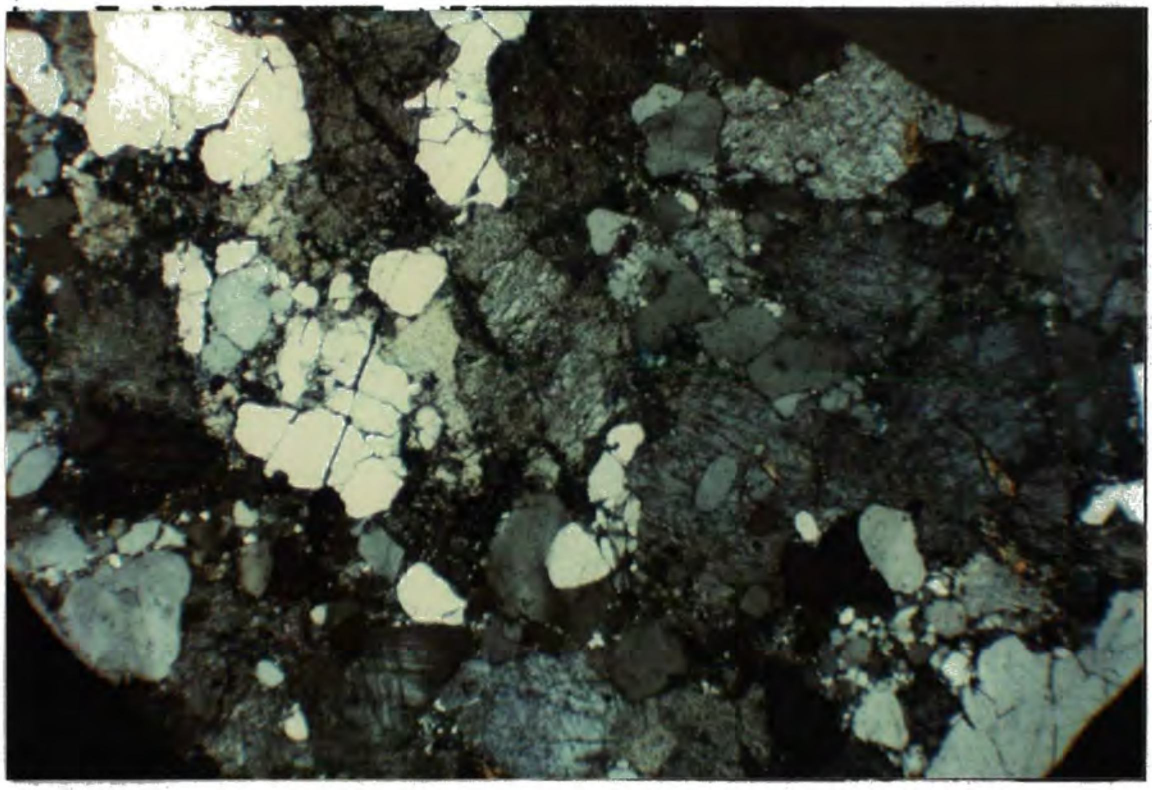

Plate 2.2 Leucocratic Lewisian Gneiss (NJ 83, 6-7)
X-polars. Field of view 9mm.
Composed predominantly of alkali feldspar (cloudy) quartz (clear) and hornblende (seen bottom right as small moderate birefringent grains). Chlorite is present (centre of slide) showing anomalous 'Berlin' blue interference colours. Note quartz forming cores to certain alkali feldspar grains. For full description of the Lewisian Gneiss see text - Section 2.b

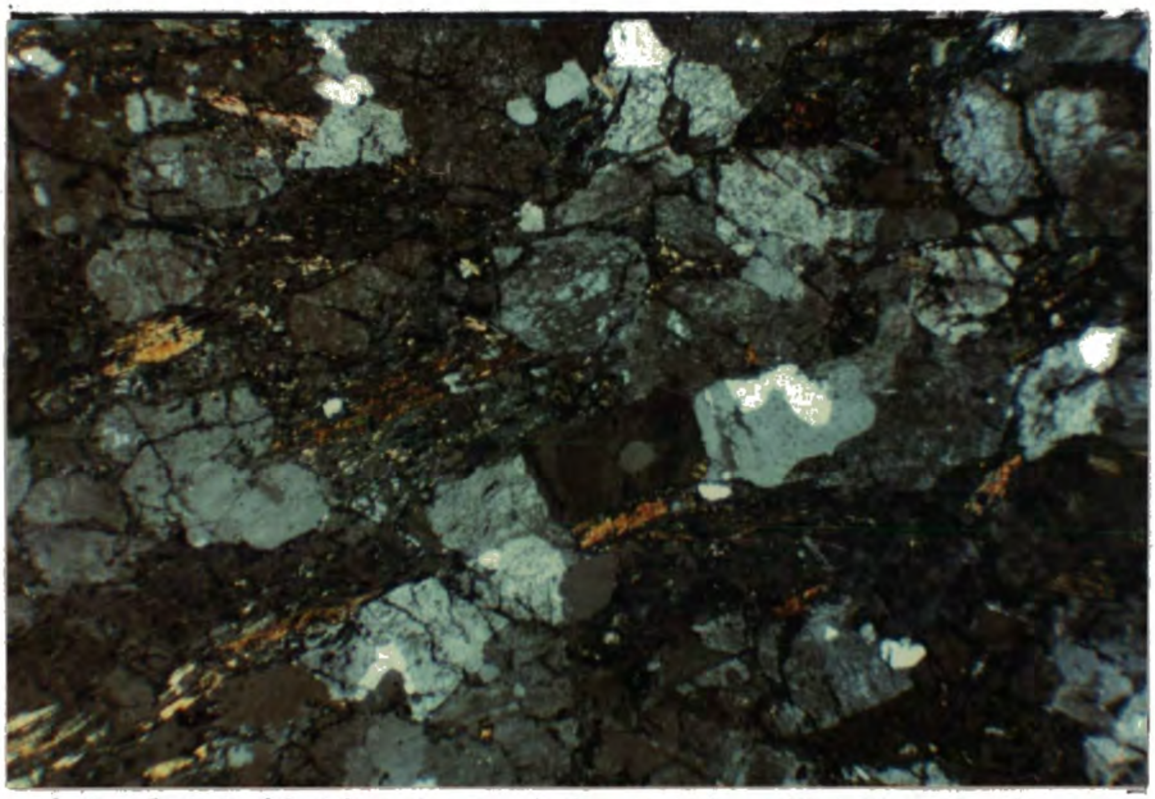

Plate 2.3 Foliation in Lewisian Gneiss (NJ 83, 32-I) X-polars. Field of view 9mm. Foliation is shown by the hornblende (bottom left to top right).

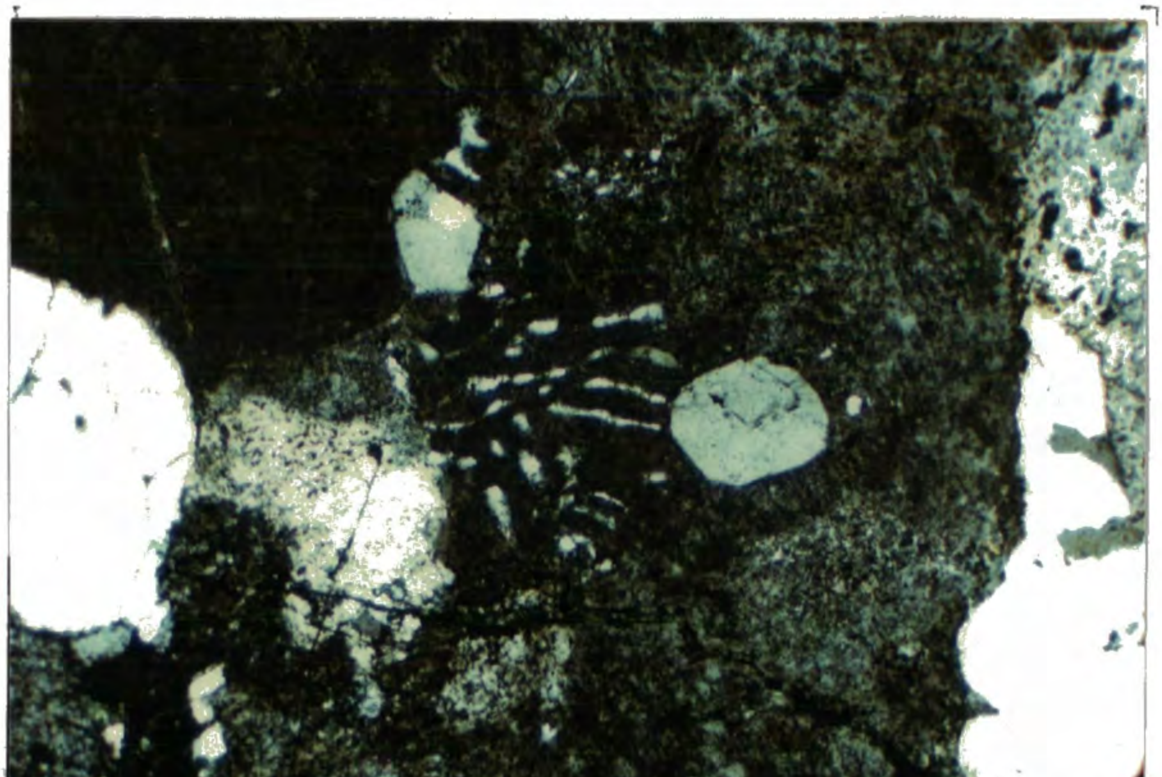

Plate 2.4 Development of granophyric texture, indicative of remelting. See text - Section 2.b. Field of view 3.5mm

Plate 2.5 Development of bench and scarp topography in Torridonian sediments to the north of Kinloch Glen. (Looking north)

Plate 2.6 Pseudo-coraline structures in rheomorphic Torridonian arkose, Allt nam Ba

Plate 2.7 Dyke in foreground has become broken up and 'back-veined' due to rheomorphism of the surrounding Torridonian arkose. Allt nam Ba.

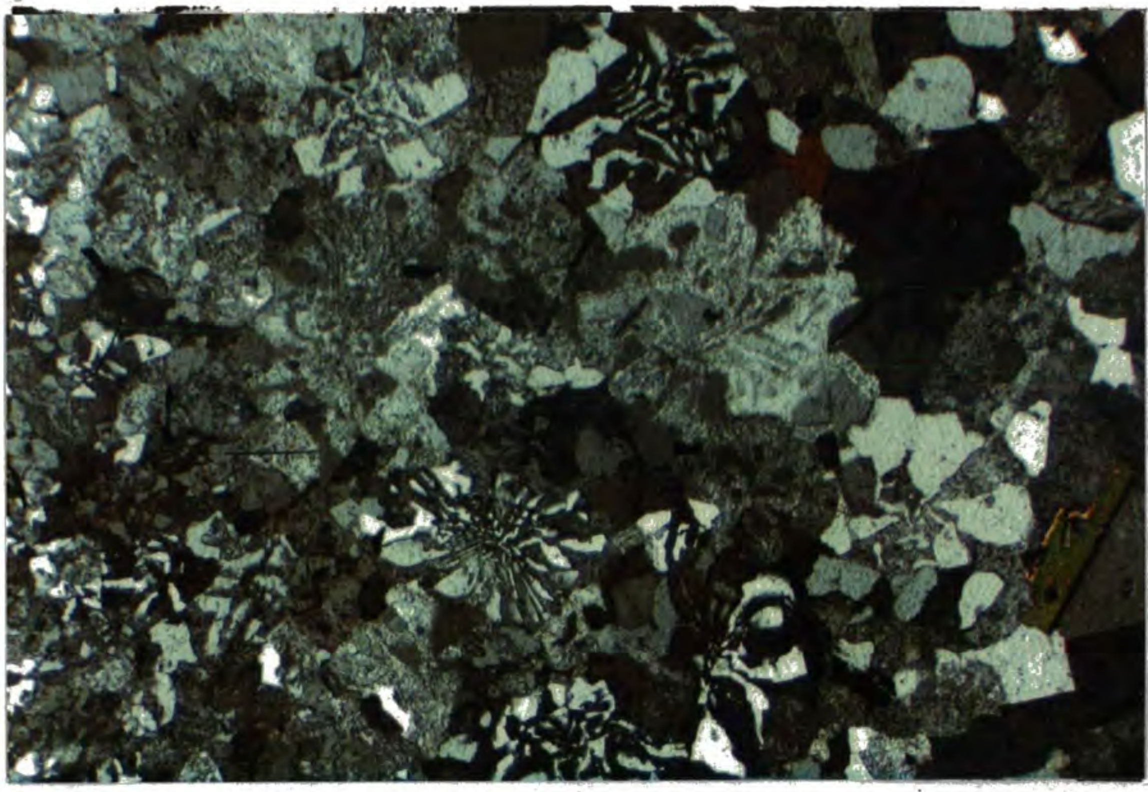

Plate 2.8 Rheomorphic Torridonian arkose, Allt nam Ba. NJ 83, 3-IO. X-polars. Field of view 3.5mm. Shows good development of granophyric texture (graphic intergrowth of quartz and alkali feldspar) due to melting and re-crystalisation of the arkose. Other minerals present are biotite, and small needles of opaque oxides (ilmenite?). A small detrital zircon can be seen just to the left of centre. See also text - Section 2.c.

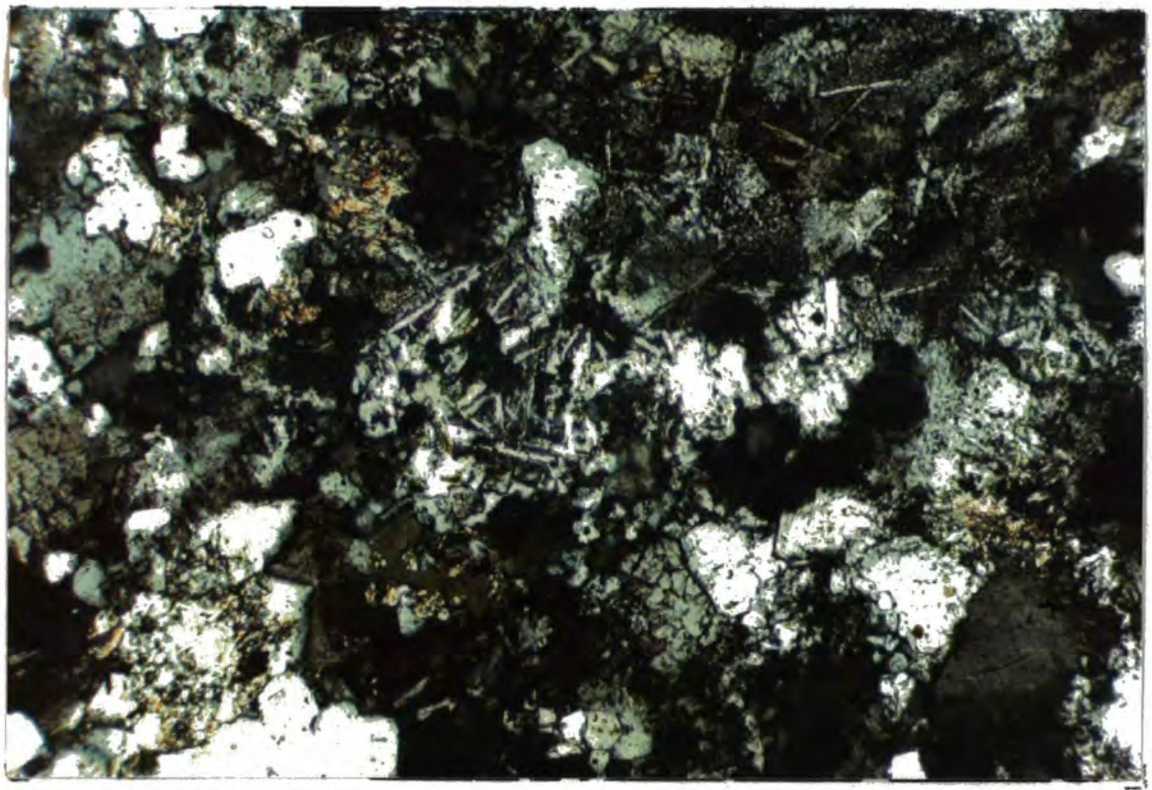

Plate 2.8a Rheomorphic Torridonian arkose (NJ 83, 3-IO). X-polars. Field of view I.5mm. Acicular needles of quartz paramorphs after tridymite in a mesostasis of quartz and alkali feldspar.

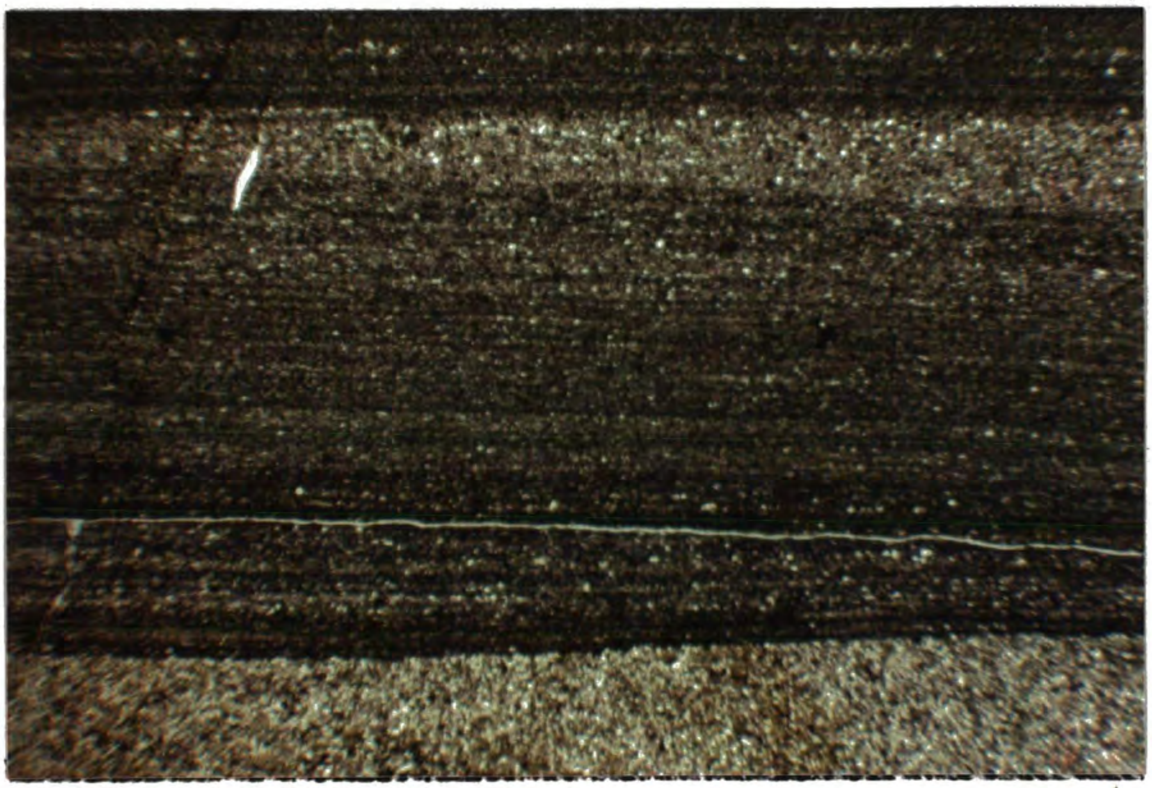

Plate 2.9 Unaltered Bagh na h-Uamha Shale (NJ 83,I-I). Plane polarised light. Field of view 9mm

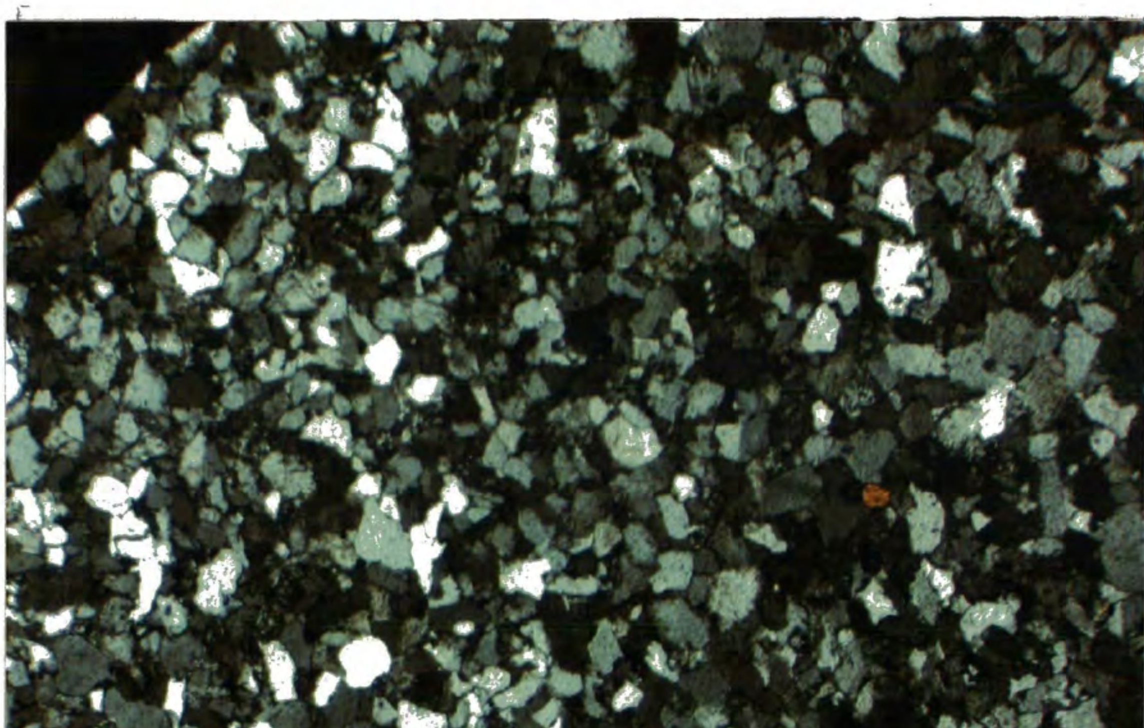

Plate 2.IO Unaltered Rudh na Roinne Grit. (NJ 83, 3-I). X-polars. Field of view 3.5mm.

Plate 2.I2 Kink banding in Torridonian Bagh na h-Uamha Shale to the west of the Inner Ring Fault. See text - Section 2.c.

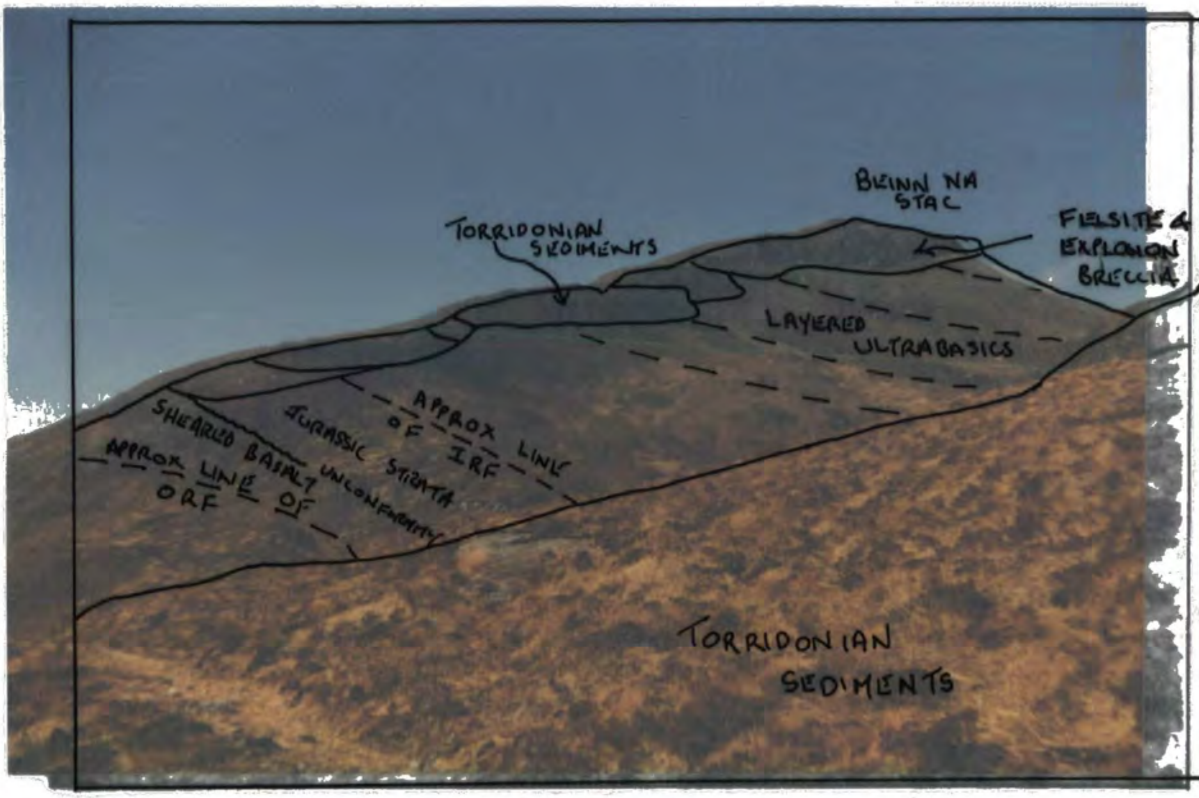

Plate 2.13 Looking southwards towards Beinn nan Stac. Note the roof like aspect of the Torridonian sediments within the MRF, and how the layering in the ultrabasic rocks is developed almost up to contact.

Plate 2.I4 A 'Pocket' of monomict explosion breccia on the Outer Ring Fault, just north of the deeply incised dyke channel at (NM 4030 9357). see text.

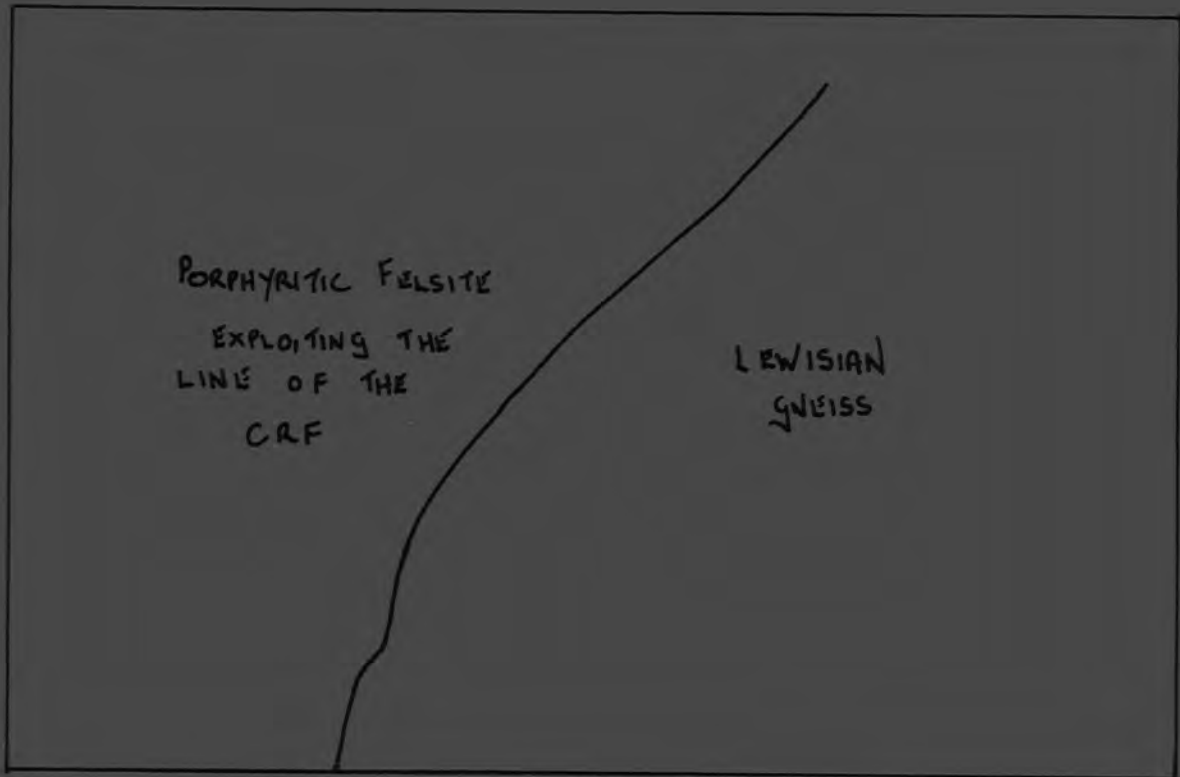
PORPHYRITIC FELSITE EXPLOITING THE LINE OF THE CRF
LEWISIAN GNEISS

Plate 2.I5 The contact of the Lewisian Gneiss with porphyritic felsite along the line of the Centre Ring Fault. Note sharpness of the contact.

Plate 2.I6 Typical 'rubbly' weathering characteristic of the porphrytic felsite. Hammer marks the junction of the felsite with Lewisian Gneiss.

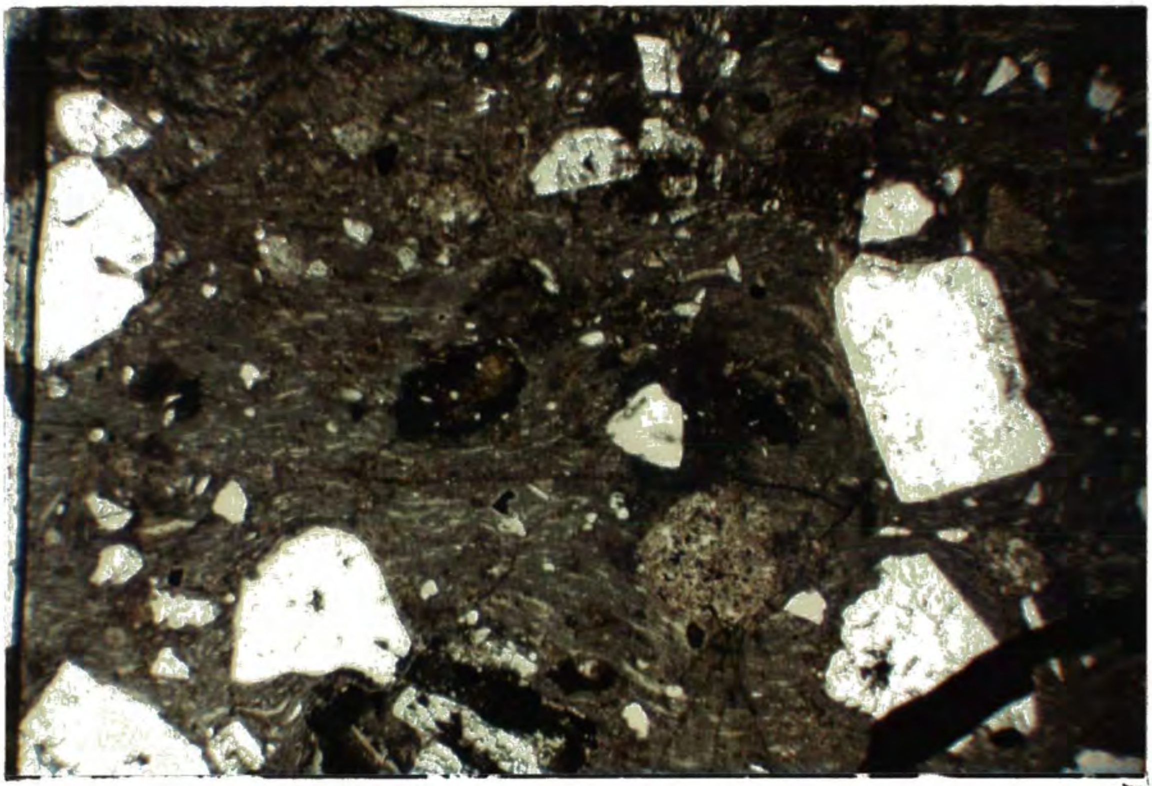

Plate 2.I7a Flow banded porphyritic felsite (NJ 85, I-I6) plane polarised light. Field of view 9mm. See text - Section 2.f.

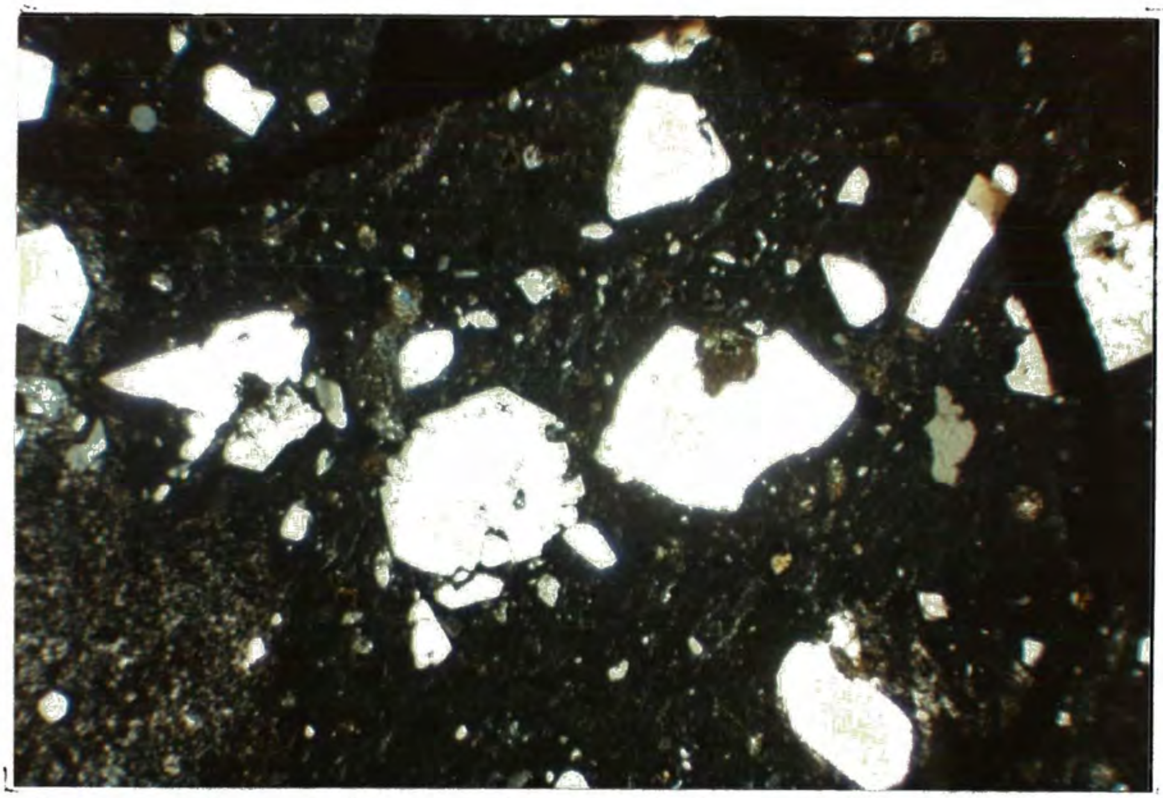

Plate 2.I7b Felsite showing partial resorbtion of feldspar phenocrysts (NJ 85, I-I6). X-polars. Field of view 9mm.

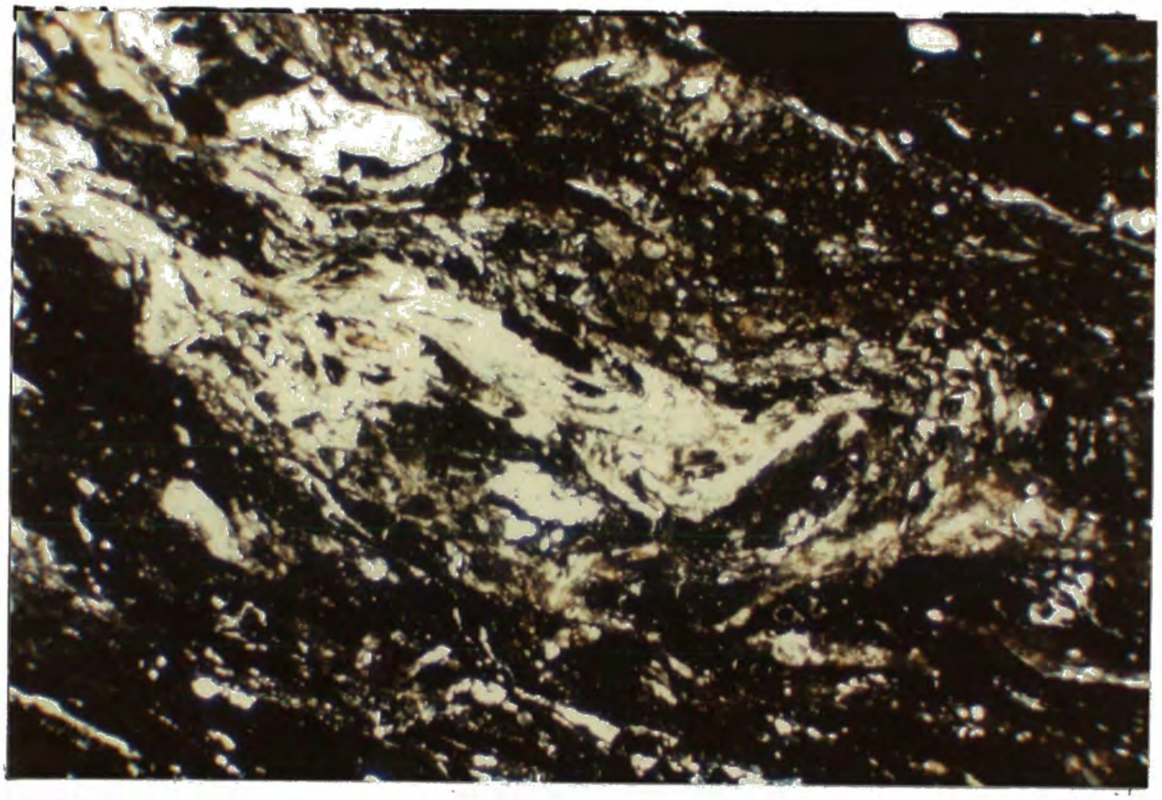

Plate 2.I7c Fiamme in felsite from along the Centre Ring Fault (NJ 83, 8-IO). Field of view 9mm

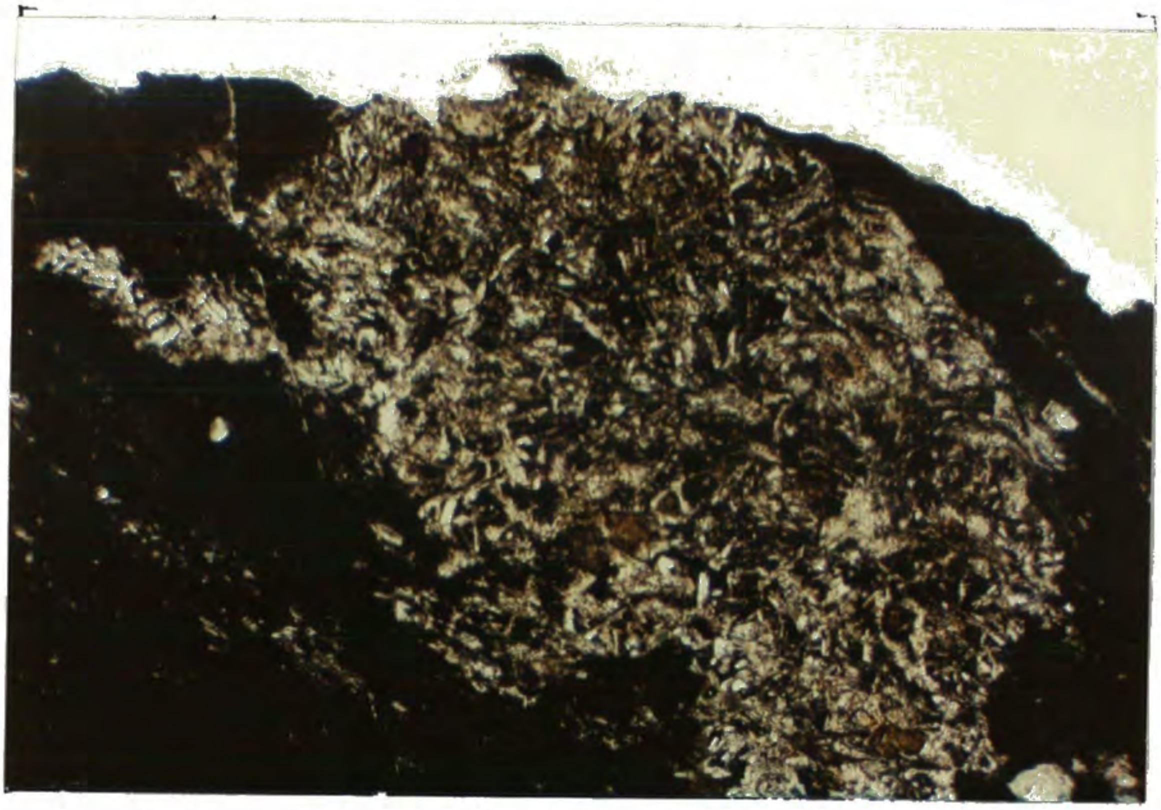

Plate 2.I7d Basaltic 'fragment' in felsite (NJ 83, 8-IO). See text - section 2.f.


BEINN NAN STAC
FELSITES & EXPLOSION BRECCIA
DEFORMED TORRIDONIAN SEDIMENTS
LAYERED
ULTRABASICS
DIBIDIL VALLEY

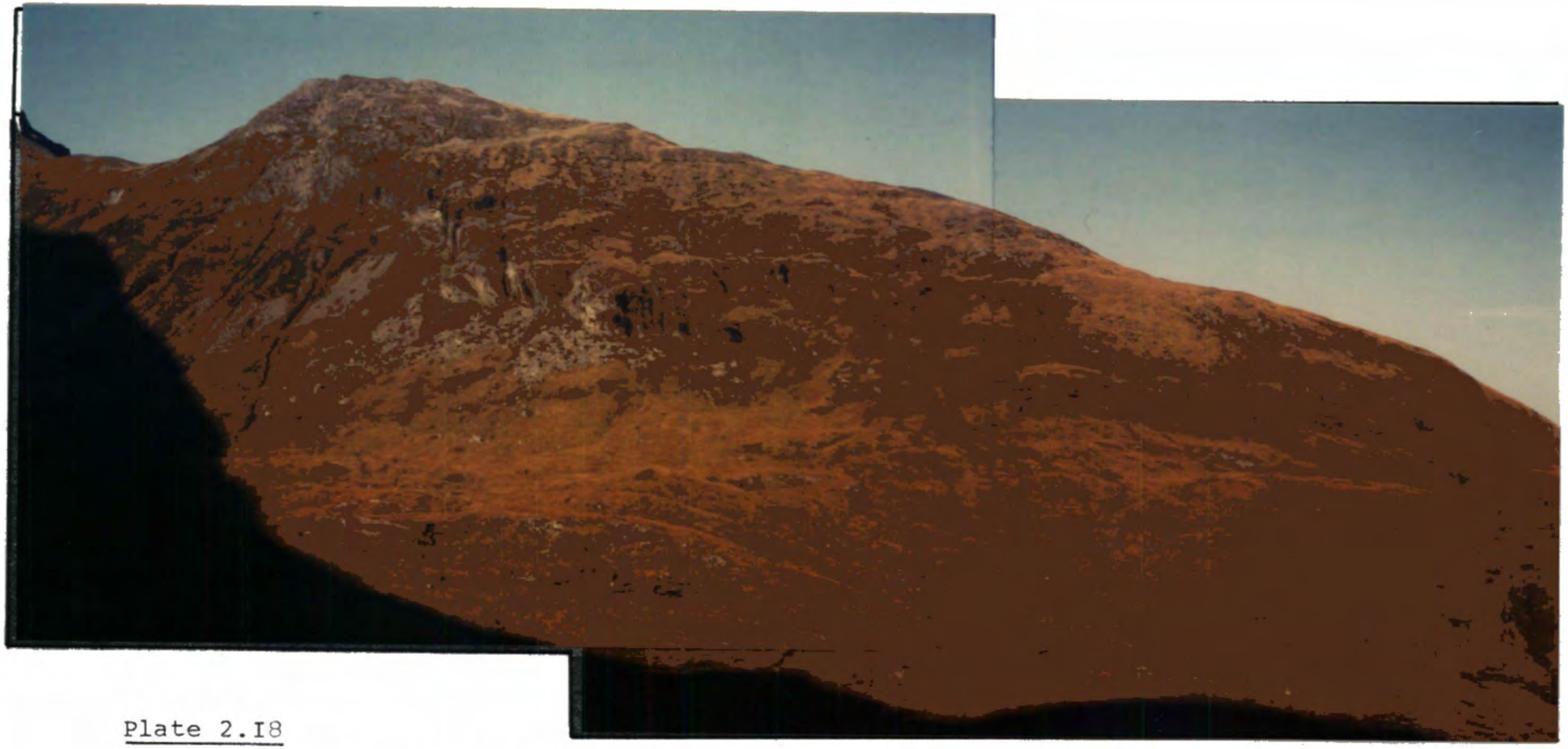

<u>Plate 2.I8</u>

Panoramic view of Beinn nan Stac from Dibidil (looking north)

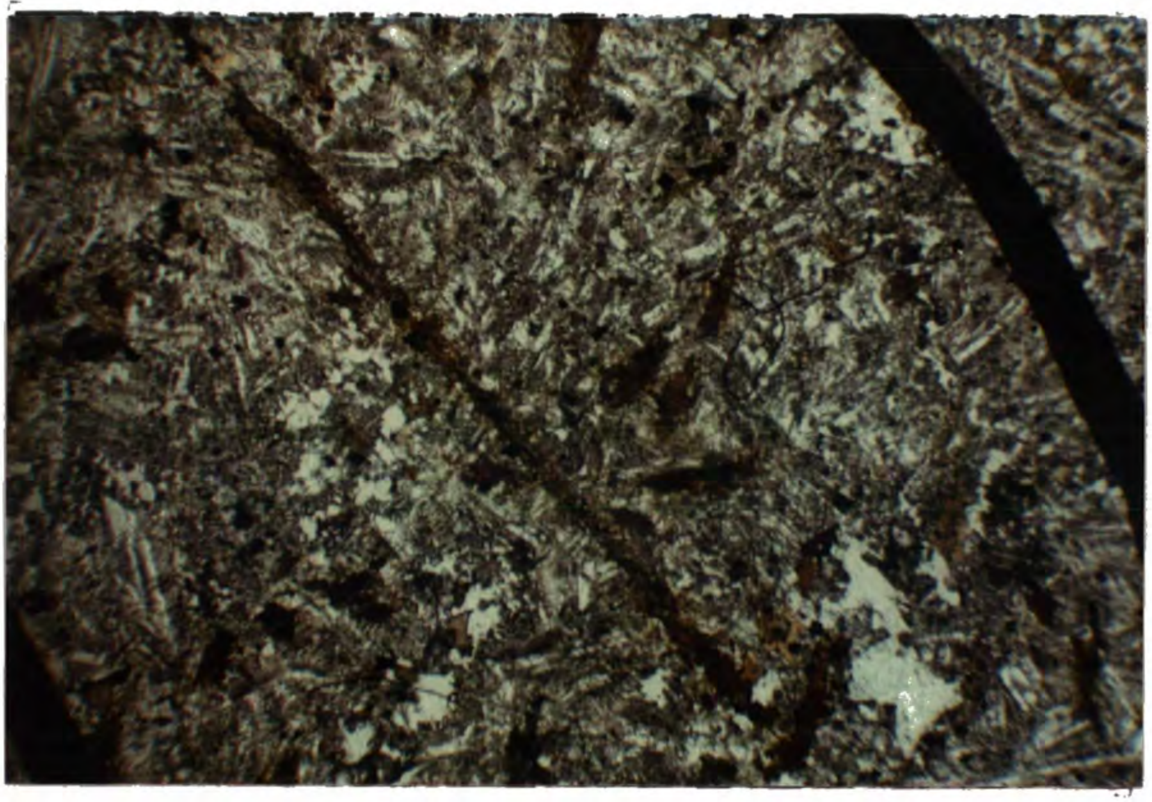

Plate 2.I9a Hybrid rock (NJ 84, 27-5). Plane polars. field of view 9mm. Shows acicular, skeletal amphiboles, but see text - Section 2.g.

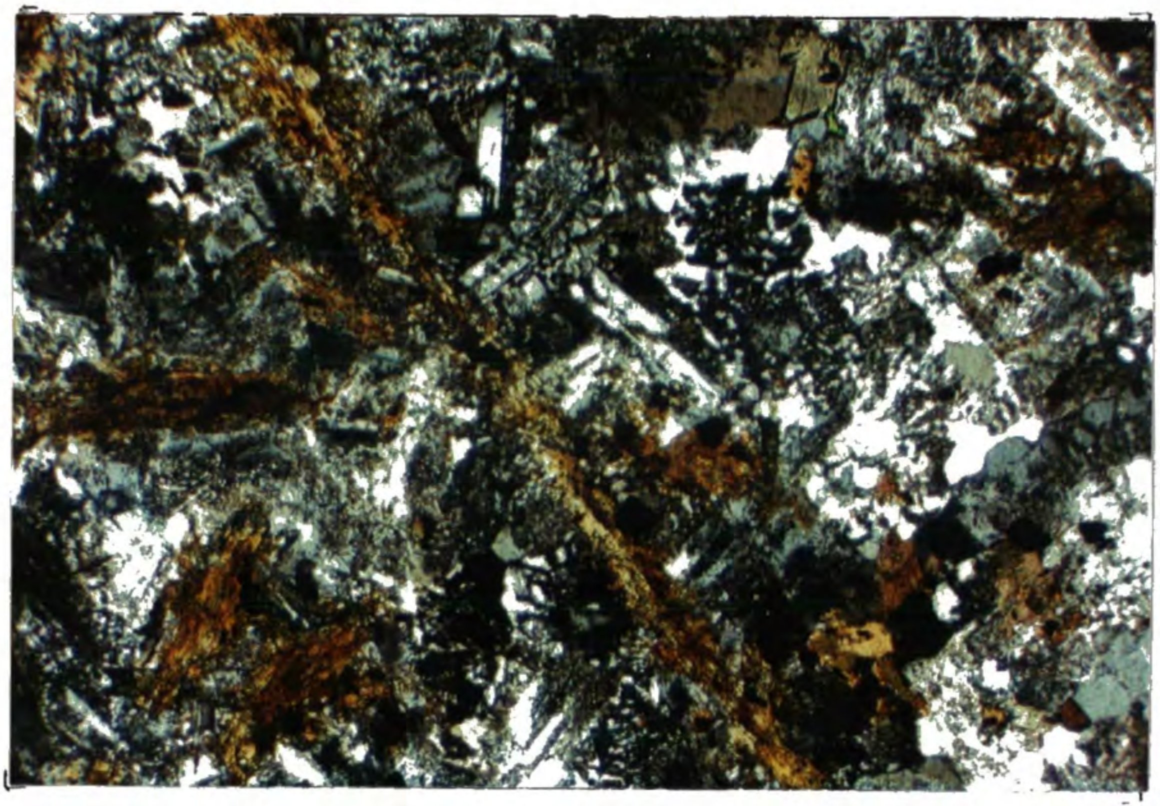

Plate 2.I9b Hybrid rock (NJ 84, 27-5).X-polars. Field of view 3.5mm. Acicular amphiboles plus graphic texture.

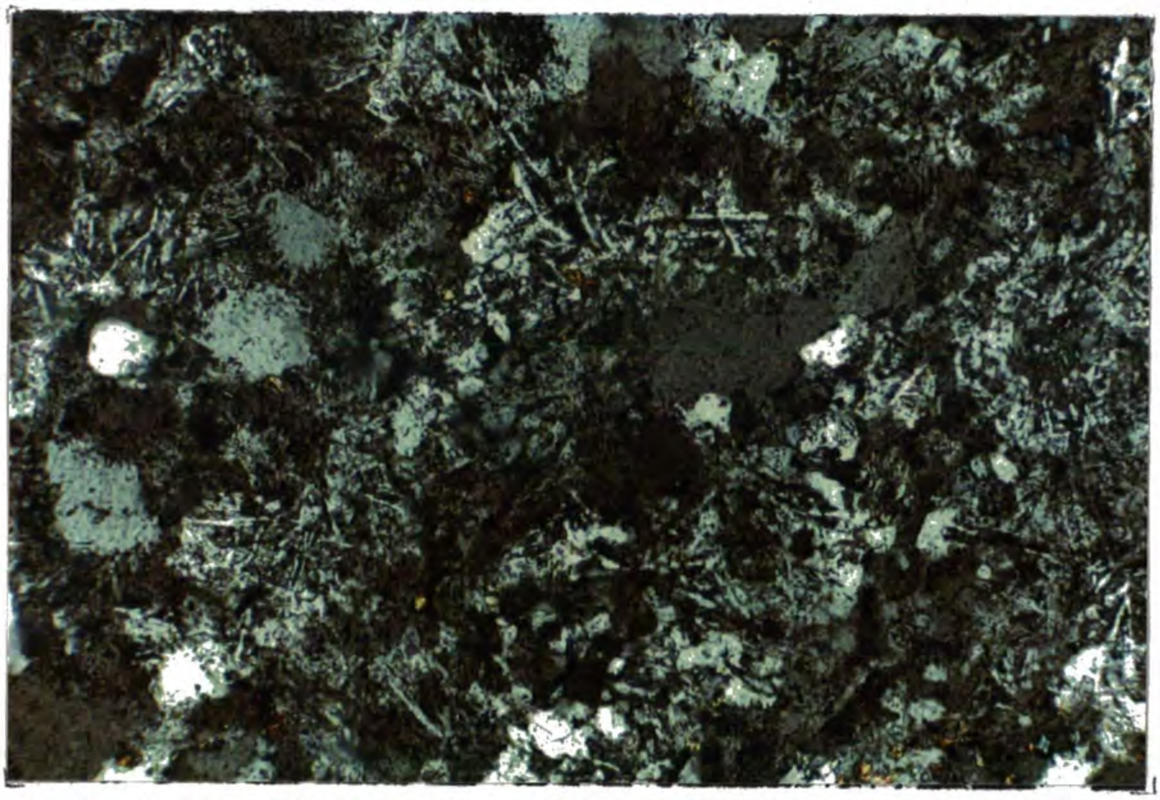

Plate 2.I9c Hybrid rock (NJ 85, 8-2). X-polars. Field of view I.5mm. Quartz paramorphs after tridymite (acicular needles) constitute c. 30% (modally) of this slide. See text - section 2.g.

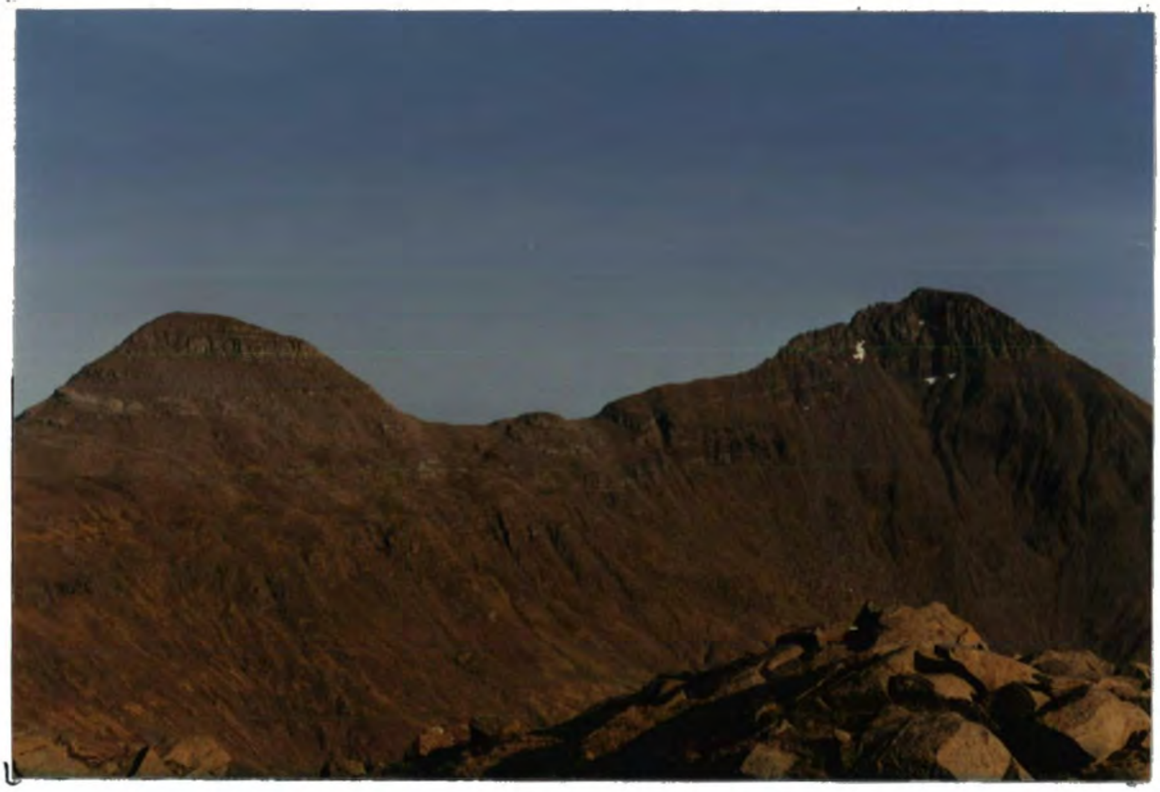

Plate 2.20 The Hallival,Askival ridge (from Barkeval), showing the layering in the ultrabasic rocks. The highest Unit (Brown 1956) is Unit 15 on the summit of Askival (the peak on the right).

Plate 2.2I Ultrabasic layering on the summit of Askival. Note the typically stepped weathering, this is due to peridotite being less resistant to erosion thus it is cut back leaving prominent ridges of allivalite.

Chapter 3

The Mesozoic Strata

3.a Description of outcrop

3.b Mesozoic lithologies

3.b.i Sandstone

3.b.ii Limestone

3.b.iii Shale

3.c Palaeontology

3.d Comparison of Rhum Jurassic rocks to other Hebridean occurrences.

Figures, Plates and Tables

3.a Description of outcrop

To the south of the valley of the Allt nam Bà, and over the eastern flank of Beinn nan Stac (Figure 2) occurs a succession of inclined and fault-bounded strata. These strata consist of beds of sandstone, limestone, sandy-limestone and shale, the succession itself being intimately associated with sheared amygdaloidal basalt lavas (see Figure 2, and Chapter 4). The sediments represent a group of Mesozoic (Jurassic) rocks (see section 3.d) caught up in the complex MRF in south-east Rhum.

On the lower north-east slopes of Beinn nan Stac (NM 4050 9408. Plate 3.1) an estimated thickness of Mesozoic rocks totals c.35 metres. This sequence can be divided up as shown in Table 3.1;

TABLE 3.1

Lithology	locality in outcrop	Thickness (metres)
Basalt	east	60(minimum)
(unconformity)		
Quartzite		7.4
Limestone		14.5
(no exposure - limestone and sandy-lst inferred)		10.5
Shale	west	c. 2.0
		from Smith(1985)

There is some lateral variation in the thickness of individual units but poor exposure precludes precise determinations being made. The sandstone unit dips at c.60^{o} to the west, the limestones and shale units are more steeply inclined at c.70^{o} west. The variation in dip between individual units of the succession needs to be explained. A clue as to the most likely cause for such variation in dip is in the presence of large sink holes in the vicinity (Plate 3.2). Such total dissolution of limestone adjacent to other more resistant units could cause localised rotation and collapse of such unsupported units.

Structural setting: the Mesozoic fault slice is bounded to the west by the low angle Inner Ring Fault (IRF) and . abuts Precambrian (Torridonian) sediments, while to the east, the contact is with the sheared amygdaloidal basalts, situated to the west of the Centre Ring Fault (CRF), (Figure 2).

3.b Mesozoic lithologies

3.b.i Sandstone

The Mesozoic sandstones of Rhum (Plate 3.6 & 3.6a) were previously thought to belong to the Torridonian 'Basal Grit'. A more detailed examination however has differentiated between true 'Basal Grit' and the rather dissimilar Mesozoic sandstone. Unlike the 'Basal Grit' the Mesozoic sandstones are composed of sub-rounded quartz grains with an approximately bi-modal size distribution (2-3mm and 0.2-0.5mm). There is little or no feldspar, this is in sharp contrast to the Torridonian which often contains greater than 50%, and therefore is variously classed as an arkose or arkosic sandstone (see also Section 2.b).

The thickness of the sandstone is rather variable.

On the lower north-eastern shoulder of Beinn nan Stac, (NM 4050 9408) 7.4 m are exposed, whereas further south some 19m are exposed. The contacts of the sandstone at both localities are with limestone to the east and the sheared amygdaloidal lavas to the west. The variation in thickness could quite simply be explained as lateral variations in thickness of the original sequence, or alternatively as the consequence of the extensive fault movement that affects all rocks hereabouts. The nature of the contact with the lava is however, an interesting one. No faulted contact is observed, but the sandstone in contact with the basalt does show evidence of local thermal metamorphism and leaching, (Plate 3.5). It is therefore postulated that the preserved contact is in fact the original landscape unconformity as preserved elsewhere in the British Tertiary Igneous Province (BTIP), this would of course explain any lateral variations in thickness of the sandstone, (see Chapter 4).

At the contact with the amygdaloidal lavas the sandstone is very pale weathering and appears to have been extensively leached. A thin section (NJ 85 19-13) reveals that the rock is even more indurated than is usual, the quartz showing evidence of embayed margins and undulose extinction. Since the sandstone lies at some distance from the underlying ultrabasic rocks, it is considered that the rather greater than normal induration was caused by extrusion of the basalt lavas onto the Tertiary land surface eroded into the Jurassic strata.

Plate 3.6 shows a typical thin section of the unleached Jurassic sandstone. The bi-modal size distribution of the quartz grains in the ranges (2-3mm and 0.2-0.5mm) is clear and ferruginous dust rims are seen around original quartz. Grain to grain contacts are low, the grains being supported by a siliceous cement. Occasionally the cement is rather more calcareous, where this does occur the original micrite often shows alteration to calc-silicate minerals, commonly wollastonite,(e.g. NJ 85 19-10 - Plate 3.7).

3.b.ii - Limestones

The Rhum Mesozoic limestones vary from relatively unaltered and quite fossiliferous rocks, through pure calcite marble to a high temperature calc-silicate mineral assemblage including Tilleyite and Harkerite (Thin Section SR 199b). As described in the introduction (Section 2.c.ii.), limestone was discovered in south-east Rhum by Geikie (1897) and 'rediscovered' later by C.J. Hughes (1960b) who first described calc-silicates from the Allt nam Bà. Hughes noted in particular the presence of 'tilleyite' from a wall like outcrop in the Allt nam Bà valley, (Emeleus and Forster. 1979, fig 5 locality IIb). This calc-silicate outcrop probably represents a large xenolith of impure limestone caught up in the marginal gabbroic members of the complex, Smith (1985). Even where the limestone is not obviously in contact with gabbroic or ultrabasic material it often still shows a high degree of thermal metamorphism. In a small easterly facing cliff, 50m south of Allt nam Bà, the original limestone is totally recrystallised to a 'sugary' textured calcite marble and in addition, contains small crystals of grossular garnet and idocrase (Plate 3.8).

Further to the south, where the limestones are more distant from the ultrabasic rocks, metamorphism is less severe and the remains of bivalves are observed. These are the exposures first discovered by Dr C.H. Emeleus and in which Dr G.Farrow noticed bivalve remains (Dunham and Emeleus, 1967). The state of preservation of these bivalves is not good enough to apply anything more than the phylum or class to them. As the limestone is traced westwards exposure is lost, however although it forms relatively few surface outcrops, its extent may be determined by the distribution of deep sink holes, (Plate 3.2).

A number of new exposures of limestone have however, been found. One of these exposures, an impure sandy-limestone, contains some of the best fossil remains to come out of the area. This assemblage is described in Section 3.c.

The limestone, and other Jurassic sediments, are now known to have a much more extensive outcrop than that shown on the published maps (cf. Emeleus 1980, Smith 1985 figure 1). The southern limit of the limestone had been thought to be about 100m north of a deeply incised dyke channel (NM 4036 9375) where the limestone was seen to be cut out beneath overthrust Torridonian sediments (Smith 1985 figure 1) along the Inner Ring Fault. Subsequently, a new exposure of limestone, sandstone and amygdaloidal basalt has been discovered on the northern slopes of Dibidil (NM.399 935), about 0.75 km south-west of the previous southern limit of the limestone. Limestone in the new outcrop (Plate 3.10) is heavily recrystallised to a pale grey marble but retains a few ill-preserved fossil remains. Overlying the heavily re-crystallised limestone (the contact not observed) is a pale weathering fine grained sandstone. This sandstone lies directly beneath overthrust Torridonian sediments, see below. The sandstone and marble appear totally inverted as amygdaloidal lavas (similar to those found further north) now lie BELOW the sediments. The junction of the basalts with the overlying Mesozoic rocks is marked by a break in slope at about 200 m altitude.

Torridonian sediments overlie the Jurassic rocks and the lavas, the junction is a low-angle thrust dipping to the south-west. The thrust is clearly defined at a number of places on the hillside and there is a tendency for the Mesozoic rocks to weather away leaving the Torridonian sediments as a well defined, (sometimes undercut) scarp. Exposure of Mesozoic rocks hereabouts is due to erosion in the Dibidil valley cutting down through the thick Torridonian succession revealing a 'window' of younger rocks beneath the thrust fault. The limestone in this outcrop is clearly that to which Geikie (1897 p351) referred and not the outcrops further north which Hughes (1960b) attributed to Geikie. The stuctural implications of this area are examined in a subsequent section (Chapter 5).

3.b.iii Shale

Just to the west of the very fossiliferous sandy-limestone exposure, about 250m south-southeast of the Allt nam Ba waterfall, (NM 4051 9410) there is an outcrop of black, indurated shale (Plate 3.1 & 3.11). Previously, all shales were postulated as belonging to the Torridonian, Bagh na h-Uamha shale member. However, the Jurassic age of this one outcrop can now be clearly established. A definitive set of fossils has been collected, including; belemnites (Passaloteuthis sp), bivalves, and corals (Montvaltia sp.- Dr.J. Senior, pers. comm.).

Like the Torridonian the Jurassic shales are indurated, dark, and finely bedded. Unlike the Torridonian they contain 6-10% angular quartz grains and up to 5% opaque grains (pyrite). The pyrite usually occurs in discrete patches which appear to have nucleated around fossil fragments (Plate 3.12). The shale is fault-bounded to the west against the IRF, where it comes against Torridonian sediments. To the east, there is a conformable junction with sandy-limestone. The shale exposure is not extensive since it is lost under overthrust Torridonian sediments on the north-eastern shoulder of Beinn nan Stac (at c. NM 4047 9403).

3.c - Palaeontology

The only fossils previously recorded from south-east Rhum were those described in Dunham and Emeleus (1967) as; 'belemnite and brachiopod remains '. These were from a slightly sheared marble (not in-situ.). C.H. Emeleus did later discover limestone with bivalve and coral remains in situ about 250m south of the Allt nam Bà valley. A tentative Jurassic age was applied, thus negating Hughes' (1960b) view of a Lewisian age.

Re-investigation of south-east Rhum has led to the discovery of much new fossil material, allowing the strata to be dated. The best fossils were from an impure sandy limestone (Plate 3.13) at about 170m altitude and 300m south-southwest of the Allt nam Bà waterfall (NM 4052 9405). The following fossil assemblage is present; belemnites (Passaloteuthis sp.), dissarticulated pectinid bivalves (Chlamys sp.), serpulid worm tubes (2-3mm in diameter) and other indeterminate fossil fragments. The preservation was typically of a cast-and-mould type.

The purer limestone also contains large quantities of fossil material although the indurated nature of this rock unfortunately precludes precise identifications. Generally the fossil material is; crinoid ossicles, echinoderm plates and spines? (Plate 3.14), with much dis-articulated bivale debris. Interestingly, some of the shell fragments preserve fine scale algal boring into the outer layers of the shell (Plate 3.15). This sort of feature is typical of slow sedimentation where shell debris lies around on the sea-floor for for some considerable time. The dis-articulated nature of the debris also suggests a moderate to high energy environment.

The highly indurated shale has proven remarkably fossiliferous. It contains well preserved belemnites (Passaloteuthis sp.), pyritized bivalves - which are often still articulated (Plate 3.12), and a well preserved solitary scleractinian coral (Monvaltia sp.),(Plate 3.16).

The sandstone is generally devoid of fossils, this is partially a primary feature but is enhanced by the generally highly baked, quartzitic nature of the rock. One section however does contain a small (5mm) solitary coral (probably (Thecosmilia sp. Plate 3.17). Table 3.2 shows the typical faunal distribution in the Rhum Mesozoic rocks. This faunal assemblage indicates a Jurassic (Lower Liassic) age for these beds.

3.d Comparison of the Rhum Jurassic rocks to other Hebridean occurrences.

Jurassic rocks outcrop to some extent on all the other Small Isles, with the exception of Canna, where it has been suggested that they may under-lie the exposed Tertiary lavas at no great depth (Binns, Mc Quillin, Kenolty et al. 1974). However, Mesozoic fragments are not found in the extensive volcanic breccias of Canna, as would be expected if the lavas were underlain by Mesozoic sediments. The above authors also record finding extensive Mesozoic sediments in a number of fault-bounded submarine basins (op cit. fig 2).

The most extensive outcrop is that on Skye, where an almost complete sequence from the Lower Lias (Broadford Beds) through Middle and Upper Lias into the Corallian is preserved. These have been described in detail by Peach et al. (1910) and Hallam (1959, 1983). Comparative Mesozoic sections are shown in Figure 3, taken from Smith (1985).

Section 3.c has shown the Rhum Mesozoic rocks to be Lower Liassic in age, therefore some correlation with the Lower Liassic (Broadford beds) of Skye would be expected. A short field season was spent examining the Broadford beds on Skye, using Hallam (1959) as a guide. The rocks consist of a series of limestones, sandstones, sandy-limestone and shales, often with abundant bivalves, brachiopods and corals, (Table 3.3). The limestones were particularly interesting, especially the Ob Lusa and Ob Breakish coral beds (Hallam, 1959). In thin section and weathering characteristics (Plates 3.18 and 3.19) they resemble the Rhum limestones (cf Plate 3.13 and 3.19).

Both Rhum and Skye limestones show numerous disarticulated bivalves, crinoid ossicles, and small corals (cf Plates 3.18 and 3.18a), the main difference between the two being that the micritic mud which forms the groundmass of the Broadford limestone is re-crystallised to calcite in the Rhum rocks. It is of particular interest to note that algal boring is well developed in rocks from both localities (see Section 3.d and Plates 3.15 and 15a).

The Rhum and Skye sandstones are also similar to each other, as shown by a comparison of thin sections NJ-84 25-4 (from Rhum) and NJ-84 35-14 (from Broadford on Skye). Both sections show rounded to sub-rounded quartz grains in a fine grained matrix. The grain to grain contacts are very low with a supporting cement. In the Broadford rock the cement is calcite (micrite) whereas in the Rhum specimen the cement has been re-crystallised to a finely disseminated form of calc-silicate (wollastonite).

At Abhainn Ashik, (NG 688 240), just to the south of Broadford, the stratigraphic section shown in Table 3.4 was measured. The alternation of lithologies - limestone, sandy-limestone and shale (cf.Tables 3.1 and 3.4) is almost identical to that preserved in the inclined fault-bounded wedge on Rhum.

The Rhum rocks therefore are considered to represent the only local remains of a once extensive Lower Liassic strata which would have covered much of the Hebridean area, including probaly the whole of Rhum. Lying as they do to the west of the Camasunary - Skerryvore fault, the Rhum Jurassic is appreciably older than that preserved to the east of the fault on Eigg. At the start of the Tertiary the relationship of the Great Estuarine group rocks of Eigg to the Broadford rocks of Rhum would have been similar to that now seen at Strat haird on Skye, shown on Figure 3.3 (taken from Peach et al (1910) figure 3, revised by Hallam (1983).

FIGURE 3.1

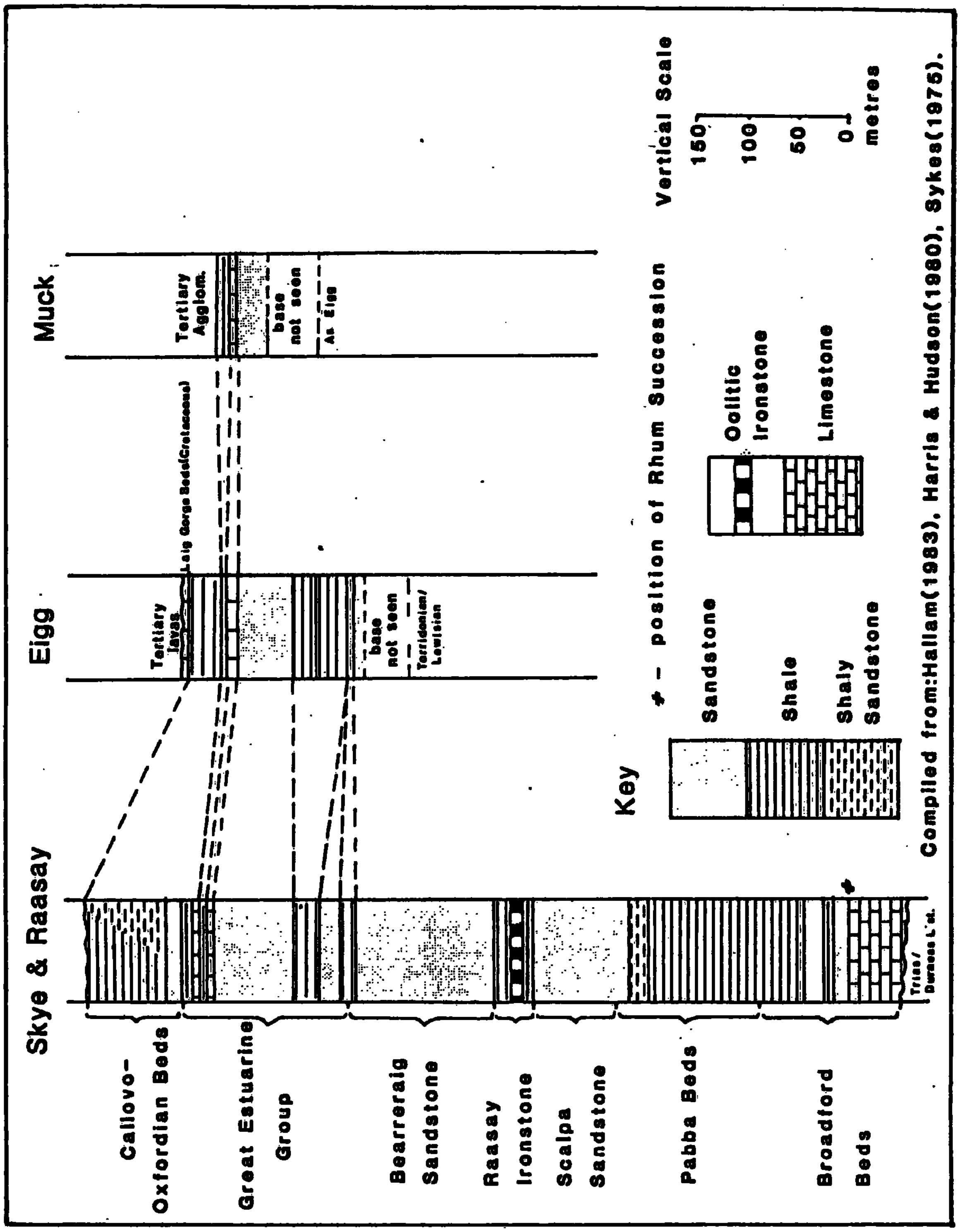

Compiled from:Hallam(1983), Harris & Hudson(1980), Sykes(1975).

FIGURE 3.2

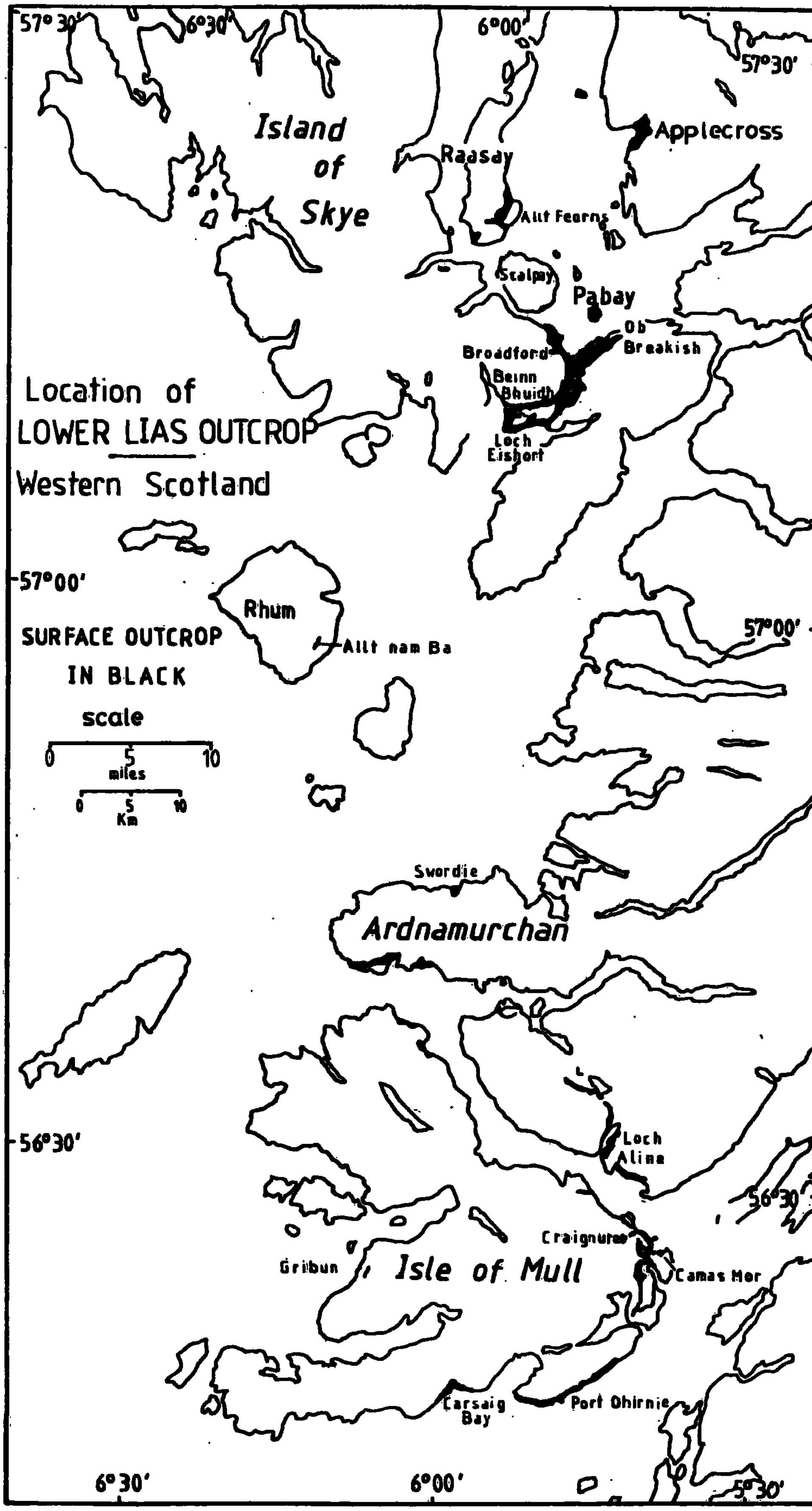

After M J Oates (1978)

FIGURE 3.3

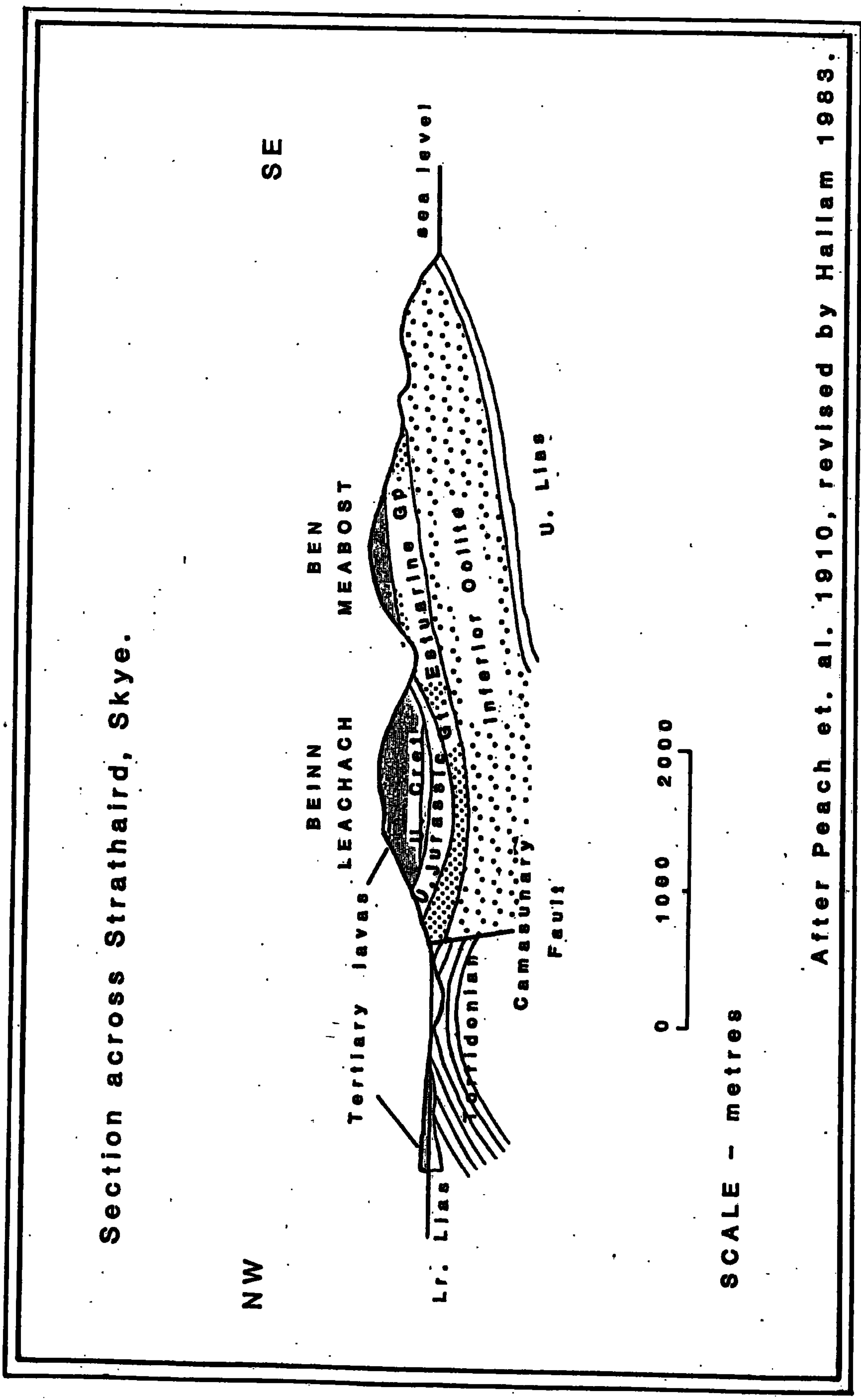
Section across Strathaird, Skye.
NW
SE
BEINN LEACHACH
BEN MEABOST
sea level
Tertiary lavas
U. Cret.
U. Jurassic Gt. Estuarine Gp.
Inferior Oolite
U. Lias
Lr. Lias
Torridonian
Camasunary Fault
0
1000
2000
SCALE - metres
After Peach et. al. 1910, revised by Hallam 1983.

Plate 3.I General view of the Allt nam Ba Mesozoic sediment locality and the Main Ring Fault (looking south from NM 405 943). Note lush 'fingers ' of grass (↗), such improved grazing is characteristic of this predominantly limestone area.

Plate 3.2 Large sinkhole just south of the Allt nam Ba waterfall. Sinkholes are a common feature of this area.

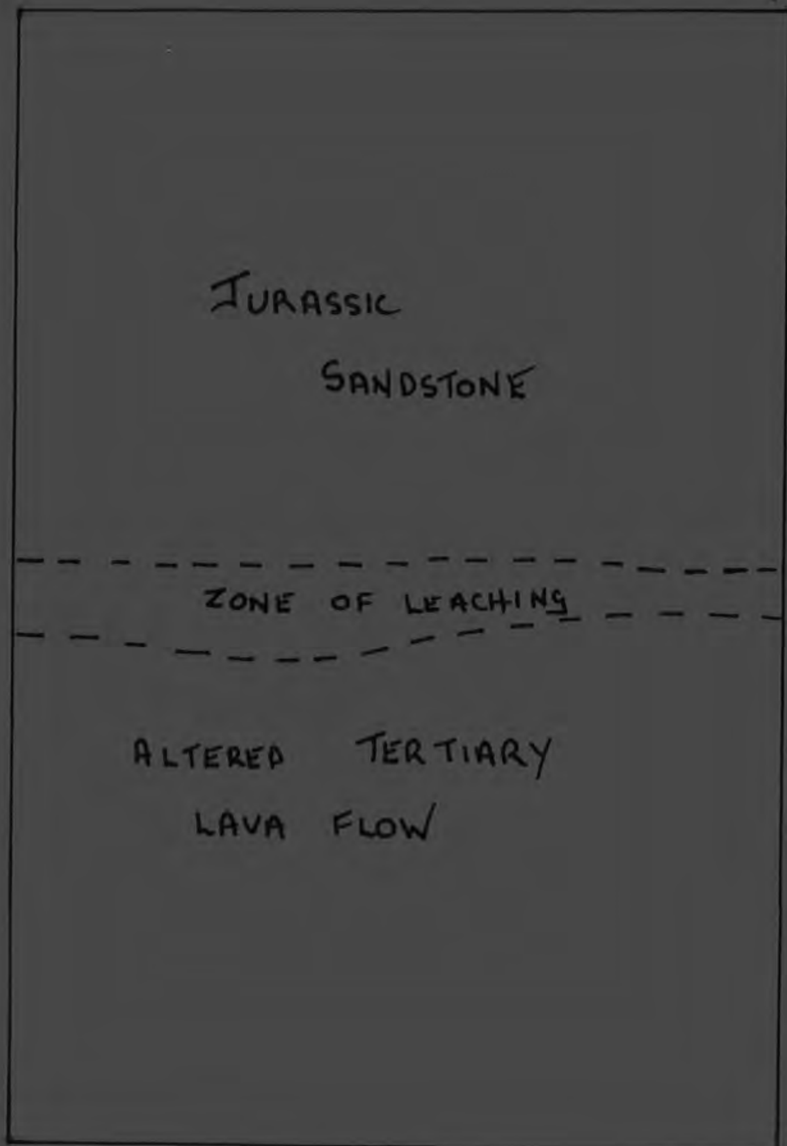
JURASSIC
SANDSTONE
ZONE OF LEACHING
ALTERED TERTIARY
LAVA FLOW

Plate 3.5 Contact of sheared basalt with Mesozoic sandstone, (see text - Section 3.b.i). Note leaching of the sandstone in direct contact with the basalt. This contact appears to be unfaulted and is thought to represent a remnant of the original Tertiary landscape unconformity, the basalt lava having flown out over the pre-Tertiary landscape.

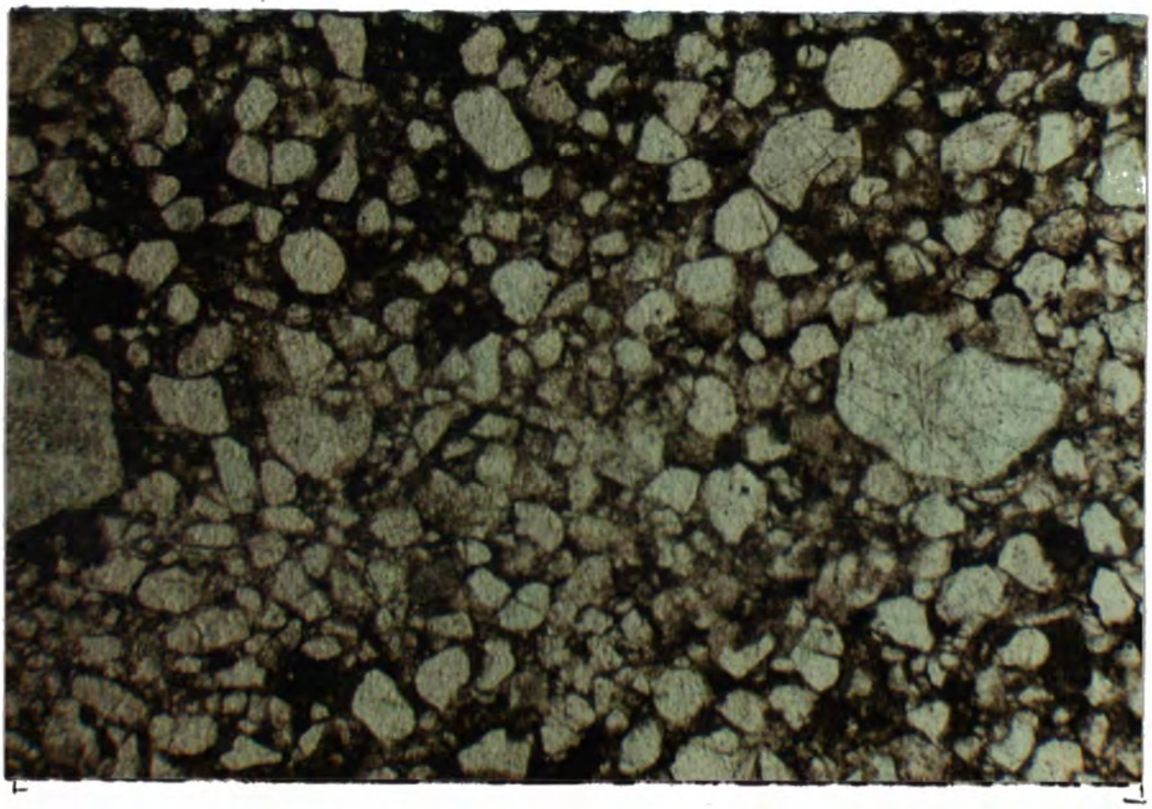

Plate 3.6 Mesozoic sandstone (NJ 84, 25-4) PPL. Field of view 3.5mm. Note sub-rounded quartz grains with bi-modal size distribution, (see text - Section 3.b.i).

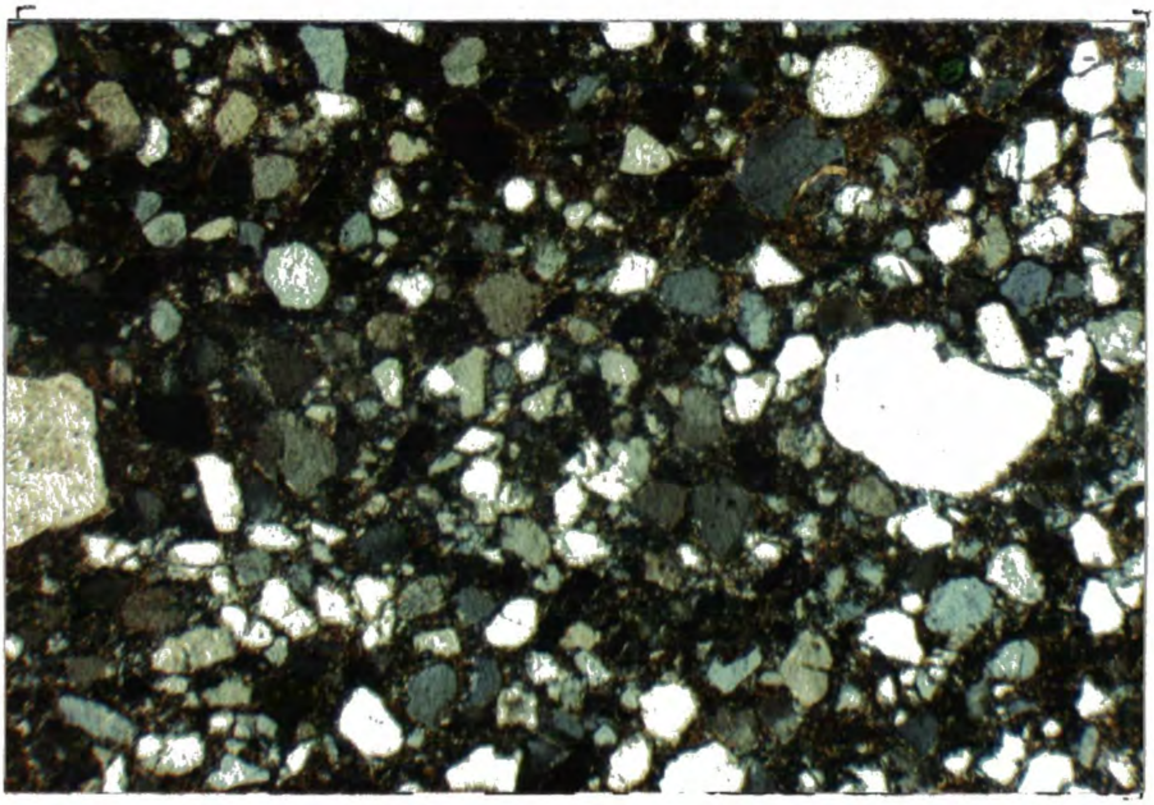

Plate 3.6a Mesozoic sandstone X-polars. note rather altered nature of the quartz and presence of calc-silicates.

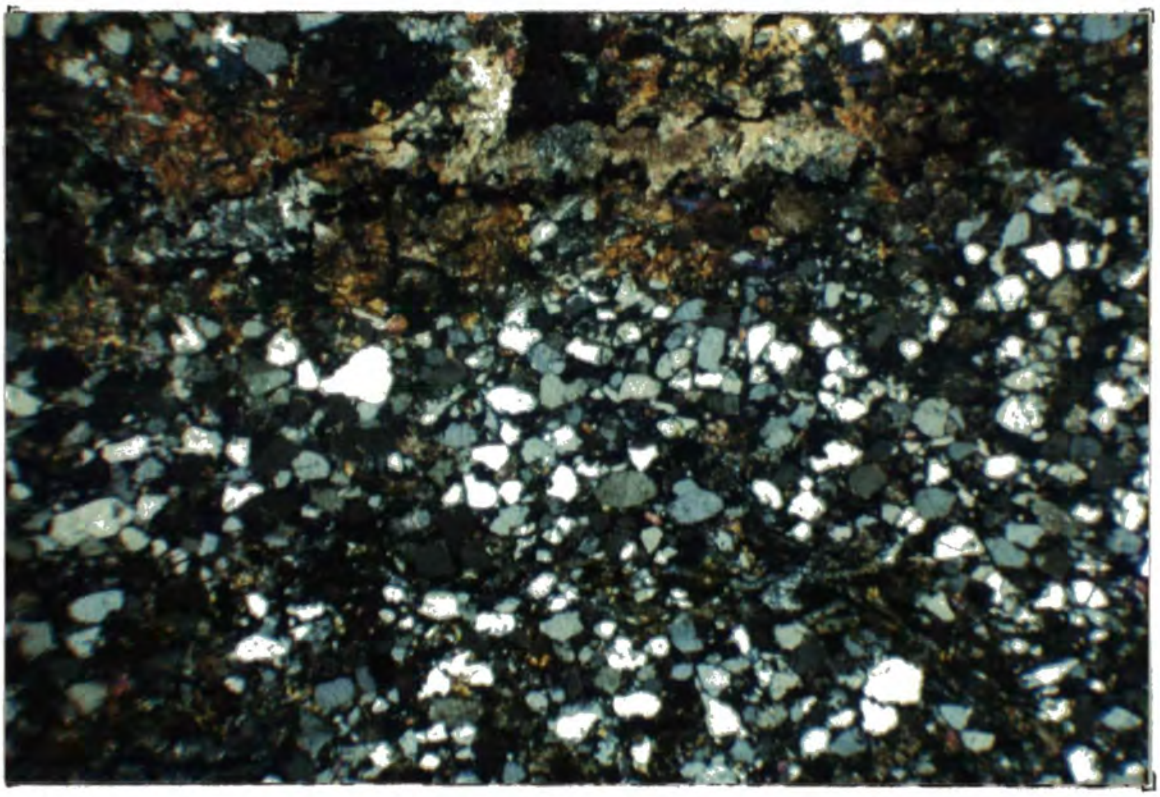

Plate 3.7 Mesozoic sandstone (NJ 84, I9-IO).X-polars. Field of view 9mm. Shows re-crystallisation of original micritic cement predominantly to the calc-silicate mineral wollastonite, some calcite and a little pyroxene (diopside) is also shown.

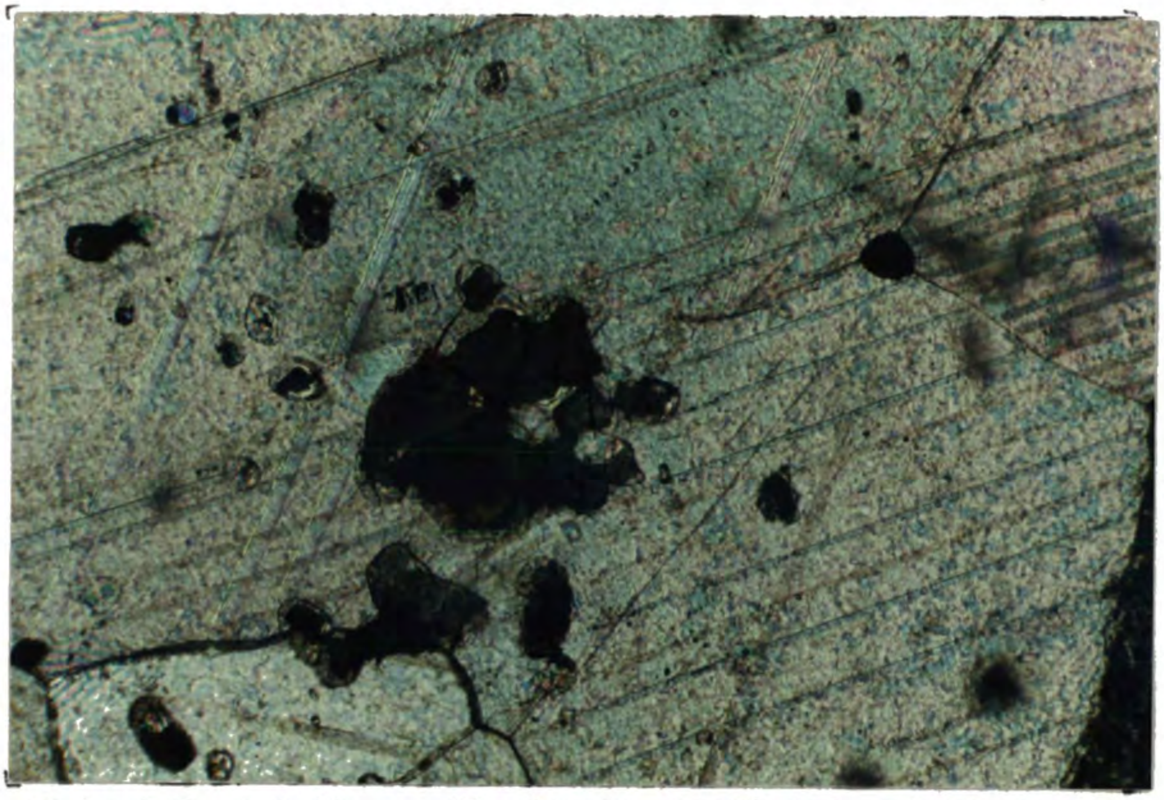

Plate 3.8 Calcite marble (NJ 83, 3-I5).PPl. Field of view I.5mm. Shows development of small (c.O.2mm) Idocrase crystals. See text - Section 3.b.ii.

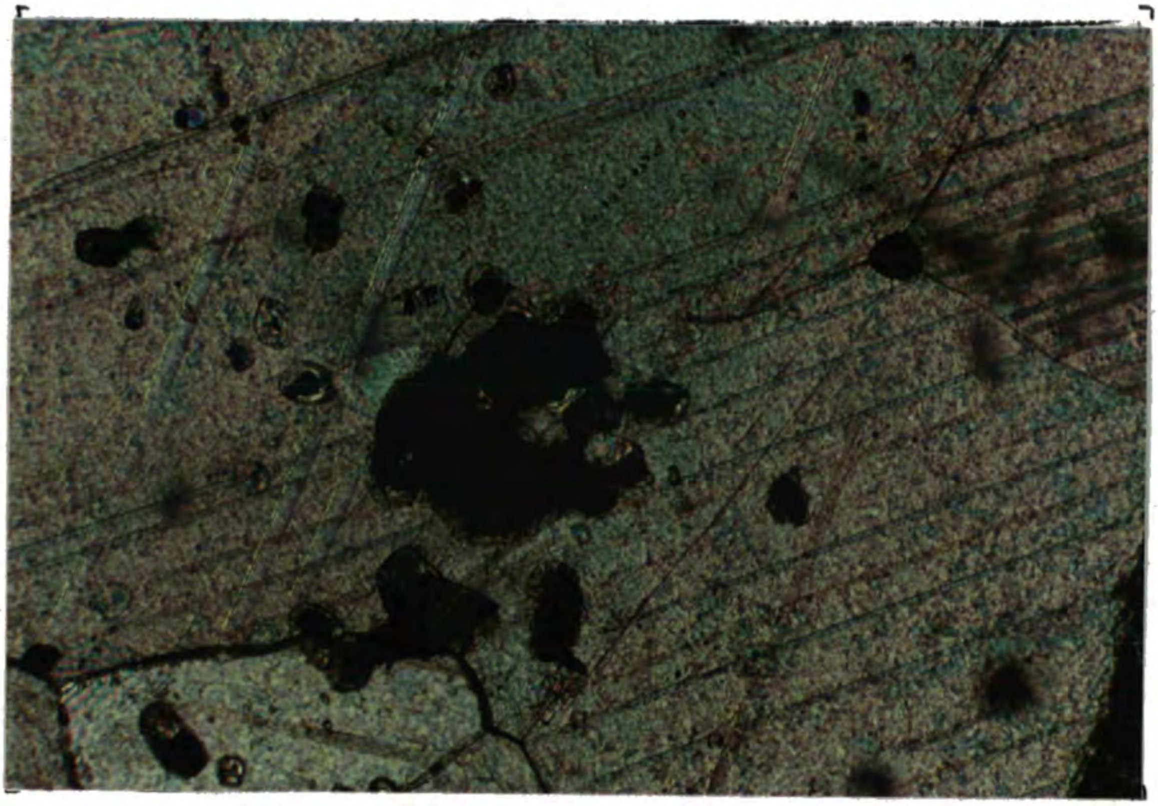

Plate 3.8a As above but X-polars. Note the very low birefringence (O.OO4) of the Idocrase.

Plate 3.IO 'Geikie's' Limestone locality in Dibidil, (NM 399 935). Note lush grass. See Section 3.b.ii.

Plate 3.IOa Limestone from above locality shows re-crystalisation to pure calcite marble.

Plate 3.II Mesozoic Shale with belemnite guard (Passaloteuthis sp.).

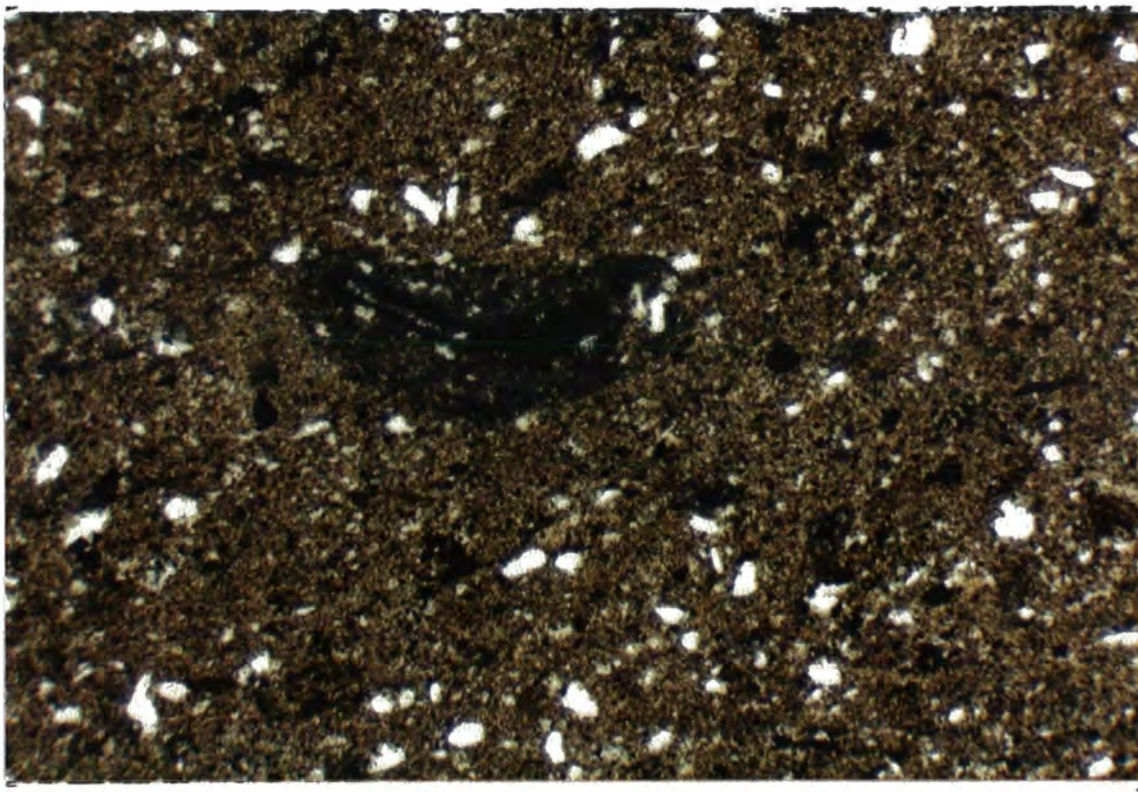

Plate 3.I2 Thin section of Mesozoic shale (NJ 84, I9-8). PPL. Field of view 3.5mm. Note angular quartz grains in finely disseminated 'shaley' matrix. The large dark area to the right of centre is pyrite nucleating around a small shell fragment (see text - Section 3.b.iii)

Plate 3.13 Impure sandy-limestone from south of Allt nam Bà (NM 4052 9405) showing cast and mould preserved bivalves - including Chlamys sp. and the remains of a belemnite phragmacone (Passaloteuthis sp.).

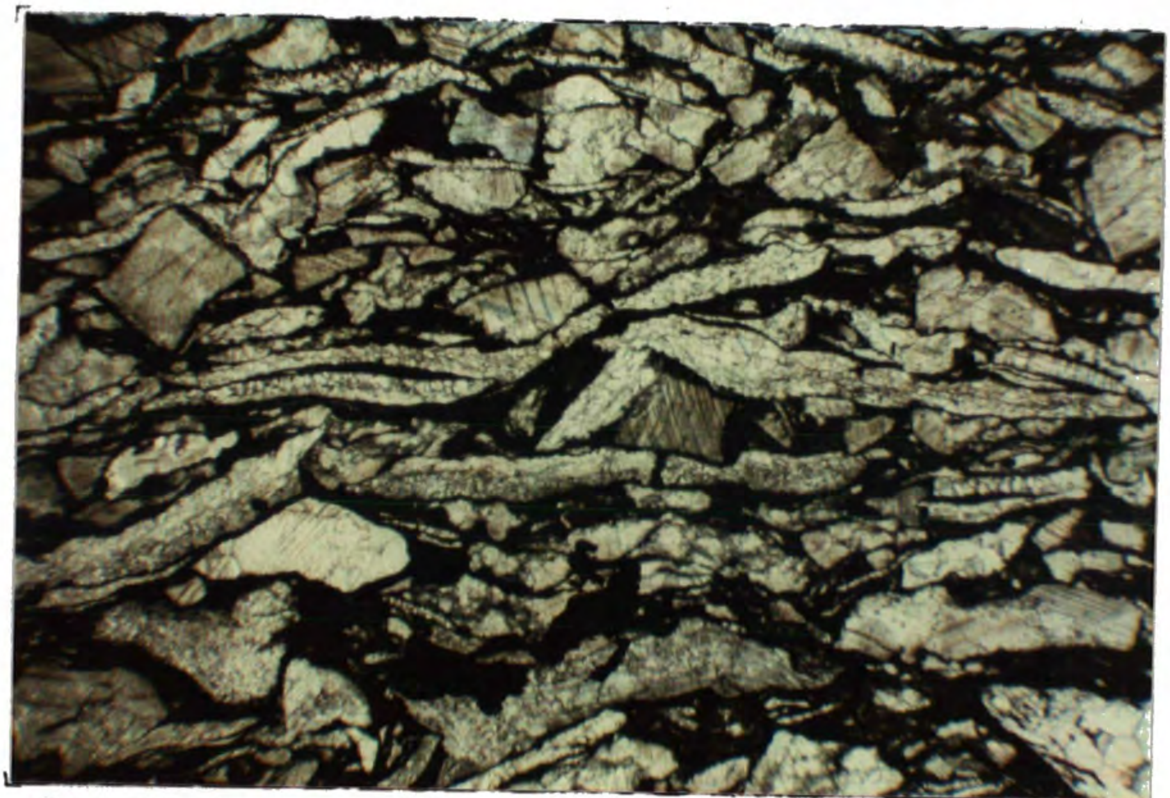

Plate 3.I4a Dis-articulated bivalve remains in Allt nam Ba limestone, (NJ 84, 5-22a). PPL. Field of view 9mm.

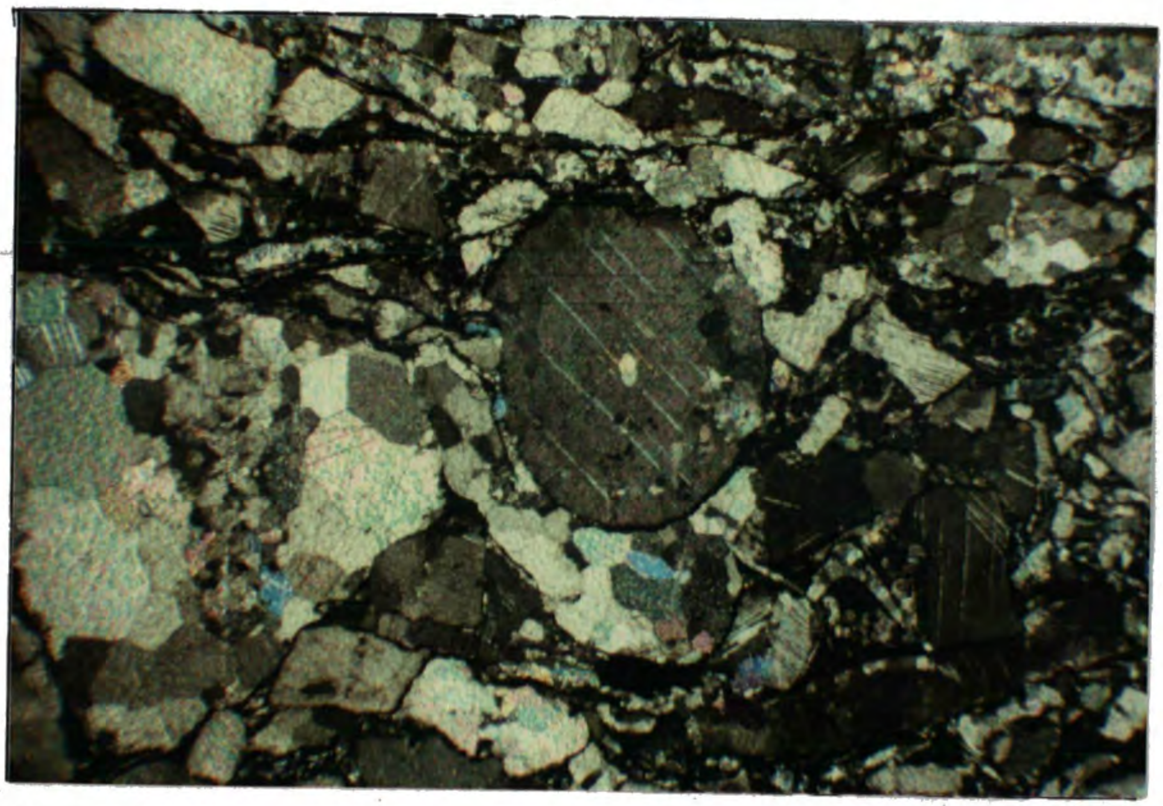

Plate 3.I4b Crinoid ossicles in Allt nam Bà limestone (NJ 84, 5-22). X-polars. Field of view 9mm.

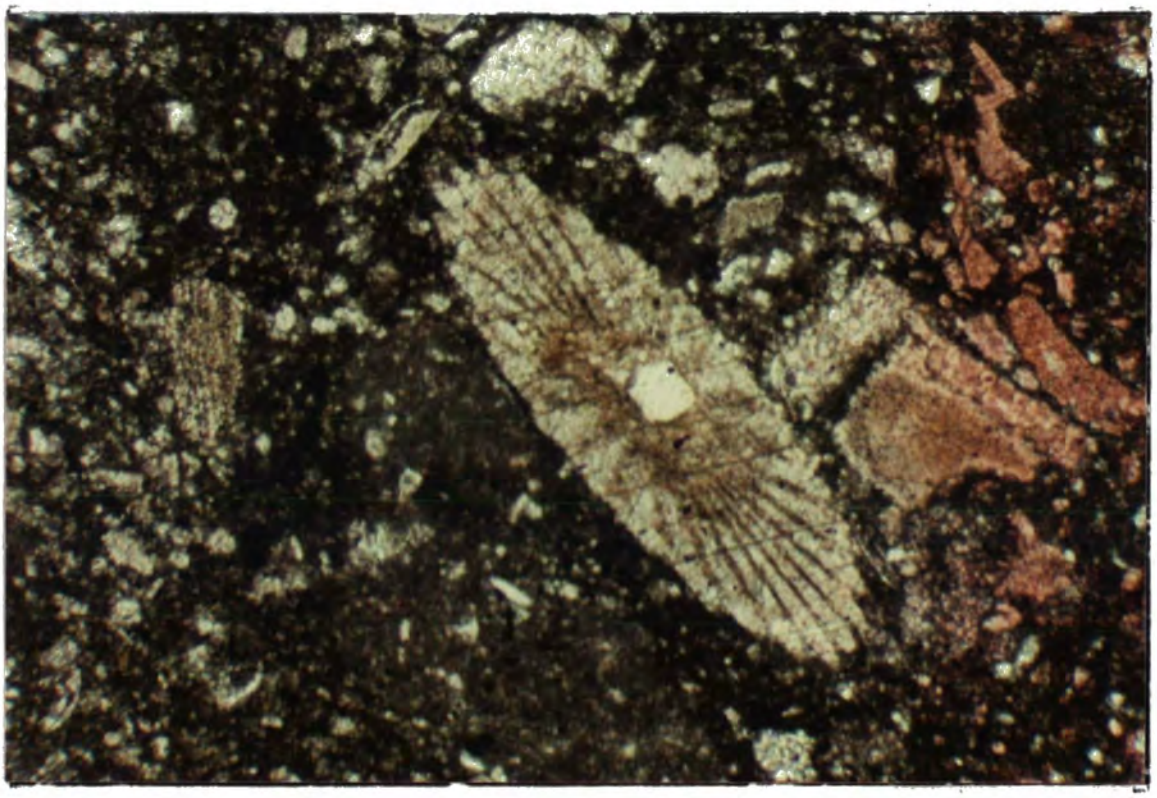

Plate 3.I4c Scleractinian coral (Thecosmilia sp.?) in Allt nam Ba limestone. NJ 84, 3-2I. X-polars Field of view 3.5mm. Note slight elongation due to shearing.

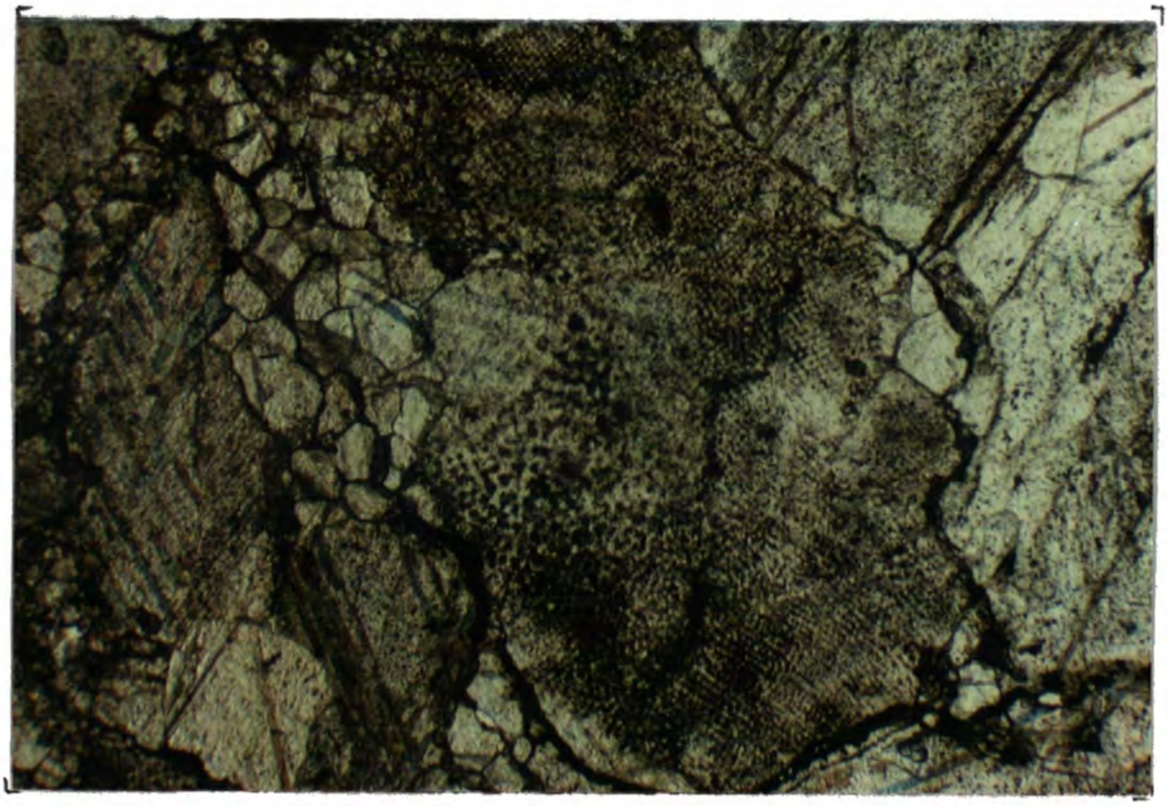

Plate 3.I4d Echinoderm plate from Allt nam Ba limestone, (NJ 85, I-4). PPL. Field of view 3.5mm.

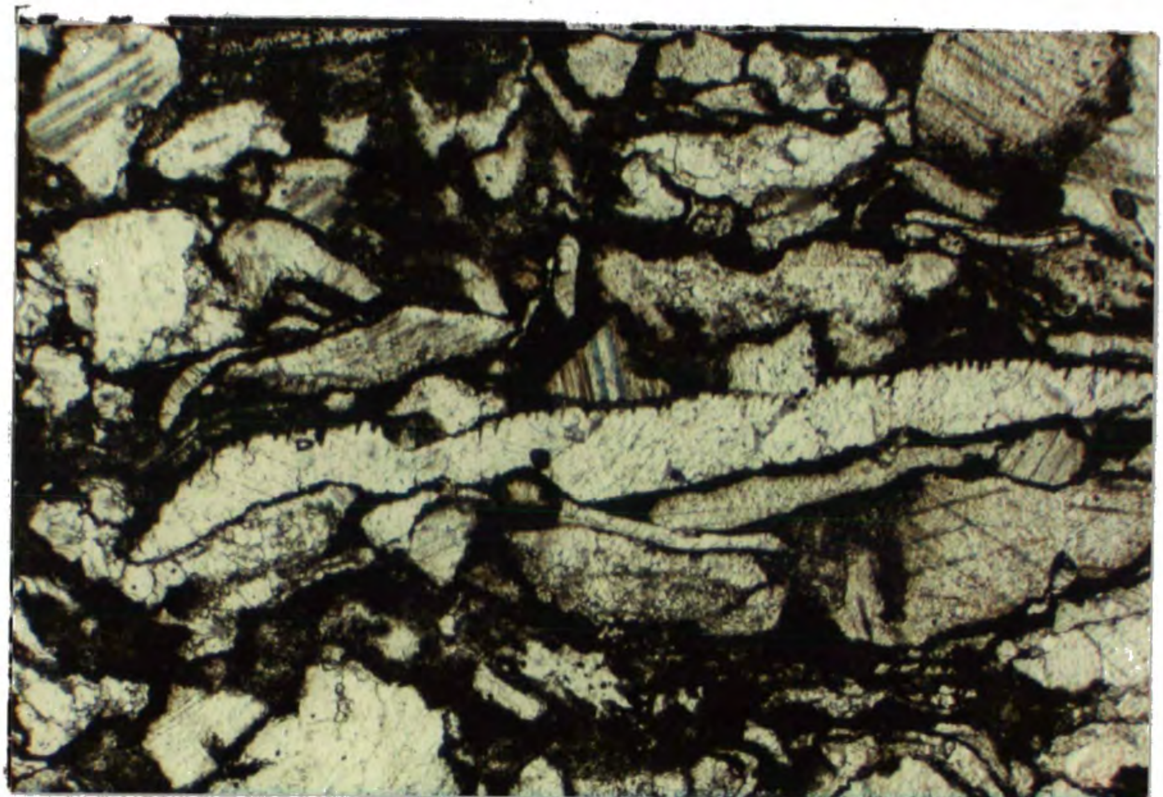

Plate 3.I5 Algal boring into bivalve debris (NJ 84, 5-221). Allt nam Ba Limestone, Rhum. PPL. Field of view 3.5mm

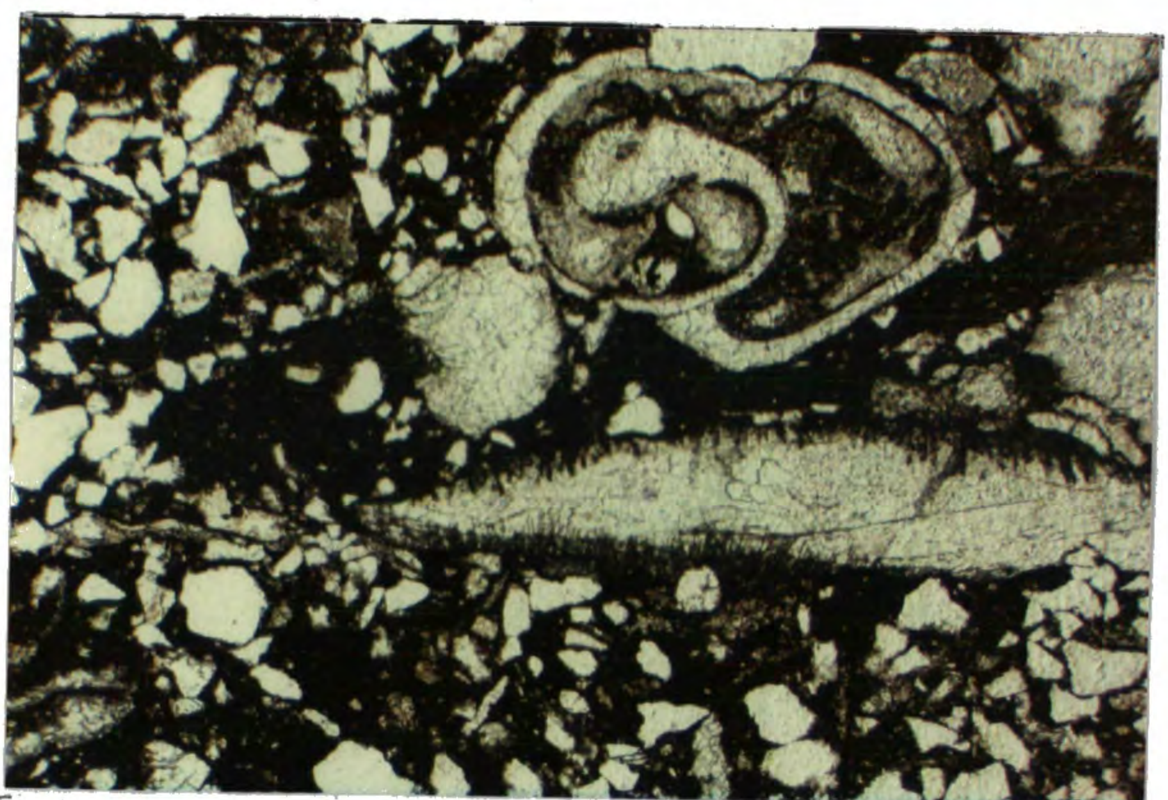

Plate 3.I5a Algal boring in Broadford bed limestone, Skye (NJ 84, 35-I2a). PPL. field of view 3.5mm.

Plate 3.I6 Scleractinian coral Montvaltia sp. from Jurassic shale south of Allt nam Ba (NM 405I 94I0).

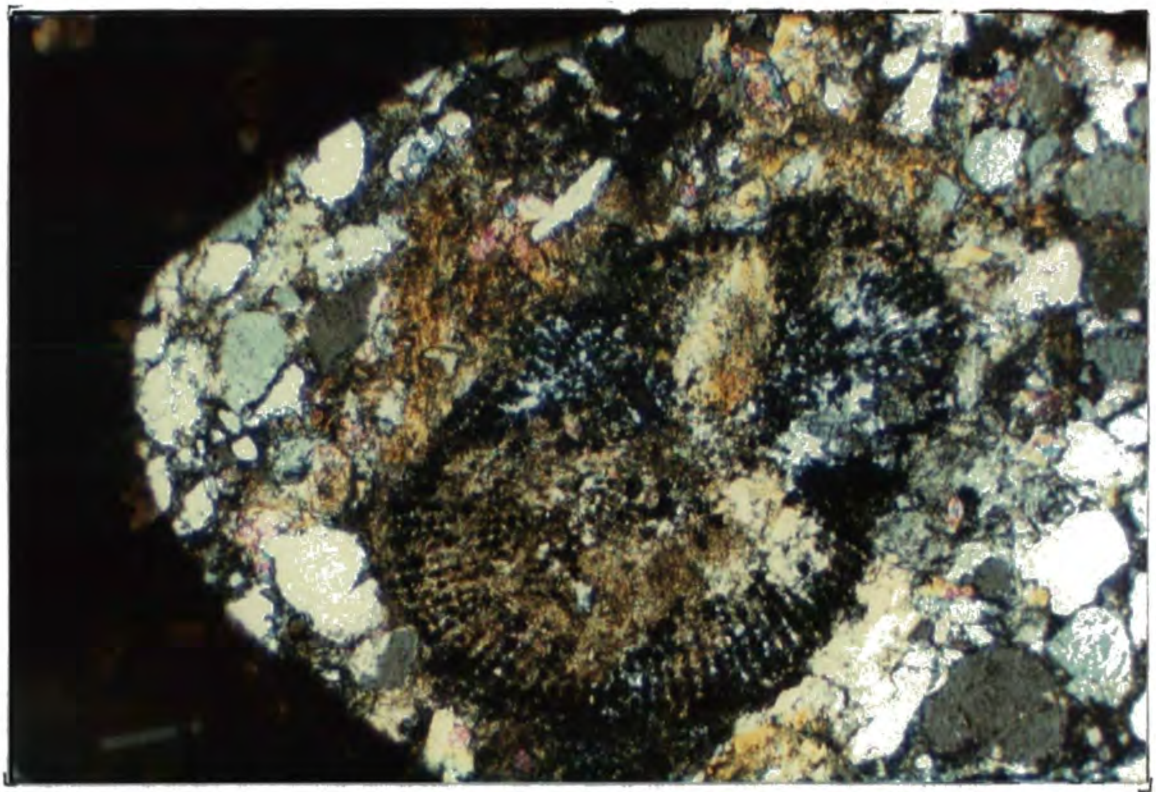

Plate 3.I7 Solitary scleractinian coral (Thecosmilia sp.) in sandstone from the southern most sandstone exposure (see Figure 2). Note also the development of diopside and wollastonite. See text - Section 3.d. X-polars. Field of view 3.5mm.

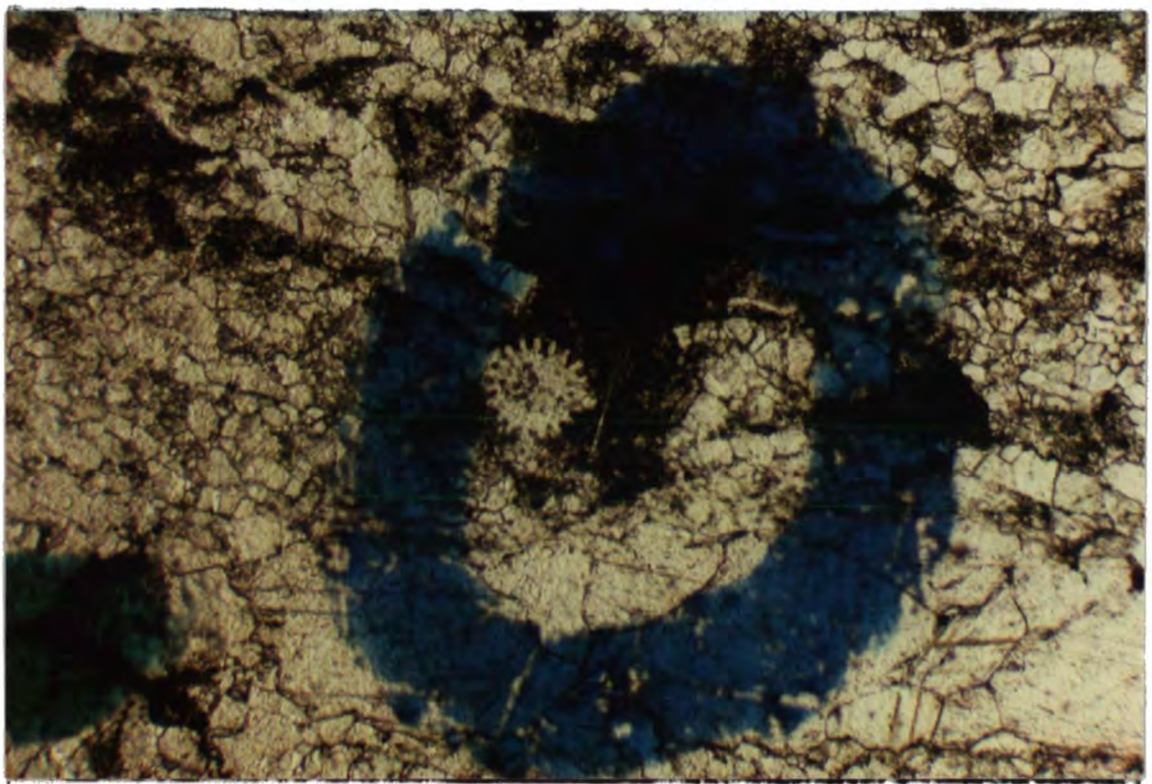

Plate 3.I8 Limestone from Allt nam Ba showing small coralite. PPL. Field of view 3.5mm. (NJ 84, 5-22L).

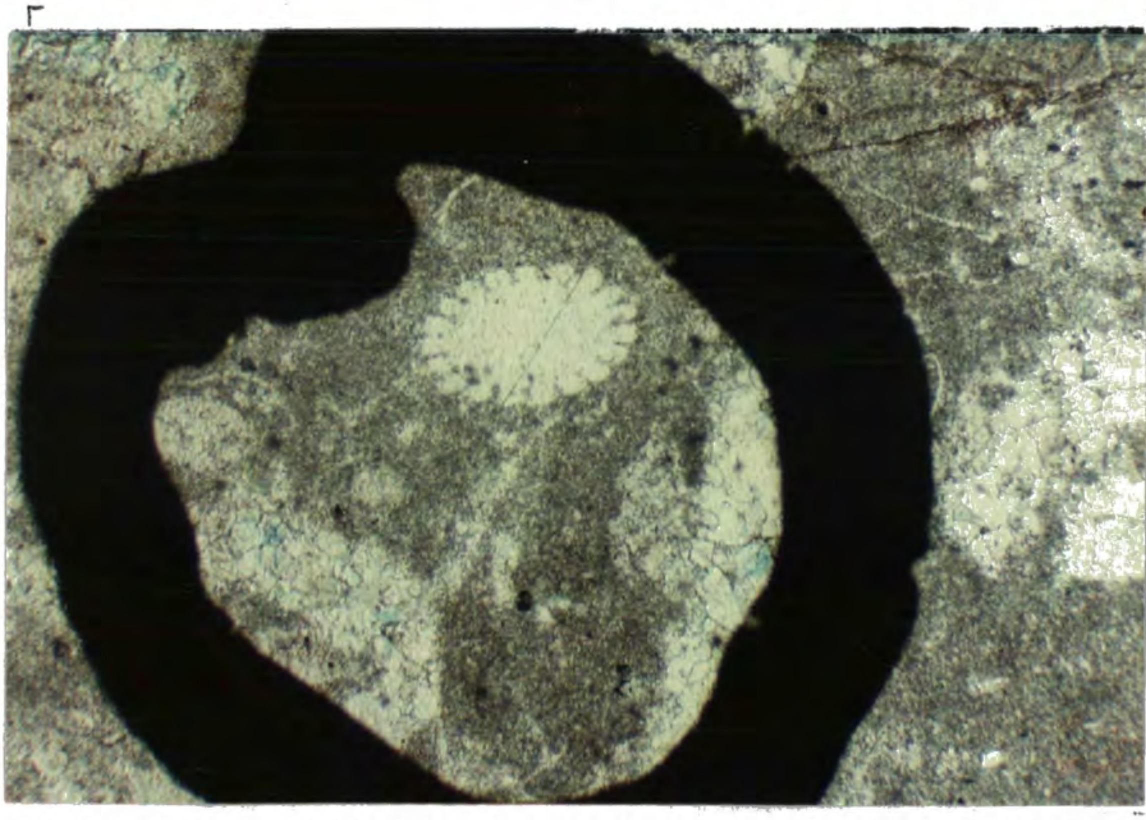

Plate 3.I8a Small coralite in Broadford limestone (Isle of Skye). PPL. Field of view 3.5mm. (NJ 84, 35-I5).

Plate 3.19 Sandy-limestone from the Abhainn Ashik stream section north of Ob Breakish, Skye (NG 688 240). Specimen shows weathering producing cast and mould preservation of disarticulated bivalves. Cf. Plate 3.13.

Table 3.2

Amonite Zone	Bucklandi	Bucklandi / Semicostatum	Semicostatum	Semicostatum	Turneri	Turneri	Unknown	Unknown	Unknown	
Key # - abundant / - occurs ? - possible fragment	Faunal assemblage									
Lithology	Thecosmilia sp.	Chlamys sp.	Crinoid ossicles	Echinoderm fragments	Montlivaltia sp.	Belemnites (Passaloteuthis ?)	Serpulid worm tubes	Bivalves	Coralites	
Sandstone(quartzite)	/									
Limestone(marble)			/	/		?		#	/	
Sandy–limestone		#				/	/	/		
Shale(hornfels)					/	/		/		

Table 3.3

Broadford Beds Faunal Assemblage

Key
x – common
o – occurs

Fauna	Ammonite Zone				
	Planorbis/Angulata	Bucklandi	Semicostatum	Turneri	Obtusum
Nautilus striatus J. Sowerby			O		
Nannobelus brevis (Blainville)			O	O	
Cardinia cf concinna (J. Sowerby)	O				
C. listeri (J. Sowerby)	O		X		
Chlamys ? calva (Goldfuss)			O		
C. textoria (Schlotheim)		O	X	O	O
Gryphea arcuata Lamarck		O	X	O	O
Hippopodium ponderosum J. Sowerby			O		
Plagiostoma giganteum (J. Sowerby)	O	O	X		
Anticquilima succincta Schlotheim	O				
Liostrea irregularis (Munster)	X	?			
L. sp			O		
Mactromya unionides (Goldfuss)			O		
Modiolus sp	O			O	
Nuculana sp	O		O		
Oxytoma inequivalva (J. Sowerby)			X		
Parallelodon cf hettangiensis (Terquem)	O				
Pholladomya sp			O	O	O
Pinna harmanni Zieten	O		X		O
Pleuromya galathea Agassiz			X	O	
P. sp	O				
Pseudolimea pectinoides (J. Sowerby)	O		O		
Terquemia arietis (Quenstedt)			O		
Bourguetia sp	O				
Pleurotomaria anglica (J. Sowerby)		O			
Procerithium sp	O				
Ptychomphalus expansus (J. Sowerby)		O			
Calcirhynchia calcaris S. Buckman		O			
Piarorhynchia juvensis (Quenstedt)		X			
Spiriferina pinguis (Zieten)		O			
S. walcotti (J. Sowerby)		X			
Zeilleria perforata (Piette)		O	O		
Isocrinus sp		O	O		
Echinoid spines			X		
Thecosmilia martini (de Fromentel)		O			

After Hallam (1959)

TABLE 3.4

Stream section at Abhainn Ashik, Skye (NG 688 240)

Lithology	Thickness (metres)	Comments
Micritic limestone	0.5	-
Sandstone	2.25	X-bedded
Sandy-limestone	1.00	-
Sandy-shale	0.25	-
Sill - dolerite	base not seen	-
Sandstone	1.00	bivalves and escape burrows
Sandy-shale	0.25	-
Sandstone	1.2	calcareous
Sandy-limestone	0.9	-
Micritic limestone	0.05	-
Sandy-limestone	0.95	-
Micritic limestone	0.95	bivalves, plus weathers similar to Rhum L'st.
Shale	0.8	liostrea
sandstone	1.00	ferruginous partings
sandy-limestone	1.66	sandy partings
micritic limestone	1.58	sandstone partings
Sill - dolerite	c. 0.75m	-
sandstone	base not seen	cast-and-mould bivalves
sandstone	2.0	fissile
Base of section.	----------	
Minimum thickness	c. 18.m	

Chapter 4

The Sheared Tertiary amygdaloidal basaltic Lavas

4.a Introduction

4.b Geological setting

4.c Mineralogy and geochemistry

4.c.i Mineralogy

4.c.ii Geochemistry

4.d Comparison with adjacent areas

Figures Plates and Tables

4.a Introduction

Emeleus, (1980) mapped a sliver of what he termed 'crushed basaltic rocks', on the south-east side of Beinn nan Stac. The present more detailed study of south-east Rhum has revealed that these basaltic rocks have a somewhat greater areal extent, and that their associations with other lithologies, particularly the Mesozoic sediments (Section 3.b.i), are rather interesting.

The sheared basalt is of lenticulate form with a length of c.1km and a maximum width of 150m (Figure 2). The whole mass is fault bounded, except where it is in contact with Mesozoic rocks. The eastern margin is formed by the ORF to the north and the CRF further south, where the ORF is seen to bifurcate. The IRF forms the westernmost boundary, until Mesozoic sediments are encountered when the boundary becomes an unconformity (section 3.b.i and Figure 2).

One of the aims of this project was to compare and, if possible, to correlate the sheared basalts with other Hebridean basaltic lavas; essentially those of Rhum, Skye, Eigg and Canna. Comparison was carried out using both a petrographic and geochemical approach, with x-ray fluorescence analysis for major and trace elements proving most useful.

4.b Geological setting

The ORF, when in contact with the basalt, is well defined; a steep slickensided fault surface (inclined 65° west) indicative of downward movement to the west. To the east of the ORF are Torridonian sediments, these are contorted, indurated, and steeply dipping westward at angles up to 60°. Also along this contact are localised bodies of 'explosion breccia' (Fig. 2 and Section 2.f), composed of highly comminuted Torridonian and basaltic rock fragments.

Direct contact between the sheared basalt and the CRF is always obscured by the presence of intervening felsite (Section 2.f).

The contact of basalt and felsite, and of the felsite and Lewisian gneiss is exposed in vertical gully walls of a deeply incised, later cross-cutting dyke (NM. 4030 9357). It appears that the felsite magma directly utilized the fault plane, so that the dip of the igneous contacts reflect the original dip of the fault. This seems a reasonable assumption to make as the igneous contacts are very sharp, and the felsite itself shows no sign of any shearing or structures to suggest that it too was caught up in movement on the CRF. The dip of the CRF therefore is 65° west (Plate 2.15).

The western margin of the basalt shows two differing contact relations; to the south of (NM.4032 9374) the basalt is in contact with overthrust Torridonian sediments (along the shallow - 45° west - IRF), whilst to the north of this point the basalts are in an unfaulted landscape unconformable junction with the Mesozoic sediments (see Section 3.b.i). Where the basalt is in close proximity to the IRF the fault plane is easily discernable, with rocks on both sides of the fault showing mylonitisation. The Torridonian to the west of the fault shows very high degrees of deformation and induration, rather greater than alteration of other Torridonian sediments caught up in the MRF. It is possible therefore (but see Chapter 6) that the folding and induration was enhanced at a date coincident with or later than movement on the IRF, due to emplacement of the underlying ultrabasic rocks (See Smith (1985) fig 3, and Chapter 6).

4.c - Mineralogy and Geochemistry

The lavas in south-east Rhum were examined both mineralogically and geochemically, in the hope that correlation could then be made with other basalts in the Hebridean province. Unfortunately extensive secondary alteration masks much of the original mineralogy, but analyses for both major and trace elements has proven more forthcoming.

4.c.i - Mineralogy

In hand specimen the lavas are melanocratic, fine grained rocks, aphyric to slightly porphyritic (feldspar-phryric) and containing characteristic small (c.5-10mm) amygdales infilled with green epidote. Small scale fractures and leucocratic veins are generaly also present. The weathered surface is reddish in colour due to a high proportion of iron oxides (up to 10% modally).

Localised deformation, both mylonitization and slickensiding occurs, especially close to the main component fractures of the MRF, because of the fairly small areal extent of the amygdaloidal basalt shearing is present throughout this body of rock (Plate 4.1).

A thin section (Plate 4.2) shows the rock to be composed of a groundmass of plagioclase laths (0.25 - 0.5mm) wholly or partially enclosed within pinkish coloured, slightly titaniferous, augite. Plagioclase compositions of the ophitic/sub-ophitic laths are An 50-55 determined optically. Phenocrysts are generally small (c. 0.5 - 0.75mm), rather rounded, and more calcic in composition - typically An 70 (labradorite/bytownite). Rounding is more related to extensive alteration around the periphery of the phenocryst than say due to resorbtion. The clinopyroxene (augite) shows alteration, often extensive, to green, finely disseminated chlorite, secondary opaque minerals and epidote. Plagioclase, in both groundmass and phenocrysts, is also altered, typically to finely disseminated sericite plus epidote. This type of alteration, termed saussuritization, is typical of the low grade hydrothermal metamorphism of basic igneous rocks. The other major constituent of the lavas is an opaque oxide phase. Modally the oxides can reach 10%, the oxides being magnetite and ilmenite +- haematite. The opaques also show some degree of alteration, with minor amounts of leucoxene, secondary haematite, and hornblende developing at the grain margins.

Infilled vesicles (amygdales) are very common at some localities. They vary in size from 2 - 10mm in diameter, and are composed of epidote, quartz, calcite, garnet and some zeolite minerals (natrolite & thompsonite - determined using x-ray diffraction), (Plate 4.3). Certain sections show amygdales which are elongated due to shearing, whilst others retain remnant concentric infilling structures, (Plate 4.3).

Shearing is common and can be observed on two scales;

first, mylonitization produces a shear fabric shown clearly in thin section NJ 84 20-9; Plate 4.4. This sample comes from the northern margin of the lava wedge (NM 4061 9407) where this mylonitic basalt serves to delimit the line of the ORF. Note the way in which the feldspar phenocrysts are shattered and typically show strained extinction. The second scale of shearing is observed in section NJ 83 6-9 (Plate 4.5). Here a plagioclase phenocryst is broken into two along a slightly mineralised shear surface, the two halves of the crystal being displaced by 2.5mm.

Because of the rather altered nature of these rocks comparisons with other basaltic lavas cannot be made on mineralogical and petrographic grounds alone. Consequently XRF techniques, allied to mineralogy and field observations have been used.

4.c.ii - Geochemistry.

The lavas of south-east Rhum were analysed using a Phillips PW 1400 X-ray fluorescence (XRF) spectrometer. Major element (Si,Al,Fe,Mg,Ca,Na,K,Ti,Mn,P) determinations were made on fused glass beads whilst trace element analysis used whole rock powder pellets. A detailed explanation of the techniques used for the production of glass beads, powder pellets, and data reduction programs are given in Appendix 1.

Tables 4.1 and 4.2 show typical major and trace element analyses of the south-east Rhum lavas. C.I.P.W norm calculations are also shown, and were calculated using the computer program 'normcal' by R.C.O. Gill, an outline of this program is given in Appendix 2.

During the processing of the geochemical data it was noted that the lavas could be grouped into two distinct categories on the basis of their major and trace element geochemistry. The first group (Group 1, Table 4.1) is characterised by a typical high temperature, less evolved geochemical signature. The group 1 rocks show high Mg (7%) and Ca (12.5%) coupled with low values for the more residual elements Fe and Na - 9% and 2.4% respectively. The fairly unevolved nature of the rocks is also reflected in trace element geochemistry, the incompatible elements show lower vaues than the group 2 lavas; Zr(77),Sr(375),Ba(144), Zn(48),V(236), the figures in parentheses are mean values expressed in parts per million (ppm). The value for Cr is higher than that for the group 2 lavas at 308ppm, this is due to it partitioning into pyroxene. The primitive nature of these rocks is shown by the low value for the Thornton - Tuttle differentiation index - a mean of 23.1 as compared with 33 for the group 2 lavas.

The group 2 lavas (Table 4.2) show a more evolved chemistry. They are much higher in Fe(16%) and Na(3.6%) and also Ti(2.6%) (possibly due to its partitioning into augite). Incompatible trace elements show enrichment when compared to the group 1 lavas; Zr(184),Sr(537),Ba(204),Zn(84),V(320). Cr conversely is depleted, with a value of only 18ppm. Figure 5 shows that both groups of south-east Rhum lavas plot predominantly in the alkali-olivine basalt field on a %anorthite v differentiation index diagram. Unfortunately alteration has produced results which occasionally plot outside this field (due to hydrous alteration) thus reducing the XRF totals to rather less than 100%. Plotted on this same diagram (Figure 4.1) are data for Eigg lavas, north-west Rhum lavas, and lava clasts from conglomerates beneath the north-west Rhum lavas. From Figure 4.1 it should be noted that it is the Eigg lavas which are the nearest geochemical eqivalent to those lavas of south-east Rhum, (see section 4.d).

4.d Comparison of south-east Rhum lavas with adjacent areas

From geochemical data given in Tables 4.1 and 4.2, the sheared lavas in south-east Rhum are shown split into two groups, both having a characteristic geochemical 'fingerprint'. Using this 'fingerprint' a correlation was attempted in order to find out if laterally equivalent lavas could be found.

On Rhum the only other lavas are those forming the north-western hills of Bloodstone, Fionchra, and Orval. These lavas have been described in detail (Emeleus 1985) with geochemistry shown in Table 4.3. From Table 4.3 it can be seen that in the main these lavas are far more evolved than those in the south-east. Figure 4.1 highlights the more evolved nature of these rocks, plotting in the fields of mugearite and hawaiite as opposed to the alkali-olivine basalt (AOB) nature of the lavas in the south-east. On the total alkali v silica diagram (Figure 4.2) the north-west Rhum lavas show a wide spread, but still most of these rocks plot in the more evolved Ardnamurchan trend, (Thompson, Esson and Dunham ,1972).

Lying beneath the lavas in the north-west of Rhum are extensive water-lain boulder conglomerates (see Emeleus 1980). These conglomerates are composed primarily of clasts of the local Torridonian sediments, Lewisian gneiss, porphyritic felsite, abundant western granophyre, a few ultrabasic cobbles and quite importantly basaltic rocks. The basaltic rock cobbles are of a far less evolved nature than the overlying lavas, although in bulk composition they do somewhat resemble the least evolved flows of Fionchra (Emeleus 1985). Essentially they are relatively low in Na, Fe and Ti and also in the incompatible trace elements (Ba, Nb, Zr, Sr, Rb), (Table 4.4).

Emeleus (1985) comes to the conclusion that these basaltic cobbles must represent the remains of an earlier lava formation, now totally removed by erosion. Perhaps not totally removed, the fault bounded south-east Rhum lavas could represent the only other remnant of this earlier lava episode. Such a theory can be proven by the use of trace element ratios which should remain essentially constant for any given lava episode. This does seem to be the case for certain of the lava cobbles and the south-east Rhum lavas. Cobble samples SR 244e and 244g with Rb/Sr and Nb/Zr values of around 0.02 and 0.02-0.032 repectively compare well with the mean group 2 Rhum lava values (Rb/Sr of 0.013 - 0.02, and Nb/Zr of 0.032). The full range of Rb/Sr and Nb/Zr ratios are given in Tables 4.5 and 4.6.

Rocks from the Eigg lava plateau plot in the field of AOB (Figure 4.1), as do the south-east Rhum lavas and the basaltic conglomerate cobbles. Therefore a geochemical comparison to the Eigg lavas was also made.

E.A Allwright, in an unpublished M.Sc thesis (1980), worked on the lava plateaus of the Inner Hebrides. On Eigg she discovered that the lavas could be split up into two distinct groups on the basis of geochemistry. Representative samples from both of these Eigg lava groups are shown on Tables 4.7 and 4.8.

The group 1 Eigg lavas (Table 4.7) are fairly primitive - high Ca and Mg, low Na, Ti and K. Incompatible trace element values are low, like the south-east Rhum lavas, and Cr shows enrichment.

The group 2 Eigg lavas (Table 4.8) are more evolved, having higher Fe, Na and Ti values but with low Mg and Ca. Incompatible trace elements are also enriched.

What is even more remarkable than the simple fact that the Eigg lavas can also be divided up into two distinct geochemical species, as can the south-east Rhum ones, is that both show almost identical ranges for trace elements within the two groups (Table 4.9).

Not surprisingly then the Rb/Sr and Nb/Zr ratios are often nearly identical - Tables 4.5 and 4.6, a resume of this data is also shown in Table 4.9. An example of the close similarity of the lavas of Rhum and Eigg is;

	Rb/Sr	Nb/Zr
south-east Rhum NJ 84 17-9	0.011	0.033
Eigg lava E7427	0.08	0.032

Figure 4.3 shows a graphical representation of the correlation between two lavas from Rhum and Eigg, the correlation is extremely good for both major and trace elements.

From the data presented above and in the associated text figures and tables, certain conclusions can now be drawn about the lavas in south-east Rhum. It would seem that prior to emplacement of the Rhum ultrabasic complex an extensive plateau lava field, composed essentially of fairly unevolved AOB, extended over what is now Eigg, Muck, Canna and Rhum. During the emplacement of the Rhum volcano the lavas over Rhum were uplifted to high structural levels (probably c.2 km higher than at present - Emeleus, Wadsworth and Smith, 1985) with subsequent extensive erosion. This erosive period on the uplifted lava plateau is possibly shown by the boulder conglomerate containing basaltic clasts now underlying the north-west Rhum lavas, but, see also Section 6.c.i - Phase 8.

Subsequent caldera collapse of the Rhum volcano early in its emplacement (Emeleus, Wadsworth and Smith, 1985) caught up a small sliver of this once extensive lava plateau, now only preserved as a fault bounded sliver on the MRF, (Figure 2, and Smith 1985, figure 3).

Figure 4.1

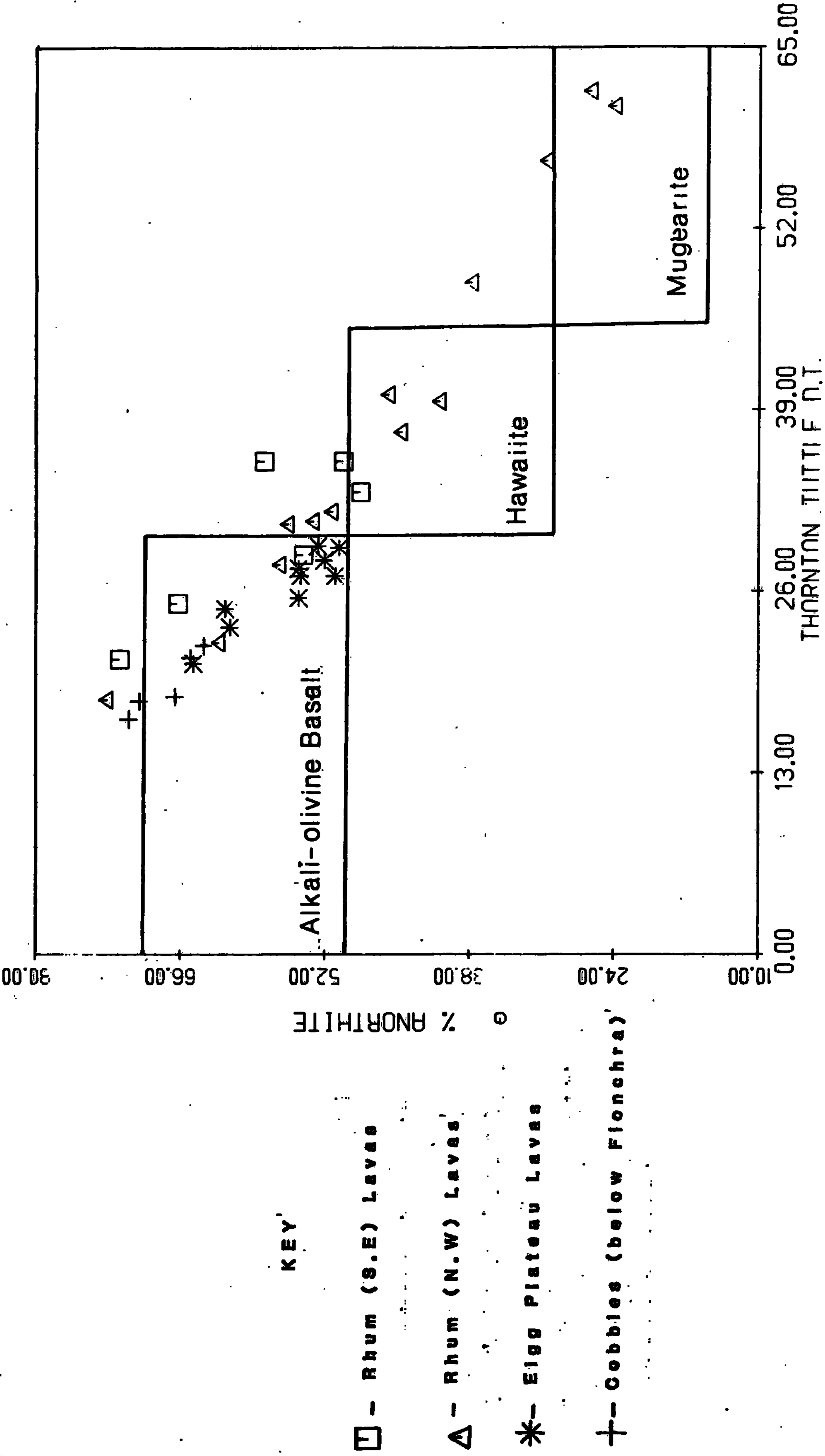
Alkali-olivine Basalt
Hawaiite
Mugearite
% ANORTHITE
THORNTON TUTTLE D.I.
0.00
13.00
26.00
39.00
52.00
65.00
10.00
24.00
38.00
52.00
66.00
80.00
KEY
Rhum (S.E) Lavas
Rhum (N.W) Lavas
Eigg Plateau Lavas
Cobbles (below Fionchra)

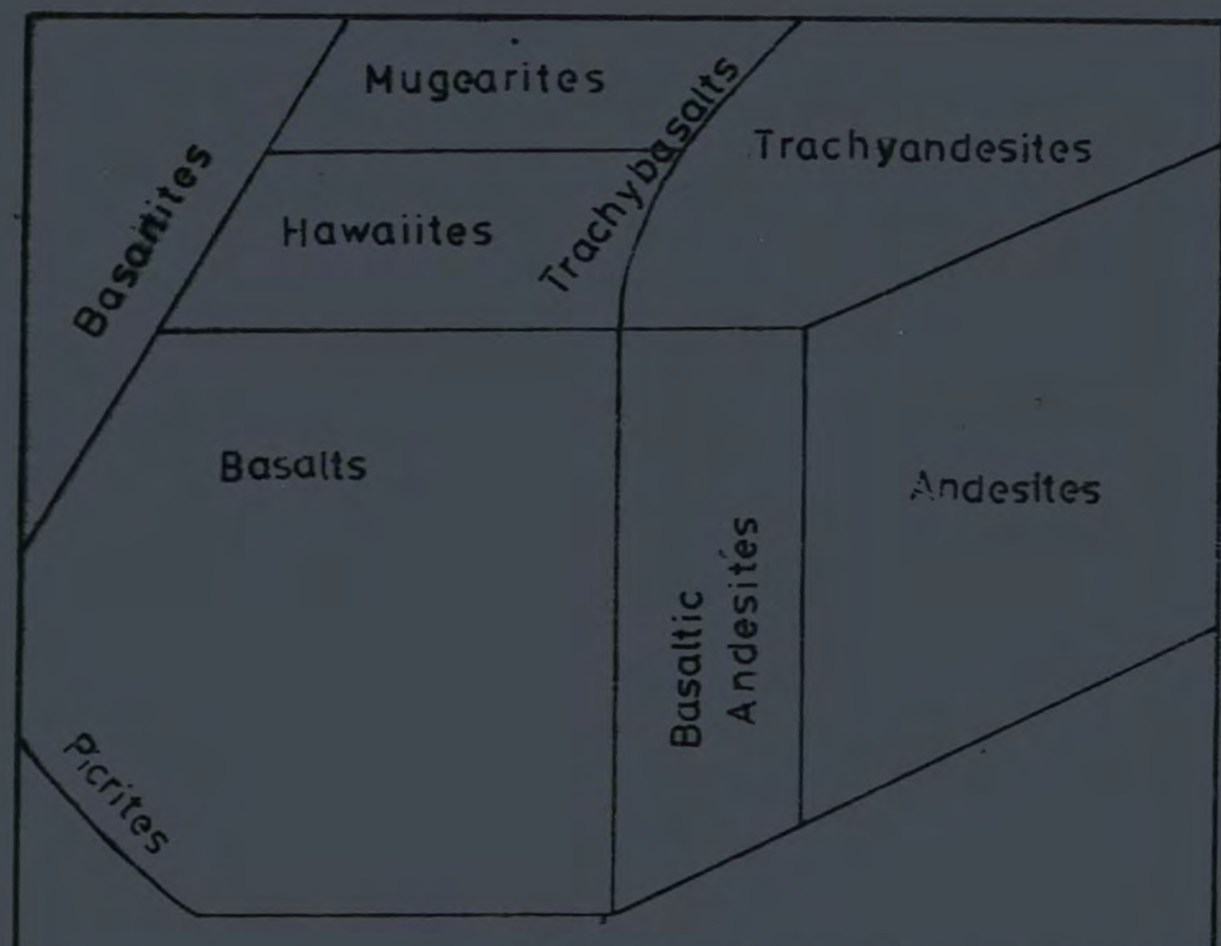

Classification ; Cox, Bell, and Pankhurst

Figure 4.2

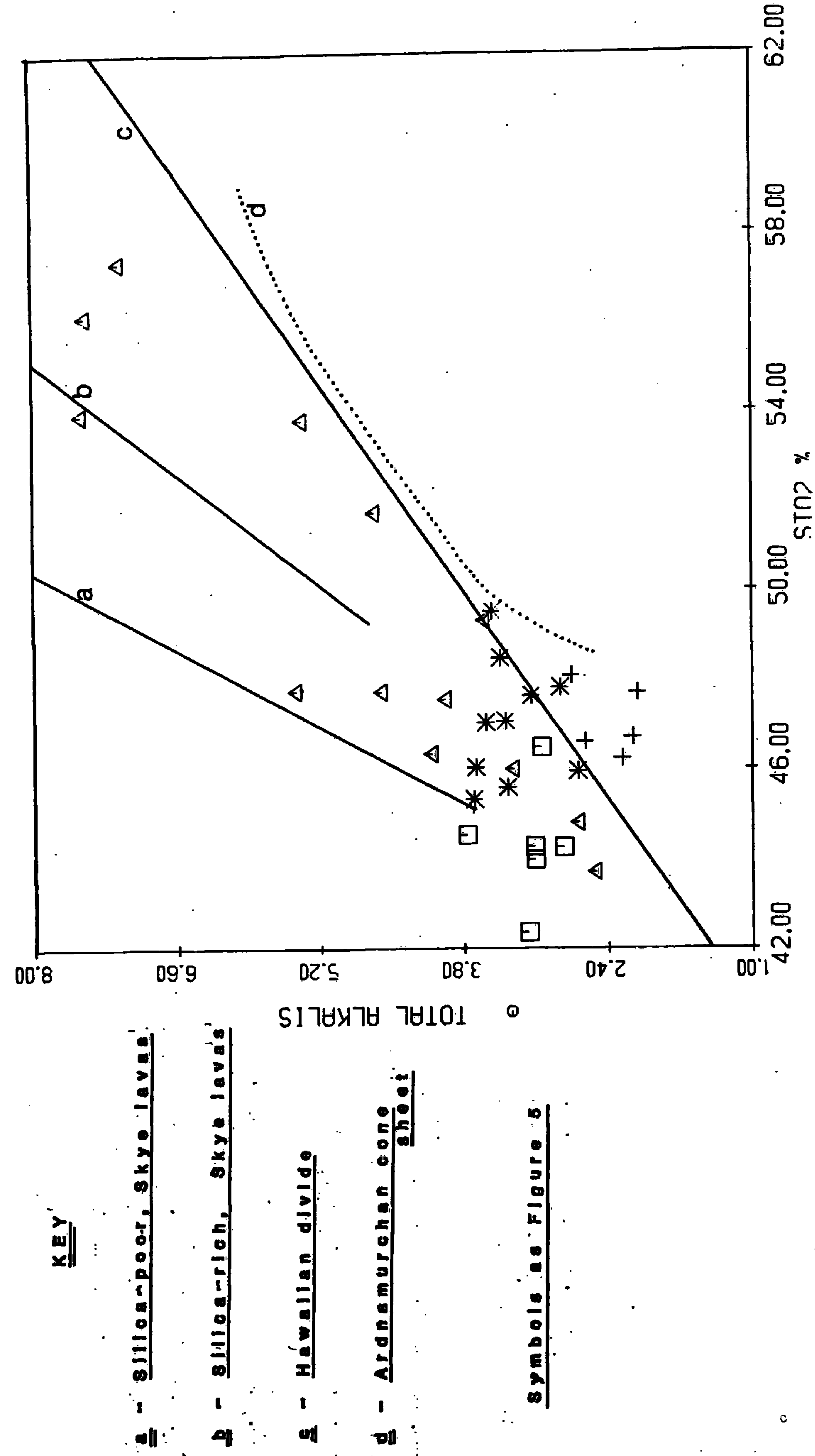

KEY
a - Silica-poor, Skye lavas
b - Silica-rich, Skye lavas
c - Hawaiian divide
d - Ardnamurchan cone sheet
Symbols as Figure 5
TOTAL ALKALIS
SiO2 %
1.00
2.40
3.80
5.20
6.60
8.00
42.00
46.00
50.00
54.00
58.00
62.00
a
b
c
d

Figure 4.3

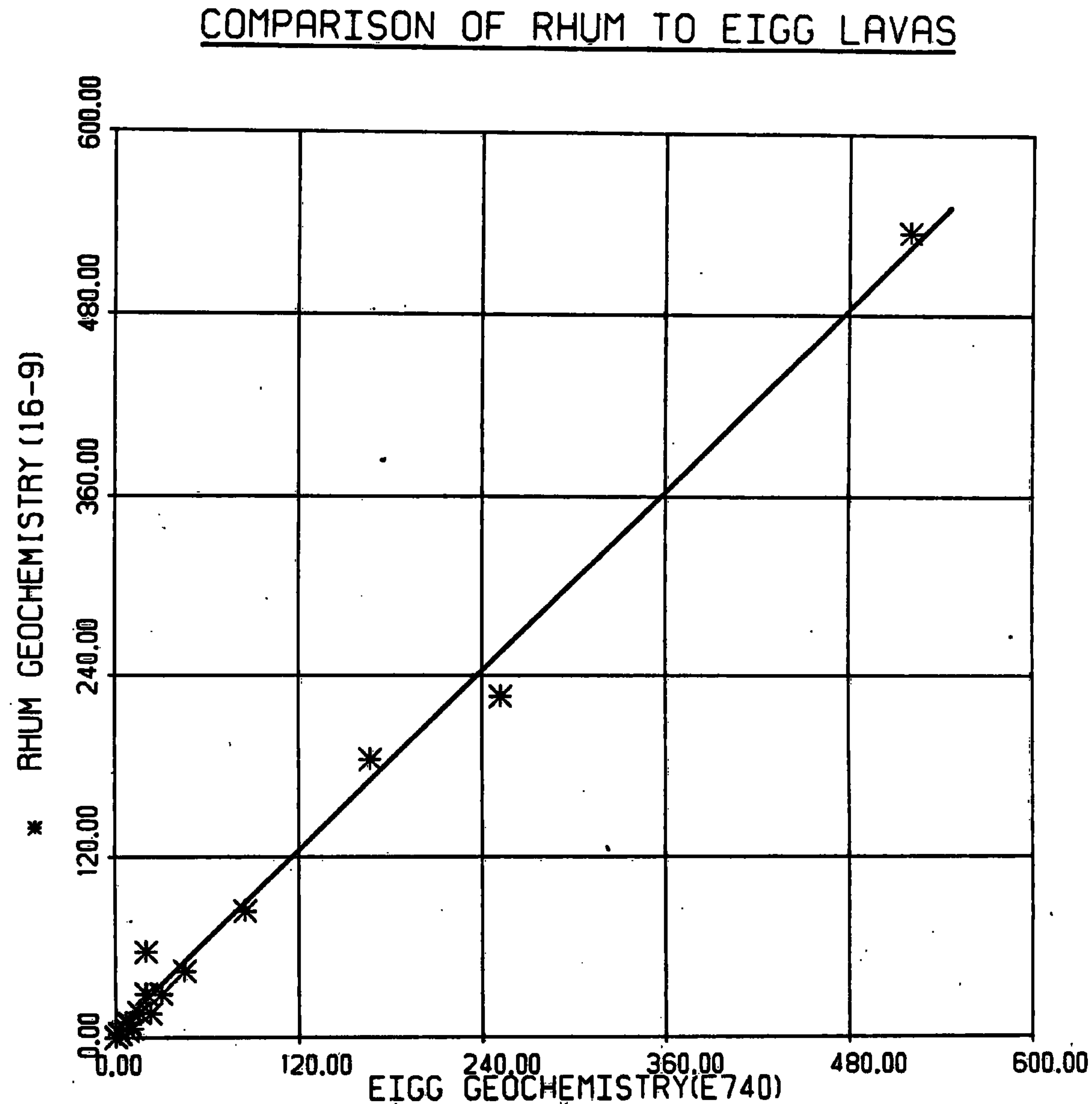

Direct plot of major and trace element chemistry of lava flow samples from Rhum (sample 16-9) versus Eigg (sample E740)

The correlation coefficient is 0.998 (1.0 being a perfect correlation)

Figure 4.3a

COMPARISON OF RHUM TO EIGG LAVAS

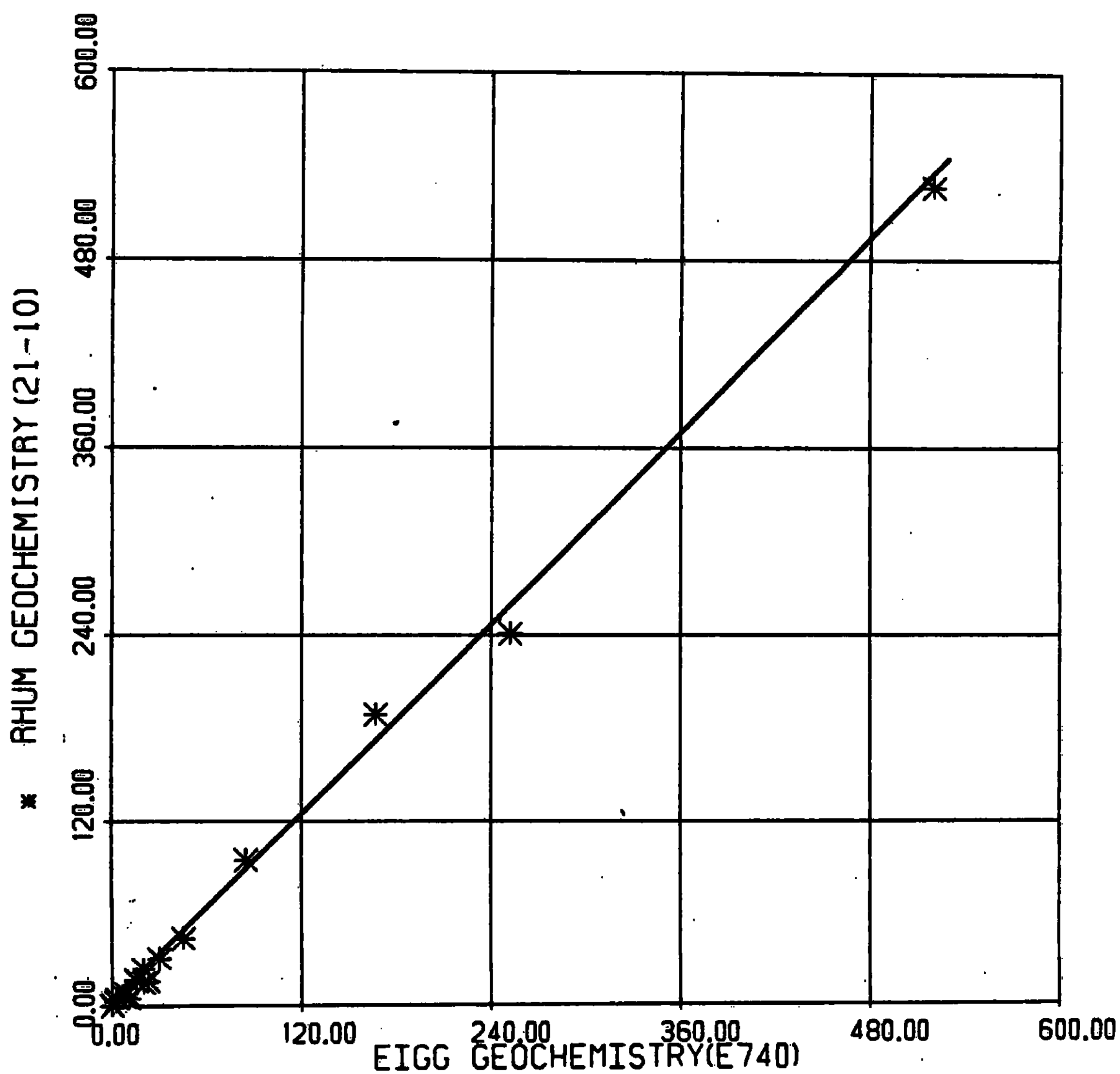

DIRECT PLOT OF MAJOR AND TRACE ELEMENT CHEMISTRY OF LAVA FLOW SAMPLES FROM RHUM (SAMPLE 21-10) VERSUS EIGG (SAMPLE E740)

THE CORRELATION COEFFICIENT IS 0.998 (1.0. BEING A PERFECT CORRELATION)

Plate 4.I One of the many vertically slickensided surfaces within the sheared basalt lava wedge. From a point close to the ORF. (NM 4o6 937).

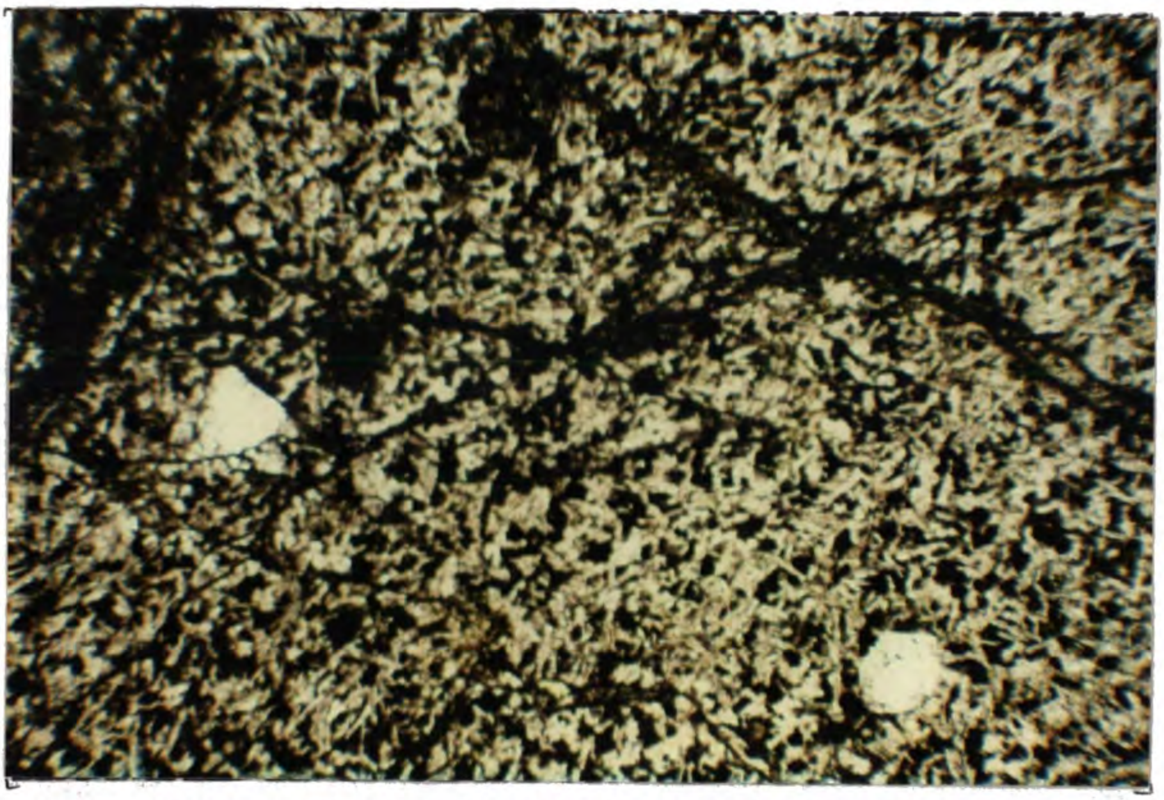

Plate 4.2 Sheared basalt (NJ 83, 6-9). PPL. Field of view 9mm. Shows phenocrysts of plagioclase (Labradorite) in an ophitic mesostasis of plagioclase laths enclosed within augitic clino-pyroxene. Note presence of opaque oxides - up to 10% modally. See also text - Section 4.c.i.

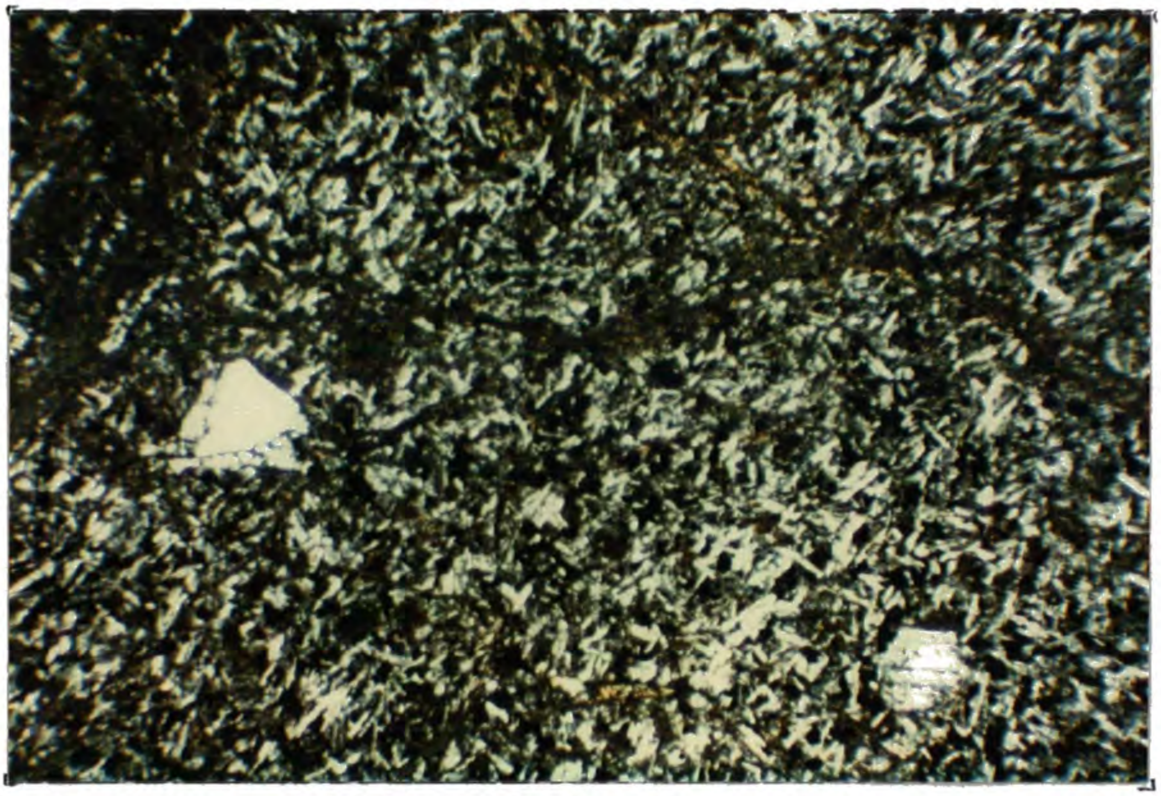

Plate 4.2.a Sheared basalt (NJ 83, 6-9). same view as 4.2 but X-polars. Note extensive alteration to green/brown chlorite, and high birefringent epidote (termed saussuritic alteration) See text - Section 4.c.i.

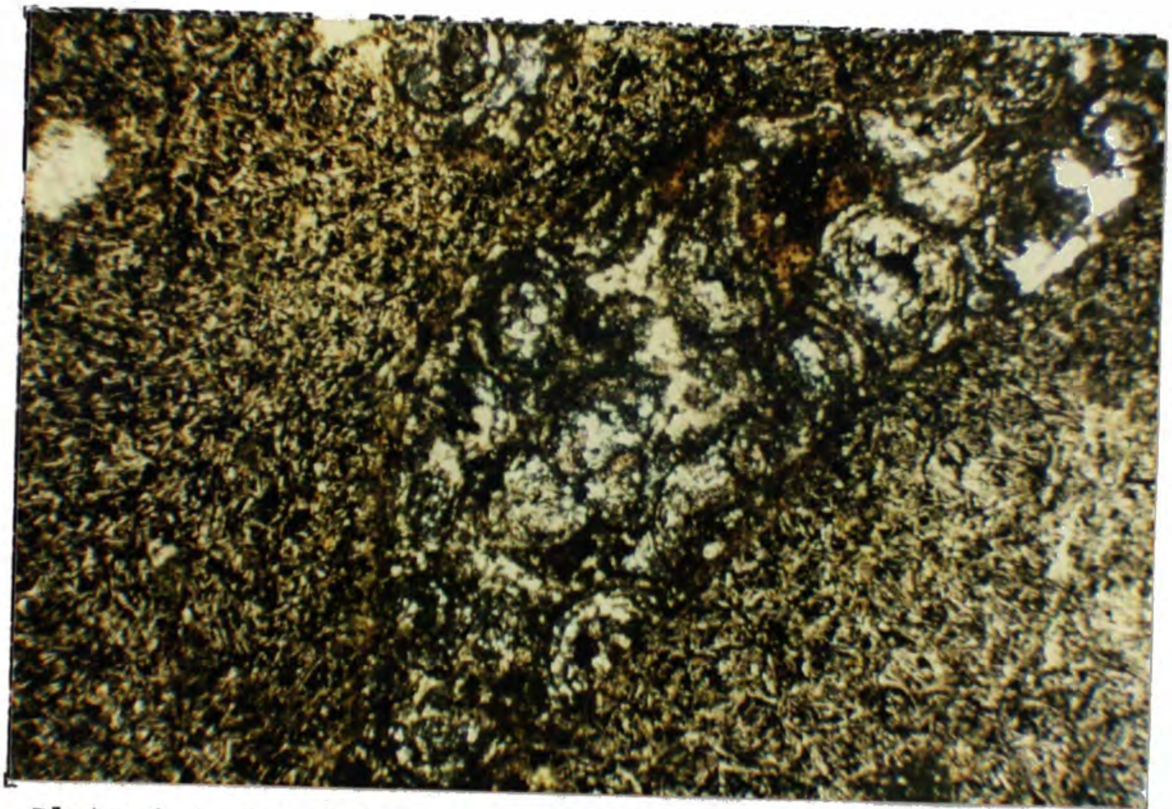

Plate 4.3 Amygdales in sheared basalt (NJ 83, 7-I3). PPL. Field of view 9mm. Shows remnant concentric infilling structures. See text-Section 4.c.i.

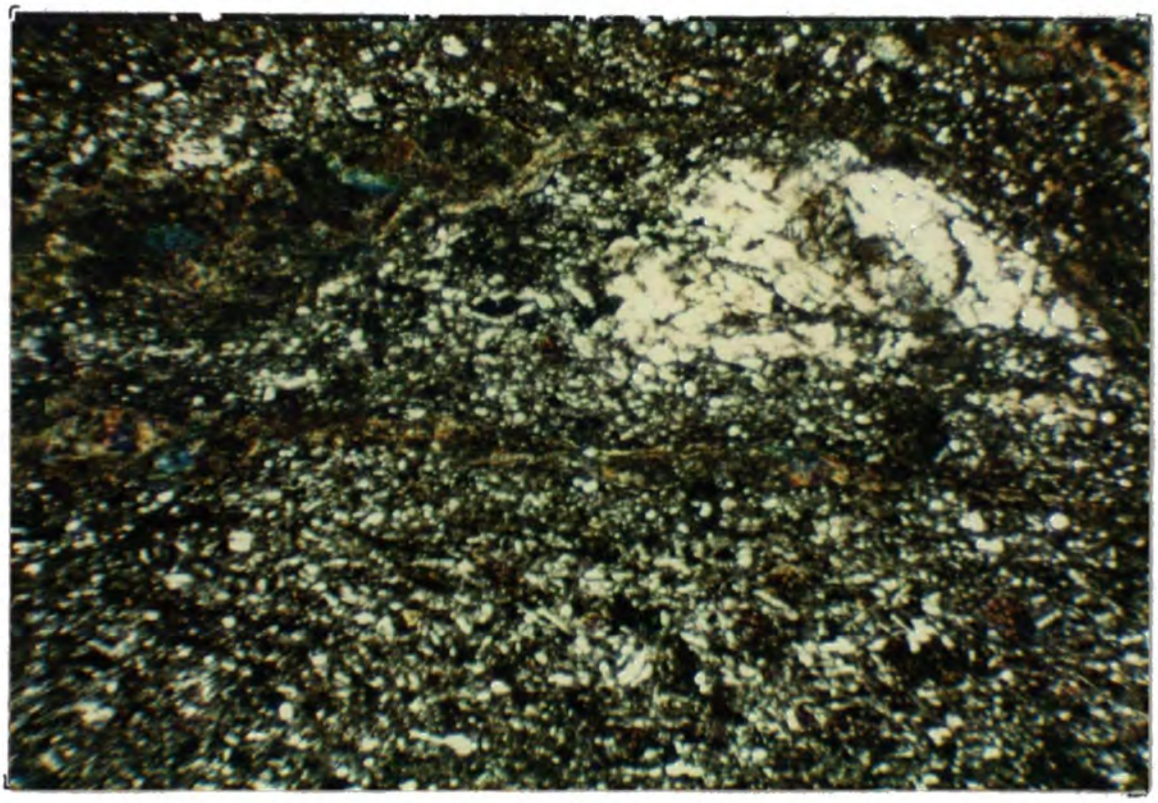

Plate 4.4 Sheared basalt (NJ 83, 20-9). X-polars. Field of view 9mm. Note development of a quite intense shear fabric (running horizontally) plus the shattered plagioclase phenocryst. See text - Section 4.c.i.

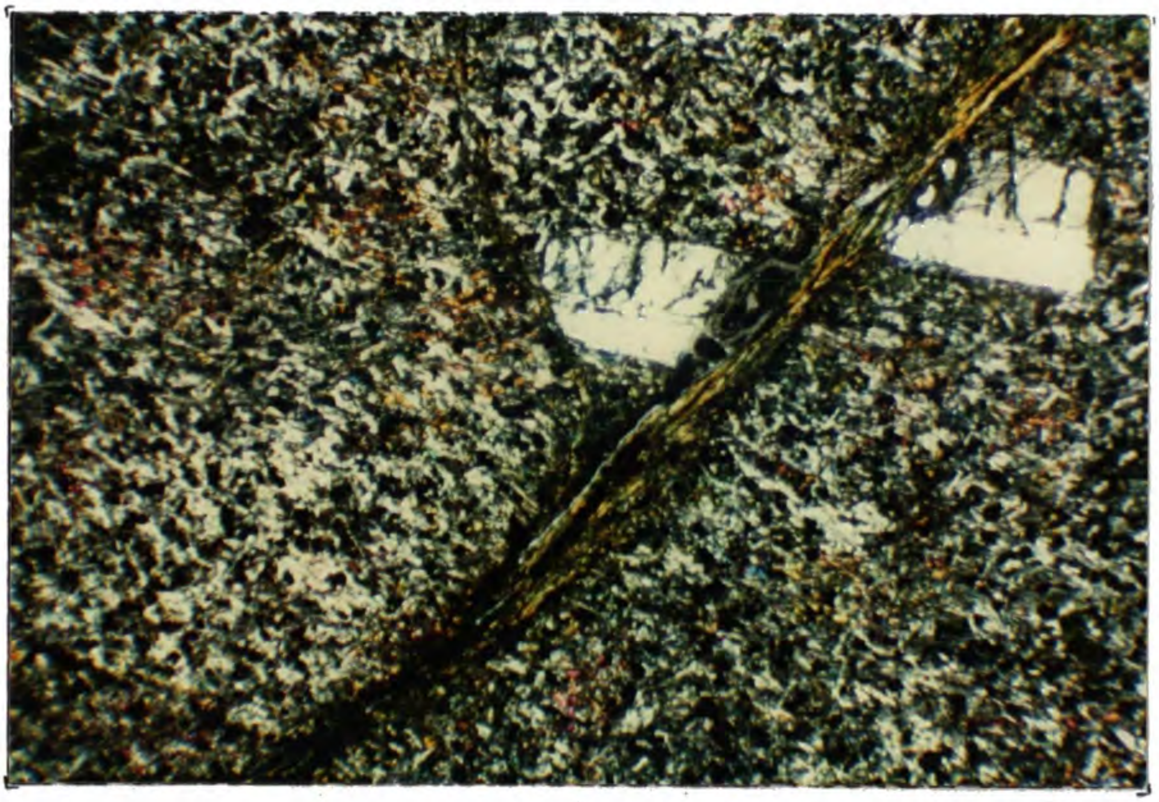

Plate 4.5 Sheared basalt (NJ 84, 6-4). X-polars. Field of view 9mm. Feldspar phenocryst sheared and displaced sinistrally by 2.5mm. Note also the mineralisation of the shear surface.

TABLE 4.1

Rhum Basic Rocks - Geochemical comparison table
Group 1 lavas (S.E Rhum)

Oxide %	NJ 84 17-3	NJ 84 21-3	NJ 84 10-2d
SiO_2	46.48	44.25	45.12
Al_2O_3	18.38	17.39	16.98
Fe_2O_3	8.77	9.14	10.02
MgO	6.49	7.33	9.30
CaO	12.06	12.86	12.97
Na_2O	2.37	2.39	2.69
K_2O	0.67	0.44	0.86
TiO_2	0.90	0.89	1.14
MnO	0.138	0.123	0.145
P_2O_5	0.10	0.08	0.10
Total	96.40	94.93	99.36
Trace Elements (ppm)			
Ba	191	96	75
Nb	2	1	1
Zr	77	77	72
Y	10	11	13
Sr	349	400	197
Rb	30	18	42
Zn	46	50	63
Cu	156	141	142
Ni	161	166	262
Pb	3	3	5
U	1	1	1
Th	0	0	1
V	251	220	260
Cr	310	305	620
Nd	2	0	0
Ga	18	18	18
La	4	15	8
Ce	15	1	6
CIPW Norms.			
Quartz	0.0	0.0	0.0
Ortho.	4.1	2.8	5.2
Albite	21.0	14.7	8.2
Anorth.	39.2	37.6	32.2
Neph.	0.0	3.7	8.1
Diop.	18.3	23.8	26.0
Hypers.	1.4	0.0	0.0
Olivine	10.5	11.7	14.0
Magnet.	3.5	3.7	3.9
Ilmen.	1.8	1.8	2.2
Apatite	0.2	0.2	0.2
Diffn. index	25.1	21.1	21.4

TABLE 4.2

Rhum Basic Rocks - Geochemical comparison table
Group 2 lavas

Oxide %	NJ 84 16-9	NJ 84 17-9	NJ 84 21-10	NJ 84 21-11
SiO_2	44.26	42.36	43.97	44.52
Al_2O_3	16.77	16.46	17.02	16.50
Fe_2O_3	16.00	15.68	15.62	15.59
MgO	4.33	4.16	6.17	3.48
CaO	9.60	9.47	8.21	8.76
Na_2O	2.88	3.10	4.67	3.56
K_2O	0.23	0.07	0.35	0.21
TiO_2	2.62	2.57	2.75	2.66
MnO	0.195	0.253	0.175	0.231
P_2O_5	0.25	0.22	0.26	0.26
Total	97.17	94.39	99.25	95.81
Trace Elements (ppm)				
Ba	226	135	241	215
Nb	6	6	5	6
Zr	184	182	189	181
Y	29	30	31	31
Sr	534	551	527	535
Rb	10	5	7	6
Zn	84	83	95	75
Cu	29	13	15	21
Ni	57	43	24	22
Pb	2	4	1	5
U	2	1	0	1
Th	0	0	0	1
V	340	308	293	323
Cr	16	23	16	16
Nd	24	11	30	27
Ga	22	20	21	18
La	18	11	16	11
Ce	36	21	30	36
CIPW Norms.				
Quartz	0.0	0.0	0.0	0.0
Ortho.	1.4	0.4	2.1	1.3
Albite	24.7	28.1	24.7	31.8
Anorth.	33.9	33.0	24.9	30.0
Neph.	0.0	0.0	8.4	0.0
Diop.	11.7	13.2	12.2	11.8
Hypers.	10.9	0.7	0.0	4.8
Olivine	5.2	12.2	15.5	7.9
Magnet.	6.4	6.5	6.1	6.3
Ilmen.	5.2	5.2	5.3	5.3
Apatite	0.6	0.6	0.6	0.7
Diffn. index	35.3	28.6	35.3	33.1

TABLE 4.3a

Rhum (north-west) lavas geochemical comparison table.

Oxide %	SR.217	SR.156	SR.213	DU.9878	SR.215
SiO_2	43.70	46.33	47.71	45.99	47.54
Al_2O_3	16.39	17.56	16.74	16.89	16.53
FeO	7.98	6.97	8.82	10.11	9.98
Fe2O3	6.11	5.23	5.55	4.68	3.33
MgO	8.50	4.33	4.96	4.61	5.06
CaO	11.46	11.59	8.00	10.16	9.81
Na_2O	2.04	3.93	3.92	2.91	3.23Z
K_2O	0.48	0.27	0.67	0.48	0.74
TiO_2	2.00	2.29	2.09	2.52	2.06
MnO	0.23	0.16	0.21	0.19	0.21
P_2O_5	0.22	0.57	0.34	0.34	0.39
Trace Elements (ppm)					
Ba	159	433	330	350	387
Nb	6	17	7	6	6
Zr	121	132	122	128	135
Y	22	24	30	27	31
Sr	337	842	444	365	412
Rb	1	6	10	10	17
Zn	91	84	91	108	87
Cu	147	-	-	127	-
Ni	363	-	-	55	-
Pb	-	-	-	-	-
U	-	-	-	-	-
Th	-	-	-	-	-
V	-	-	-	-	-
Cr	420	-	-	122	-
Nd	-	-	-	-	-
Ga	-	-	-	-	-
La	-	-	-	-	-
Ce	-	-	-	-	-
CIPW Norms.					
Quartz	0.0	0.0	0.0	0.0	0.0
Ortho.	2.9	1.6	4.0	2.9	4.4
Albite	12.8	24.0	33.1	25.0	27.2
Anorth.	34.6	29.8	26.5	32.1	28.5
Neph.	2.5	5.2	0.3	0.0	0.1
Diop.	17.7	20.5	9.6	14.5	14.9
Hypers.	0.0	0.0	0.0	2.0	0.0
Olivine	22.9	10.2	18.7	16.1	17.8
Magnet.	2.2	2.9	2.9	2.2	2.2
Ilmen.	3.9	4.4	4.1	4.9	3.9
Apatite	0.5	1.4	0.8	0.8	0.9
Diffn. index	18.2	30.8	37.4	27.9	31.7

This data is extracted from results collated by C.H Emeleus (1985).

TABLE 4.3b

Rhum lavas (north-west) geochemical comparison table

Oxide %	SR.165	SR.237	SR.189	SR.230	SR.232
SiO_2	49.30	51.70	53.75	56.06	57.26
Al_2O_3	14.47	15.27	15.61	16.89	15.44
FeO	4.73	9.19	5.78	3.02	3.99
Fe2O3	12.85	4.31	5.56	7.65	6.37
MgO	3.00	3.05	2.83	2.42	1.75
CaO	8.15	8.05	7.25	5.27	5.60
Na_2O	2.60	3.79	4.01	4.57	4.81
K_2O	0.99	0.87	1.36	2.95	2.67
TiO_2	2.71	2.07	2.04	1.98	1.85
MnO	0.21	0.18	0.18	0.16	0.17
P_2O_5	0.56	0.50	1.00	0.88	0.85

Trace Elements (ppm)					
Ba	1022	1002	1252	1486	1488
Nb	10	9	13	10	13
Zr	236	236	219	320	300
Y	38	38	46	52	46
Sr	509	521	671	635	609
Rb	12	47	34	60	62
Zn	142	127	137	139	130
Cu	35	63	-	3	2
Ni	3	4	-	0	0
Pb	-	-	-	-	-
U	-	-	-	-	-
Th	-	-	-	-	-
V	-	-	-	-	-
Cr	10	10	-	4	6
Nd	-	-	-	-	-
Ga	-	-	-	-	-
La	-	-	-	-	-
Ce	-	-	-	-	-

CIPW Norms.					
Quartz	2.7	1.9	5.5	0.3	3.7
Ortho.	6.0	5.2	8.2	17.6	15.9
Albite	22.4	32.5	34.5	39.0	41.0
Anorth.	25.3	22.4	20.9	17.0	12.8
Neph.	0.0	0.0	0.0	0.0	0.0
Diop.	10.4	12.5	7.6	3.0	8.2
Hypers.	24.6	17.4	14.1	13.6	9.2
Olivine	0.0	0.0	0.0	0.0	0.0
Magnet.	2.2	2.9	3.0	3.7	3.7
Ilmen.	5.2	4.0	3.8	3.8	3.5
Apatite	1.4	1.2	2.4	2.1	2.0
Diffn. index	31.0	39.6	48.1	56.8	60.7

This data is extracted from results collated by C.H Emeleus (1985).

TABLE 4.4

Geochemistry of Cobbles from conglomerate at base of Fionchra

Oxide wt.%	SR.244c	SR.244d *	SR.244e	SR.244f *	SR.244g
SiO_2	47.70	46.60	46.23	46.70	48.08
Al_2O_3	15.52	15.09	16.44	15.48	16.24
Fe_2O_3	12.71	11.82	12.99	11.78	11.14
MgO	8.94	8.25	7.45	8.88	6.31
CaO	11.31	10.61	12.76	10.88	12.48
Na_2O	1.62	1.93	1.78	1.95	2.21
K_2O	0.49	0.69	0.48	0.21	0.54
TiO_2	1.32	1.83	1.59	1.26	2.42
MnO	0.21	0.159	0.27	0.161	0.31
P_2O_5	0.18	0.19	0.18	0.15	0.27
Total	100.00	97.20	100.00	97.49	100.00
Trace Elements(ppm)					
Ba	-	91	60	46	76
Nb	-	4	2	3	5
Zr	-	133	102	82	152
Y	-	19	28	26	36
Sr	-	247	218	201	292
Rb	-	39	4	12	6
Zn	-	84	80	88	88
Cu	-	100	149	113	79
Ni	-	130	145	188	125
Pb	-	5	5	6	6
U	-	1	1	1	1
Th	-	1	1	3	4
V	-	340	351	286	444
Cr	-	253	391	434	404
Nd	-	7	2	15	23
Ga	-	23	21	18	22
La	-	19	19	16	11
Ce	-	20	22	15	35
CIPW Norms					
Quartz	0.0	0.0	0.0	0.0	0.0
Ortho.	2.9	4.2	2.9	1.3	3.2
Albite	13.9	17.0	15.2	17.1	18.9
Anorth.	34.0	31.6	35.4	34.0	33.1
Neph.	0.0	0.0	0.0	0.0	0.0
Diop.	17.6	17.5	22.6	16.8	22.6
Hypers.	17.9	17.2	3.9	18.5	10.7
Olivine	8.5	3.7	14.4	4.8	4.0
Magnet.	2.2	4.7	2.2	4.7	2.2
Ilmen.	2.5	3.6	3.1	2.5	4.6
Apatite	0.4	0.5	0.4	0.4	0.7
Diffn. index.	16.8	21.2	18.1	18.4	22.1

* Denotes major element chemistry by XRF using fusion beads. The other results are by C.H. Emeleus, using raw rock powders and normalised to 100%.

TABLE 4.5

Rubidium:Strontium ratios(Rb/Sr)
Rhum & Eigg Lavas

RHUM LAVAS(S.E)

NJ 84 17.3	0.086(1)
NJ 84 21-3	0.045(1)
NJ 84 16-9	0.020(2)
NJ 84 21-10	0.013(2)
NJ 84 21-11	0.011(2)

RHUM LAVAS(N.W)

SR 217	0.003
DU 9868	0.009
SR 156	0.007
SR 213	0.02
DU 9878	0.027
SR 215	0.04
SR 230	0.096
SR 232	0.10

EIGG LAVAS

E 7467	0.028(1)
E 7469	0.033(1)
E 7636	0.021(1)
E 7649	0.031(1)
EA 8	0.021(1)
E 7427	0.008(2)
E 7429	0.020(2)
E 7430	0.013(2)
E 7458	0.013(2)

COBBLES(FIONCHRA)

SR 244c	---
SR 244d	0.16
SR 244e	0.018
SR 244f	0.06
SR 244g	0.021

The numbers in brackets refer to which group of lavas the sample belongs to.(See text)

TABLE 4.6

Niobium:zirconium ratios (Nb/Zr)
Rhum and Eigg lavas

RHUM LAVAS (S.E)

NJ 84 17.3	0.026(1)
NJ 84 21.3	0.013(1)
NJ 84 16.9	0.033(2)
NJ 84 17.9	0.033(2)
NJ 84 21.10	0.027(2)
NJ 84 21.11	0.033(2)

RHUM LAVAS (N.W)

SR 217	0.05
DU 9868	0.041
SR 156	0.13
SR 213	0.057
DU 9873	0.063
SR 215	0.044
SR 230	0.031
SR 232	0.043

EIGG LAVAS

E 7467	0.088(1)
E 7469	0.029(1)
E 7636	0.038(1)
E 7649	0.035(1)
EA 8	0.13(1)
E 7427	0.032(2)
E 7429	0.043(2)
E 7430	0.066
E 7458	0.06

COBBLES (FIONCHRA)

SR 244c	-----
SR 244d	0.03
SR 244e	0.02
SR 244f	0.037
SR 244g	0.033

Numbers in brackets refer to the 'group' to which a particular lava belongs (see text)

TABLE 4.7

Eigg Lavas - Geochemical comparison table
Group 1 Lavas

Oxide %	E7467	E7469	E7636	EA8	E7649
SiO_2	45.95	47.05	47.62	47.81	49.51
Al_2O_3	16.10	16.00	15.04	8.32	15.21
Fe_2O_3	12.35	11.67	12.31	9.88	10.20
MgO	10.21	8.90	9.84	9.78	9.65
CaO	10.89	11.22	10.03	11.39	10.36
Na_2O	2.40	2.82	2.72	2.55	2.91
K_2O	0.29	0.57	0.42	0.31	0.61
TiO_2	1.45	1.43	1.60	1.07	1.22
MnO	0.21	0.19	0.19	0.17	0.16
P_2O_5	0.14	0.15	0.22	0.12	0.17
Total	100.0	100.0	100.0	100.0	100.0

Trace Elements (ppm)					
Ba	122	198	250	97	281
Nb	8	3	5	10	4
Zr	91	105	133	75	113
Y	19	22	24	17	19
Sr	284	303	336	324	353
Rb	8	10	7	7	11
Zn	76	84	74	58	70
Cu	113	125	94	98	79
Ni	322	234	208	81	144
Pb	-	-	-	-	-
U	-	-	-	-	-
Th	-	-	-	-	-
V	-	-	-	-	-
Cr	430	420	496	375	480
Nd	-	-	-	-	-
Ga	-	-	-	-	-
La	-	-	-	-	-
Ce	-	-	-	-	-

CIPW Norms.					
Quartz	0.0	0.0	0.0	0.0	0.0
Ortho.	1.7	3.4	2.5	1.8	3.6
Albite	17.6	18.3	23.0	21.5	24.6
Anorth.	32.3	29.3	27.6	33.8	26.6
Neph.	1.4	3.0	0.0	0.1	0.0
Diop.	17.0	20.7	16.9	17.8	19.2
Hypers.	0.0	0.0	1.9	0.0	3.5
Olivine	24.7	20.0	22.4	20.5	17.5
Magnet.	2.1	2.2	2.2	2.3	2.2
Ilmen.	2.8	2.7	3.0	2.0	2.3
Apatite	0.3	0.4	0.5	0.3	0.4
Diffn. index	20.8	24.7	25.5	23.4	28.2

This data is extracted from results collated by E.A Allwright (1980). Unpub. M.Sc. Thesis U. of Durham.

TABLE 4.8

Eigg Lavas - Geochemical comparison table
Group 2 lavas

Oxide %	E7430	E7429	E7427	E7458
SiO_2	45.31	45.58	47.02	46.02
Al_2O_3	15.46	14.87	15.61	16.25
Fe_2O_3	15.76	16.23	14.67	15.36
MgO	7.88	8.17	7.34	6.96
CaO	8.88	8.70	8.84	8.67
Na_2O	3.27	2.92	3.13	3.27
K_2O	0.43	0.45	0.45	0.41
TiO_2	2.57	2.81	2.56	2.60
MnO	0.2	0.21	0.19	0.20
P_2O_5	0.25	0.31	0.26	0.25
Total	100.0	100.0	100.0	100.0
Trace Elements (ppm)				
Ba	252	284	254	266
Nb	11	8	6	10
Zr	167	184	189	178
Y	30	37	37	33
Sr	520	451	508	529
Rb	7	9	4	7
Zn	85	94	85	84
Cu	20	42	17	13
Ni	20	41	49	12
Pb	-	-	-	-
U	-	-	-	-
Th	-	-	-	-
V	-	-	-	-
Cr	23	70	45	24
Nd	-	-	-	-
Ga	-	-	-	-
La	-	-	-	-
Ce	-	-	-	-
CIPW Norms.				
Quartz	0.0	0.0	0.0	0.0
Ortho.	2.5	2.7	2.7	2.4
Albite	21.9	24.2	26.5	25.7
Anorth.	26.2	25.2	27.2	28.5
Neph.	3.1	0.3	0.0	1.0
Diop.	13.3	13.3	12.5	10.8
Hypers.	0.0	0.0	2.5	0.0
Olivine	25.2	26.3	21.1	23.9
Magnet.	2.1	2.1	2.1	2.1
Ilmen.	4.9	5.3	4.9	4.9
Apatite	0.6	0.7	0.6	0.6
Diffn. index	27.6	27.1	29.1	29.2

Data extracted from results collated by E.A.Allwright, unpublished M.Sc Thesis, University of Durham (1980).

TABLE 4.9

Ranges of trace element values - Rhum (SE) and Eigg

Rhum (SE) - group 1.		Eigg - group 1.
Zr	72-77	75-113
Y	10-11	17-20
Sr	350-400	380-353
Cu	141-156	94-125
Ni	161-166	81-322
Cr	305-310	375-500
Rhum (SE) - group 2.		**Eigg - group 2.**
Zr	181-189	167-190
Y	29-31	30-37
Sr	527-551	450-530
Cu	13-29	13-40
Ni	22-57	20-50
Cr	16-23	23-70

Values for Nb/Zr and Rb/Sr ratios

	Nb/Zr	Rb/Sr
Rhum (south-east) lavas group 1	c. 0.032	0.045-0.086
Rhum (south-east) lavas group 2	c. 0.032	c. 0.013
Rhum (north-west) lavas	0.040-0.120	0.003-0.009 0.096-0.100
Cobbles (below Fionchra)	0.020-0.032	0.060-0.021
Eigg lavas - group 1	c. 0.032	c. 0.028
Eigg lavas - group 2	c. 0.032	c. 0.013

Chapter 5

Structure of the Main Ring Fault

5.a Introduction

5.b The MRF in south-east Rhum

5.b.i The Outer Ring Fault (ORF)

5.b.ii The Centre Ring Fault (CRF)

5.b.iii The Inner Ring Fault (IRF)

Figures Plates and Tables

5.a Introduction

The Main Ring Fault (MRF), Figure 2.1, forms an essentially annular boundary to the igneous rocks of the Rhum complex enclosing both the ultrabasic rocks and the acid volcanics of western Rhum, (the NMC; Dunham, 1968, and the SMC; Hughes, 1960a). The acid volcanics are totally bounded by the fault, whereas the ultrabasic rocks often transgress (thermally erode ?) the line of faulting. In south-east Rhum however, the MRF is no longer a simple single arcuate fracture (Figure 2) but comprises 3 sub-parallel fractures. These component fractures have been defined earlier (section 2.a and Smith, 1985) as the Outer Ring Fault (ORF), Centre Ring Fault (CRF), Inner Ring Fault (IRF). Each of the components of the MRF in south-east Rhum is described in detail below. Plate 5.0, an aerial photograph of south-east Rhum, picks out the major lineations produced by the MRF.

5.b The MRF as seen in south-east Rhum

The single arcuate fracture of the MRF in south-east Rhum is never observed directly, its course is infered to lie along a deep gully (Plate 5.1 and 5.1a) produced by the erosion of easily weathered marginal gabbro. The Torridonian to the east of the fault line is highly deformed (dips up to 70 degrees west) and often exhibits signs of rheomorphism with the occasional production of true hybrid rocks (Section 2.c). Emeleus and Forster (1979), describe the path of the MRF in this area as a 'moat like' feature, the cover photo (op cit) is an aerial view of Rhum from the south-east which shows up this feature admirably. To the west of the marginal gabbro are the unit 1 peridotite and allivalite of the Lower Eastern Layered Series (Faithfull 1985). The unit 1 allivalite dips west at angles of c. 30 - 40 degrees, and is described in Section 2.e.

It seems therefore that in south-east Rhum the line of the MRF has been 'exploited' during emplacement of the ultrabasics with severe thermal metamorphism of the Torridonian to the east of the marginal gabbro. Transgression of the MRF caused by the ultrabasics/gabbro perhaps indicates that thermal erosion of the MRF also took place at this stage.

5.b.i The Outer Ring Fault

At a point just south of the calc-silicate 'dry stone wall' locality (Emeleus and Forster, 1979, location II 1b. and Figure 2), the MRF may bifurcate. This bifurcation of the fault is not observed directly due to masking by marginal gabbro. It is possible that the MRF was 'double' to the north of Allt nam Bà but all evidence is now lost. Just to the south of the presumed point of bifurcation the fault plane of the ORF is observed, it is marked by the presence of pockets of explosion breccia, and intense mylonitization of the basaltic rocks to the west of the fault. As will be outlined in Chapter 6, this particular portion of the ORF has been utilized on at least two occasions. Along this northern portion of the ORF the displacement on it must have been down to the west; juxtaposing sheared Tertiary basalts against Torridonian strata (Figure 2). The fault plane dips c.65° west and can be traced southwards to a point where the fault once again bifurcates (NM 4054 9386). The ORF now separates basal Torridonian/Lewisian Gneiss from Torridonian Rudha na Roinne grit. Consequently displacement within this southern portion of the ORF must have been upward to the west. Mylonite, slickensiding and pockets of explosion breccia all serve to delimit the fault plane hereabouts.

The Lewisian Gneiss is foliated, with the foliation generally trending c. 340°. Along the ORF however, the foliation is bent around (in c. 1m) to become coincident with the line of faulting, this implies that there must have been a component of horizontal movement, and presumably a fair degree of heating as no brittle shearing is observed.

Explosion breccia is very common along the southern portion of the fault plane, especially to the south of the deeply incised cross-cutting dyke (Figure 2 and Plate 2.14). Ultimately, to the north of the dyke channel, explosion breccia becomes associated with porphyritic felsite and the fault plane becomes obscured. The explosion breccia and felsite presumably exploited the existing structural weakness of the ORF (see Chapter 6). Explosion breccia can be traced over the south-eastern shoulder of Beinn nan Stac into the Dibidil valley where exposure is lost beneath thick peat.

5.b.ii The Centre Ring Fault

The CRF is the shortest of the three components comprising the MRF in south-east Rhum. The CRF juxtaposes Lewisian Gneiss/basal Torridonian sediments against the sheared basaltic lavas lying south-west of the point of bifurcation of the CRF and ORF (Figure 2). The fault plane is never observed directly with the CRF always exploited by porphyritic felsite.

The felsite along the fault becomes far more abundant southwards, eventually terminating the Lewisian Gneiss exposure completely (Figure 2). Explosion breccia is associated with this felsite and forms extensive outcrops between the ORF and CRF.

To the west of the CRF are the sheared Tertiary basaltic lavas, which show signs of extensive shearing (Plate 4.1). At (NM 4015 9375) the CRF is cut out by the later IRF.

The last phase of movement on the CRF must have been downwards to the west, thereby juxtaposing Lewisian Gneiss against Tertiary basaltic lava, (Plate 2.15).

5.b.iii The Inner Ring Fault

This fault forms the inner-most fracture and separates the sheared Tertiary lavas and Mesozoic sediments from the heavily deformed Torridonian strata within the MRF.

The northern portion of the IRF is not observed as it, like the MRF north of the Allt nam Bà waterfall, has been presumably thermally eroded by the marginal gabbro. To the south of the Allt nam Bà valley the IRF is still not well defined, but must separate Jurassic fossiliferous shale from the unfossiliferous Torridonian Bagh na h-Uamha shale. The fault plane is easily discernable further south. Here Jurassic limestone has dissolved along the interface with Torridonian rocks producing a prominent undercut scarp feature (Plate 5.3). Often there are considerable sink holes along the contact, with the 'hanging wall' Torridonian rocks commonly collapsing into them.

The dip (c. 45^{o}) of the IRF is rather less than that of either the ORF or CRF. Where the Mesozoic sediments eventually wedge out (Figure 2), sheared basalt is now brought into contact with Torridonian sediments inside the Ring Fault. Dark flinty mylonites are developed for c. 1m in rocks on both sides of the IRF.

Where the oft mentioned deeply incised dyke channel crosses the IRF (Figure 2), it exposes a small tract of Jurassic sandstone (altered to quartzite). This is the southern-most visible extent of Jurassic strata on the MRF system, although the presence of deep sink holes along the IRF for some tens of metres south of this point indicate the presence of calcareous rocks. The IRF continues south-wards, cutting off the CRF, and can be traced over the south-western flank of Beinn nan Stac into the lower Dibidil valley, where exposure is lost. Rocks which are exposed on the line of the IRF before it is lost are highly brecciated and deformed Torridonian sediments.

A cross section through the MRF system in south-east Rhum is given in Smith (1985, figure 3 - Appendix 3).

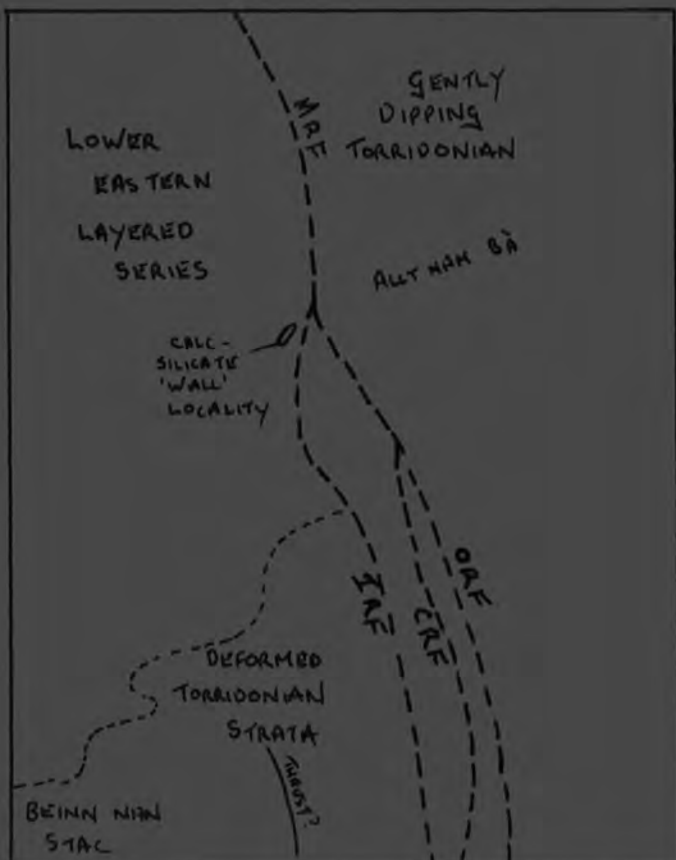
GENTLY
DIPPING
TORRIDONIAN
MRT
LOWER
EASTERN
LAYERED
SERIES
ALLT NAN BÀ
CALC-
SILICATE
'WALL'
LOCALITY
ORF
CRF
DEFORMED
TORRIDONIAN
STRATA
THRUST?
BEINN NAN
STAC

Plate 5.0 Aerial view of south-east Rhum.

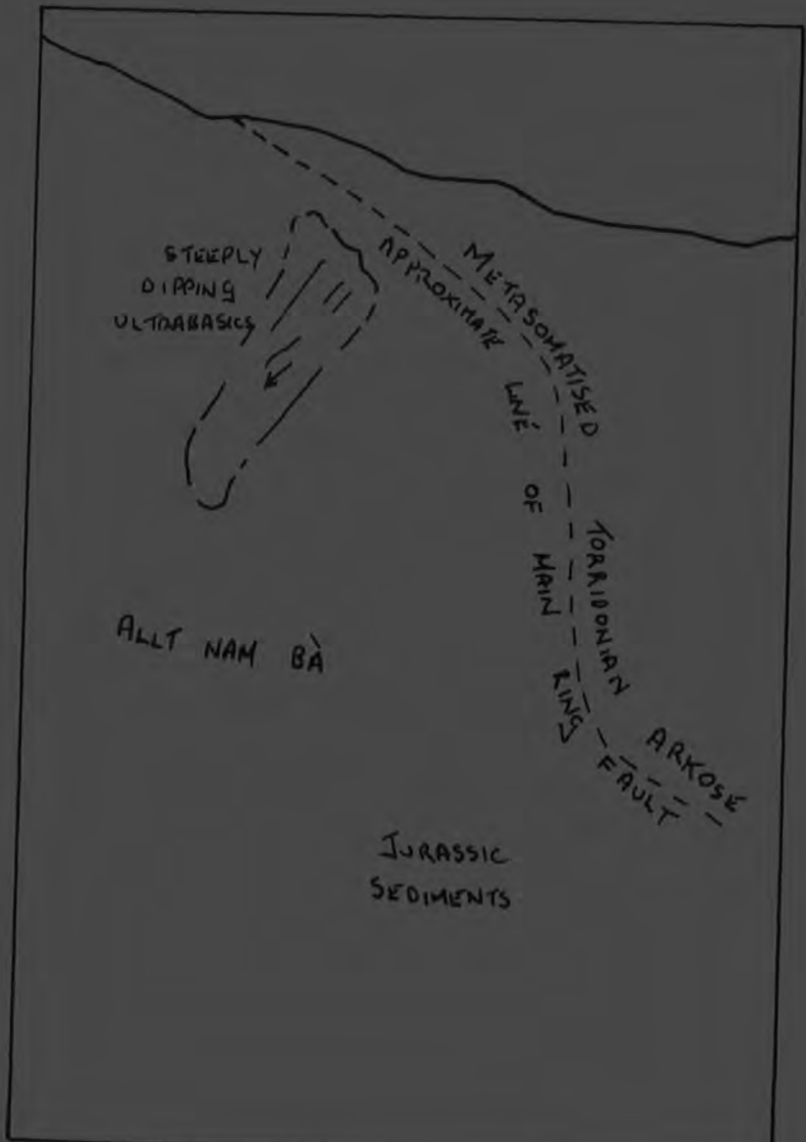
STEEPLY
DIPPING
ULTRABASICS
APPROXIMATE LINE OF MAIN RING FAULT
METASOMATISED TORRIDONIAN ARKOSE
ALLT NAM BÀ
JURASSIC
SEDIMENTS

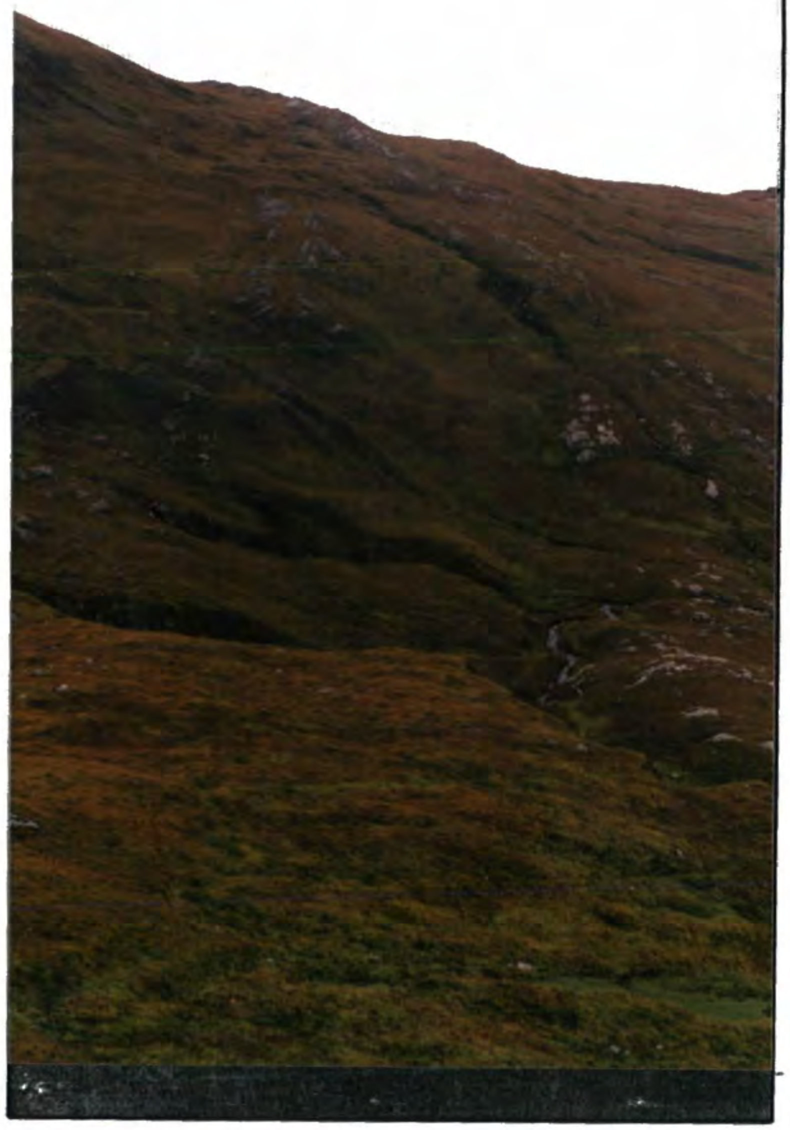

Plate 5.I General view looking north, taken from the Mesozoic limestone locality (NM 405 943). Note the gully formed by the easily weathered gabbro along the line of the MRF, and also the inclination of the Unit I peridotite/allivalite. (See text).

Plate 5.Ia Shows the moat and ridge feature caused by the easily weathered marginal gabbro leaving a gully against the more resistant rheomorphosed Torridonian arkose. In the foreground is the calc-silicate dry-stone wall just below the Allt nam Ba waterfall.

Plate 5.2 The Steep slickensided fault plane of the ORF against the sheared Tertiary lavas. See also Plate 3.I.

Plate 5.3 The IRF seen dipping c. 45° west. Note the undercut nature of the 'hanging wall' of Torridonian sediments (to the left of the shot) due to dissolution of limestone adjacent to the fault plane.

Chapter 6

The Main Ring Fault in south-east Rhum and its implications to the early tectonic history of the volcanic complex.

6.a Introduction

6.b The development of calderas

6.c Formation of the Rhum caldera

6.c.i Phases in the development of the Rhum caldera

Figures Plates and Tables

6.a Introduction

Emeleus, Wadsworth and Smith (1985) proposed a model for the early history of the Rhum volcanic centre in terms of an early caldera forming event. Initiation of the caldera was thought to be due to the diapiric uprise of acidic magma, now expressed at the surface by the 'western granophyre'. Such a thesis seems reasonable in the light of recent work which appears to suggest that caldera forming events preceded or where integral parts of many of the Tertiary intrusions of the British Tertiary Volcanic Province (BTVP) eg; Mull - Bailey et. al. (1924), Bott and Tantrigoda (1987). Arran - King (1954), and Skye - Bell (1966,1976) Thompson (1980). More recent studies on the Rhum Complex, especially in the south-east, suggest that a slight modification is required to the Emeleus et. al. (1985) model.

Calderas are a common feature of other volcanic provinces associated with the emplacement of acid/intermediate lavas to high crustal levels, for example; Timber Mountain (Christiansen, Lipman et. al. 1965. Lipman, 1976), Valles (Smith, Bailey and Ross, 1961), Sabolka (Almond, 1977). An excellent further reference list is given in Lipman (1984).

In order to help correlate the features found on Rhum with the stages in the development of better documented calderas, a summary of the primary stages in the development of calderas is given below.

6.b The development of Calderas.

Stage 1

Pre caldera forming events, especially in the Scottish Tertiary, appear to be dominated by an intense phase of basic dyke intrusion, producing surface fissure eruptions and the consequent development of an extensive lava plateau, (of Walker 1975). Magma for this dyke phase was probably ponded at the base of the crust, with batches rising under excess hydrostatic pressure to reach the surface. However, basic dykes are also seen to cut later rocks of the Rhum complex (eg. felsite and explosion breccia), so dyke formation seems to have continued throughout the formation of the Rhum caldera (see also section 6.c.i Phase 1).

Stage 2

Caldera development is initiated by emplacement of magma less dense than the surrounding country rocks to high structural levels in the crust. At low levels in the crust the buoyant magma can rise by a method of diapirism as the crust tends to deform in a ductile manner.In the cooler more brittle upper crust the emplacement is by stoping. The buoyant acidic magma is most likely derived by a combination of primary differentiation of the ponded basic magma of Stage 1 plus partial-melting of the surrounding crustal rocks, (Thompson 1980, 1982. Thompson et.al. 1986).

Stage 3

Emplacement of the buoyant magma to high structural levels tends to deform the crust with the development of an early phase of regional tumescence. Early acid vulcanism and continued dyke emplacement are common during this stage.

Stage 4

Tumescence culminates in ring fracturing with associated vulcanism in the form of vent agglomerates and other types of pyroclastic rock eg. ignimbrites and welded tuffs. The association of such rocks with acidic vulcanism is typical of Plinian type explosive eruptions, the best documented of which is the Askja volcano in Iceland (Thompson 1980).

Stage 5

Expulsion of volatiles during ring-fracture vulcanism produces regional detumescence as the magma pressure is lost. Detumescence occurs along the bounding ring fractures, developed during Stage 4, and a caldera is formed at the surface. As caldera formation is governed by the ring fractures an essentially annular margin is produced. The actual margin of the caldera may lie some distance outside the line of annular faulting, due to the collapse inwards of the walls. Such collapse, along with the associated acid/pyroclastic vulcanism, infills the caldera often to considerable depths. The depth of infill by pyroclastic rocks and 'collapse breccias' is dependent on the initial extent of collapse (Lipman 1976, 1984). It is of interest to note that Lipman (1976) states that the floors of calderas generally collapse as intact plugs, especially in Precambrian cratonic crust, and not in a totally random, piecemeal fashion. This can preserve stratigraphically high level crustal successions at low structural levels (cf Figure 6.1 to Lipman 1976 figure 2).

Stage 6

A common feature of many calderas is resurgence (Smith and Bailey 1968), the causes of which are not totally understood but four hypotheses are generally propounded:

i. Continued uprise of magma

ii. Hydrostatic rebound

iii. Regional detumescence and centripetal pressure

iv. Return to magma pressure maximum

All four of these mechanisms are evaluated in a review of the mechanics of such mechanisms by Marsh (1984). It is probably the case that all these mechanisms take place to some extent. Resurgence is mentioned at this point in order to introduce the possibility that the floor of calderas can be re-elevated to high structural levels, this is an important factor in the development of the Rhum caldera.

Stage 7

Post resurgent vulcanism is a typical waning caldera feature with late stage acid vulcanism including pyroclastic flows and in some calderas the development of ring dykes (Smith and Bailey 1968). Erosion can also be an important factor during this stage, and this was probably the case on Rhum.

Formation of the Rhum Caldera - Introduction

On Rhum it is quite possible that all of the caldera forming events outlined above took place however, extensive erosion has stripped off much vital evidence. A further complication is also present in the form of the Ultrabasic Complex which post-dates the early caldera forming events (Emeleus et. al. 1985). The rocks of the caldera (granophyre, felsite, explosion breccia, tuffisite and country rock (inside the MRF)) seen in the NMC, SMC and south-east Rhum, are often in roof like relations to the UB complex (Plate 2.18, fig. 1 of Emeleus et.al. 1985, and fig. 3 of Smith 1985). As indicated in Stage 5 above, the initial caldera could have filled to a considerable depth (c. 2 - 3 km) with the UB complex being injected into the base of the overlying caldera fill. Dunham and Emeleus (1967), Faithfull (1985) and Emeleus (1987) came to the conclusion that the UB Complex was probably emplaced within 1 km of the surface. Consequently the caldera infill is more than thick enough to cater for this. Emplacement of the UB Complex is discussed further in Phase 8 below.

6.c.i Phases in the development of the Rhum caldera

As in Walker's (1975) model for the development of the Tertiary Volcanic Centres, it is envisaged that the first phase in the development of the Rhum centre was one of extensive basic dyke formation. Dyking was probably initiated by the ponding of basic magma at the base of the crust, with batches of this magma rising under excess hydrostatic pressure towards the surface. Magma pressure was high enough to allow the dykes to reach the surface producing fisssure eruption and the development of an extensive lava plateau. Remnants of this lava plateau are retained on the nearby isles of Eigg and Muck to the east. However, basic dykes also cut later rocks of the caldera (felsites and explosion breccias within the MRF zone) and so basic magma must have been available throughout much of the history of the Rhum caldera. There is a further problem in that the feeders for the extensive lava plateau have not, as yet, been discovered. The plateau lavas are of alkali-olivine basalt affinities (Allwright, 1980) and geochemical evidence presented in chapter 3 shows that a small sliver of this lava plateau is caught up in the MRF in south-east Rhum, so proving the existence of the lava field over Rhum during its early history (see also Smith, 1985 and Emeleus et al 1985). Dagley and Musset (1986) have recently proven by palaeomagnetic study that the plateau lavas of Eigg and Muck pre-date the development of the Rhum centre.

Phase 2

The hot basic magma which ponded at the base of the crust began to generate a body of acidic magma above it by a process involving fractional crystallisation and partial fusion of the sialic crust (Fig. 6.1). In the hot ductile lower portion of the crust, greater than 12 km depth, the acidic magma would begin to rise upward diapirically. The diapir grew by continued fractionation/partial fusion, with heat energy supplied from below by the hot basic liquid. The density of this basic liquid was also such that it too rose towards the surface, albeit more slowly, (cf Walker 1975).

The relative densities of possible parental liquids, (either olivine tholeiite (Thompson 1982) or picrite (Cox 1980)) have been calculated by Bott and Tantrigoda (1987) for the Mull Volcanic Centre. The densities of these basic melts vary (see below) but none has a dry density greater than 2750 kg/m^3 and even with only a small water content this value is significantly reduced (to around 2700 kg/m^3 for a picrite). Similar basic rocks could be parental to the Rhum Ultrabasic Complex.

Parental magma	Pressure	
	surface	11 km depth
Mg rich Ol. Tholeiite (1300 celsius)		
a)anhydrous	2670 - 2727	2700 - 2750
b)0.5% water	2630 - 2670	2690 - 2700
model picrite (1400 celsius)		
a)anhydrous	2690 - 2725	2730 - 2755
b)0.5% water	2645 - 2680	2685 - 2720
From Bott and Tantrigoda 1987. ρ in $kg\,m^{-3}$		

The basement rock beneath Rhum is predominantly Lewisian Gneiss, which has a density of around 2750 kg/m^3 at the surface rising to around 2800 kg/m^3 at depth. Consequently there is a sufficient density contrast between basic magma and the country rocks to allow them to rise towards the surface behind the more buoyant acid magma (with a density of c. 2500 kg/m^3 - but again dependant on depth and water content).

Certain batches of the basic magma continued to rise towards the surface without encountering the diapir, these fed the surface fiss ure eruptions thus extending the lava plateau.

Phase 3

As the acid diapir approached the surface localised tumescence occured warping upward the overlying crust. On Rhum doming of the country rocks outside the MRF is clearly seen in the attitude of dip and strike of the Torridonian strata around the northern margin of the Complex (Fig. 2.1). The Torridonian rocks are affected for about 1 km from the MRF, the dips increasing towards the fault to a maximum of 85 degrees. Country rocks within the MRF also show some evidence of doming in terms of their distribution and structural attitudes (Emeleus et. al. 1985).

Phase 4

In order to explain the present distribution of Lewisian gneiss around the margins of the complex and caught up between the ORF and CRF in south-east Rhum, it is necessary to invoke a period of uplift. Following Emeleus et. al. (1985) it is proposed that continued uprise of the acid diapir culminated in fracturing of the country rocks around the periphery of the dome of Phase 3. The result was the development of the annular MRF. The central plug of strong Precambrian cratonic crust was pushed upward by magma pressure (Fig. 6.1) thus elevating Lewisian basement to high structural levels. This raised central plug would, presumably, have been subjected to intense erosion thus stripping off much of the cover of Tertiary plateau lavas and possibly some of the underlying thin Mesozoic sediments, although these would tend to be protected by the overlying lava flows.

During this phase the acidic magma diapir must have approached close to the surface, certainly into the brittle upper part of the crust. This less ductile upper crust (< 12 km) does not allow diapirism to occur, rather, emplacement of magma in this region is by a process of fracturing and stoping (dense blocks of country rock sinking into the less dense magma which is consequently displaced upwards). One common method of stoping is by sub-surface cauldron subsidence, where a large relatively intact cylinder of country rock becomes detatched and sinks (Fig. 6.1). Often the surface expression of such a cauldron subsidence at depth is the production of a caldera (Walker 1984). The Mull caldera, centred on the late Loch Bá centre has recently also been ascribed by geophysical evidence as the surface expression of a sub-surface cauldron (Bott and Tantrigoda 1987). The acid magma which exerted a positive magma pressure on Rhum is probably now represented by the 'western granophyre'.

Phase 5

Deflation of the buoying acid magma, due to escape of volatiles along the propagating fractures of the MRF, would have had two effects; firstly, the production of large quantities of pyroclastic deposits and secondly, the relaxation of diapiric pressure must have caused the central piston to subside producing a caldera(Fig. 6.1).

On Rhum this explosive phase of de-gassing and detumescence is shown by large quantities of explosion breccia, which is always in close spatial association to porphyritic felsite. These two rock types are prevalent in the SMC (Hughes 1960a) and NMC (Dunham 1968) and in smaller quantities in south-east Rhum, such rocks are described in detail in section 2.f. In essence these rocks were originally ascribed to a near surface but essentially sub-terranean origin, and formed by in-situ brecciation of the country rock by 'gas boring' along vents and sub-surface planes of structural weakness. There are possible vents in the NMC in Coire Dubh and Cnapan Breaca (Dunham 1968) but recent re-investigation (Williams 1985) has shown that some at least of the NMC felsites are more akin to eutaxitic textured welded tuffs (ignimbrites). Ignimbrites are sub -aerial, or near surface feeders to surface pyroclastic flows, and typically form in a caldera environment.

Recent re-examination of some of the felsites and explosion breccias in the SMC has shown that they too contain features reminiscent of ignimbrites/pyroclastic flows (C.H. Emeleus pers comm.). More work is at present being carried out in this area which may prove that these deposits could have formed in a caldera environment.

From section 2.f it is shown that some of the south-east Rhum felsites contain features reminiscent of fiammé and glass shards, again features indicative of a high level origin. Similar textural features are also found in the NMC 'felsites' ', described by Williams

(1985).

Evidence for the second consequence of deflation, ie. downward movement of the central piston, is best seen in south-east Rhum. The ORF has in part at least (Smith 1985) not been utilized during the deflation of the central piston, rather a new fracture line (the CRF) has developed sub-parallel to the ORF (Fig.2). Stranded between the two faults is a sliver of Lewisian strata (Gneiss 'whaleback', Plate 2.1 and 2.1a) now at a high structural level. The remainder of the central piston seems to have subsided essentially intact (see Stage 5) along the same plane of faulting as was produced during the phase of central uplift (phase 4 above), Emeleus et. al. (1985).

Phase 6

The size of the caldera produced in phase 5 (above) can be estimated from the approximate margins of the present day MRF and by using the relative caldera sizes produced statistically by Walker (1984).

The MRF on Rhum has a somewhat asymmetrical form, with a north-south dimension (measured approximately along the line of the Long Loch fault) of 8 km and an east-west diameter slightly less than this (c. 6 km). The western extent of the MRF is sub-marine so the value for the east-west dimension is only an estimate. Taking a diameter for the Rhum Complex of c. 8 km and applying Walker's findings an idea of the minimum size of the Rhum caldera comes out at c. 12 km. On geological evidence from south-east Rhum the total

downward movement of the central plug was of the order of 2 km (Emeleus et. al. 1985, Smith 1985). The subsidence in south-east Rhum took place along the northern portion of the ORF and the CRF (Smith 1985), both these fractures exhibit evidence for acid/explosive vulcanism; the ORF has pockets of explosion breccia along it (Fig. 2, and section 2.f), whilst the trace of the CRF is exploited by felsite (section 2.f). The felsite intrudes along the plane of the CRF in a manner somewhat analogous to a ring dyke (Anderson 1936), features produced during phases of subsidence (cf the Loch Bá felsite ring dyke of Bailey et. al. 1924). An interesting feature of the Rhum felsite 'ring dyke' is the presence of blebs of basic material (Plate 2.17d and section 2.f). This could provide evidence for the coexistence of acid and basic magma at depth. On Mull the Loch Ba felsite is also noted for the abundant elongate dark mafic inclusions it contains.
These are thought to represent stringers of basic magma incompletely assimilated with the felsite magma prior to injection as a ring dyke (Blake et. al. 1965. Marshall and Sparks 1984), a similar situation is envisaged for Rhum. The important significance of the coexistence of acid and basic magma is discussed below.

Phase 7

On collapse of the central piston the ensuing caldera on Rhum was gradually infilled with debris - both collapse breccias (now best represented by the deformed Torridonian sediments within the MRF Plate 2.18) and pyroclastic deposits (of phase 5 above). In previous work on the early tectonic history (Emeleus et. al. 1985, Smith 1985) the IRF of south-east Rhum was ascribed to possible resurgent uplift, with uplift of the central block not occuring along the pre-existing line of weakness (ie.the ORF and CRF). This phase of resurgent uplift was required in order to juxtapose older Torridonian strata (Bagh na Uamha shale) west of the IRF against the Jurassic sediments/Tertiary lavas to the east (Fig.1). However, recent discoveries in Dibidil and on Beinn nan Stac, have revealed new exposures of Jurassic sediments and Tertiary lavas (Fig.2) totally overlain by Torridonian shale. The boundary between the Toridonian and Jurassic/Tertiary appears tectonic, a low angle thrust dipping c. 30 degrees west. The Torridonian above the thrust seems to be faulted into a series of large blocks (see Plate 2.18), rather reminiscent to the sort of feature caused by rotational slumping/faulting at the margins of a caldera (Fig. 6.1). The faulted blocks could have accumulated on the caldera floor (collapse breccias ?) and become intercalated with tuffs and volcanic rocks evacuated from the underlying acidic magma chamber. Such caldera infill has been termed 'mega breccia' (Lipman 1976), and is a common feature of the Lake City caldera of the western San Juan Mountains. Both the SMC and NMC, along with the rocks described from Beinn nan Stac, could reasonably have formed in such a collapse dominated environment.

The problem remains however that if downward caldera collapse had been the terminal phase in the early history of the Rhum centre this would not account for the fact that Lewisian gneiss and basal Torridonian are only found inside the MRF (Emeleus et. al 1985). Therefore evidence for renewed central uplift is clear.

Phase 8

This phase can be tied in with the required late phase of central uplift (see phase 7) and also the emplacement of the ultrabasic rocks.

The envisaged cauldron subsidence at depth (Phase 4) which produced the sub-terranean magma chamber into which original acid magma was displaced upward, must have become somewhat evacuated by continued acid magmatism (seen on Rhum as felsite, explosion breccia and Tuffisite) erupted into the surface caldera. As in Walker's (1975) model it is thought that the acid diapir of Phase 2 was followed by a basic (ultrabasic ?) column. This following basic magma must presumably have begun to infill the partially evacuated acidic magma chamber underlying the surface caldera. Magma mixing, with the injection of hot basic magma into stagnant semi-crystalline acid magma chambers induces vigourous convection, vesiculation and as a consequence renewed magma pressure (Sparks et. al. 1977). This renewed magma pressure could produce resurgent uplift of the original central plug of the caldera, thereby raising rocks within the annular ring fault to high structural levels. Magma mixing as a trigger for Plinian type eruption and caldera formation has also been postulated as a mechanism for the emplacement of the western

Redhills Complex of Skye (Thompson 1980).

Once elevated to a high structural level, erosion of the central plug would once more have taken place, stripping off most of the remaining lavas and Mesozoic rocks - apart from the lower fault bounded blocks trapped, by resurgent uplift, at lower levels.

There is evidence on Rhum of major erosion, in the form of coarse pebble conglomerates beneath the north-west Rhum lavas (Emeleus 1985), but these must have been formed after the emplacement of the Ultrabasic Complex. The conglomerates contain clasts of acidic rocks (both granophyre and felsite), large quantities of Torridonian sediments and Lewisian gneiss, basaltic fragments (some of which show chemistries similar to the early plateau lavas - Chapter 4) and, importantly, a few clasts of allivalite. However, NO unequivocal examples of Mesozoic clasts have yet been identified. As these conglomerates contain allivalite clasts the erosive event which produced them must have begun to unroof the Layered Complex. Therefore these conglomerates can not provide evidence for erosion caused by resurgent uplift of the central plug, as a consequence of the emplacement of the ultrabasic rocks at depth.

The Rhum Caldera mega-breccias, collapse breccias and pyroclastic deposits would have lain above the evacuated acidic magma chamber, therefore, on emplacement of basic/ultrabasic magma into this chamber, they would form roof material. Such roof like relationships are seen on Beinn nan Stac where explosion breccia, felsite and Torridonian sediments inside the MRF (Fig.2) (plus presumably the whole MRF zone of south-east Rhum) overlie the layered ultrabasics as seen in Plate 2.18 (cf Smith 1985 figure 3 to Plate 2.18). Layering in the ultrabasics is developed almost directly up to the contact, presumably because the overlying caldera fill was already pre-heated prior to emplacement of ultrabasics by convected and conducted heat from the original acid magma chamber, consequently any chilling was minimised.

Generally hybrids and 'marginal gabbro' are present along the margins of the ultrabasic rocks (section 2.g). As already stated hybrids and marginal gabbro can be seen to form either in situ (such as below the summit of Beinn nan Stac) or as discrete intrusions (such as north of Allt nam Bà and in the SMC - R. Greenwood pers comm.). Such phenomena are easily explained by the model outlined above, as the ultrabasic liquid is injected into the partially evacuated acid magma chamber ultrabasic and any remaining acid liquid can readily mix to produce hybrids (along with intense convection and vesiculation). The production of hybrids by such a mixing process is rather more feasible than producing all hybrids by in-situ anatectic melting of surrounding crustal rocks (predominantly Torridonian arkose). Anatectic melting requires a great deal of energy applied to the system to produce even a small amount of remelting (D.M.Hirst pers. comm). Undoubtedly some in-situ melting has taken place (the gradational contacts observed in places below the summmit of Beinn nan Stac - Fig.2), and is proven by isotope data from a number of hybrid/ultrabasic junctions (R. Greenwood pers. comm.) but such hybridisation is complimented by those produced by magma mixing. Evidence for the co-existence of acid and basic magmas and resultant magma mixing is also documented from elsewhere in the BTVP: Thompson 1980, 1982. Thompson et al. 1986. Marshall and Sparks 1984.

In conclusion therefore magma mixing seems to have played an intrinsic part in the development of many intrusive centres in the BTVP not least of which in the emplacement of the Rhum Volcanic Complex.

Appendices - Contents.

Appendix 1 - X-Ray Fluorescence analysis Technique.

Appendix 2 - CIPW Norm Calculation Program 'normcal'

Appendix 3 - Smith N.J. 1985. Reprint from The Geological Magazine. Volume 122 No. 5. p439-445. 'The Age and Structural Setting of Limestones and Basalts on the Main Ring Fault in south-east Rhum'

Appendix 4 - Emeleus C.H, Wadsworth W.J, Smith N.J. 1985. Reprint from the Geological Magazine. Volume 122 No. 5 p451-457. 'The Early Igneous and Tectonic History of the Rhum Tertiary Volcanic Centre'.

Appendix 1

X-ray Fluorescence analysis

Introduction

A1.a Preparation of samples

A1.a.i Rock grinding

A1.a.ii Production of fused glass beads

A1.a.iii Production of pressed powder pellets

A1.b Data reduction techniques

A1.b.i Major elements

A1.b.ii Trace elements

Plates and Tables

X-Ray Fluorescence - Introduction

Analysis of silicate rock and mineral samples was carried out by x-ray fluorescence (XRF) methods using a Phillips PW 1400 XRF spectrometer (Plate A.1). Rock samples were analysed for 10 major and 18 trace elements:-

Major elements; Si, Al, Fe, Mg, Ca, Na, K, Ti, Mn, P.

Trace elements; Ba, Nb, Zr, Y, Sr, Rb, Zn, Cu, Ni, Pb, U, Th, Cr, Nd, La, Ce, Ga, V.

Following convention major elements were determined as oxides and expressed as weight percent, and trace elements calculated as parts per million (PPM).

Fused glass beads were used for major element analysis, after the method of Norrish and Hutton (1969), whilst for trace elements whole rock pressed powder pellets were used. Sample preparation techniques are described in Section A1.a.

Raw count data obtained from the XRF spectrometer was compared statistically to international standard samples of precisely determined composition and calibration curves plotted. Data reduction techniques are described in section A1.b. All analyses were corrected for mass absorbtion effects using the tables published by Heinrich (1966). A discussion of the theory of XRF analysis is beyond the scope of this project but it is discussed in detail in Jenkins and de Vries (1967), Norrish and Chappell (1977).

A1.a Preparation of samples

A1.a.1 Rock grinding.

Rocks for both major and trace element analyses have first to be ground to a fine powder. Grinding techniques are described in detail in Fitton, James and Thirlwall (1984). Basically a sample of around 100 grams of unweathered rock chips is placed in a 'Tema' swing mill and ground for around 3-4 minutes. The resulting fine powder should feel smooth if rubbed between thumb and forefinger, if it does not then continue grinding for a further minute before repeating the test.

A1.a.ii Production of fused glass beads.

1. Powdered rock samples were first dried at 110 degrees celsius for around an hour.

2. Between 0.45 and 0.5 grams of dried sample were accurately weighed into a clean Pt/Au crucible. The weight of the crucible and crucible + sample were recorded.

3. The weight of sample (from 2 above) was multiplied by 5.000 to give the weight of flux to be added. The weight of crucible + sample + flux was calculated and recorded.

4. Flux (Johnson Mathey 'Spectroflux 105') was added to make up to the total calculated in 3. above. The flux was dried overnight at 500 degrees celsius to expel any flux volatiles and the dried flux kept in a desiccator during the work period.

5. The crucibles, covered with Pt lids, were placed on a silica tray and put in a furnace at 1050 celsius for at least 20 minutes.

6. The resulting molten liquid was then taken out of the furnace and swirled to ensure thorough mixing. The melt was then poured onto a graphite disc surrounded by a stainless steel collar and the fusion bead formed by moulding the molten bead with an aluminium plunger. The whole operation from furnace to fusion bead should take around 10 seconds, the plunger was removed from the cast bead after about 5 seconds. The aluminium plunger and graphite discs were kept on a hotplate

maintained at 220 celsius to avoid quenching of the melt. The platinum crucible with any remaining globules of melt were placed onto a Meker burner.

7. The stainless steel collar was then removed from the graphite disc and the graphite disc and fusion bead covered with a silica dish. The fusion bead should have a uniform 'orange peel' surface texture, if it does not or is wedge-shaped or cracked then break it up and replace the fragments in the Pt crucible, replace lid, reheat until fused, and repeat step 6.

8. The crucible was removed from the Meker burner and any remaining droplets of melt shaken out into a beaker of de-mineralised water. The crucible was then quenched in the water to dislodge any remaining glass and then placed in warm 50% HCl for 10-15 minutes. The now clean crucible was then rinsed in de-mineralised water before being dried in the oven at 110 celsius.

9. After about five minutes the graphite disc and mould were removed to the cooling block. When cool (about 1 hour) the fusion bead was trimmed with pliers to remove any excess glass and a self adhesive identification label applied to the non analytical surface (the side in contact with the graphite disc). After numbering, the bead was put into a self sealing polythene bag making sure NOT to touch the analytical surface with the fingers.

The equipment used for the preparation of fused glass beads is shown in Plate A.2.

A1.a.ii Preparation of pressed powder pellets.

1. Approximately 7 grams of rock powder were weighed into a clean glass beaker. Pellets should NOT be made with less than 5 grams of powder.

2. Six drops of 'Mowiol' (2% aqueous soution of PVA) were added to the beaker of rock powder.

3. This was mixed thoroughly with a glass rod for around 2 minutes, or until an even consistency was obtained.

4. The powder was then put into the assembled stainless steel mould (Plate A.3) and tamped down using a glass tamping rod.

5. The stainless steel plunger was then inserted into the mould and the fully assembled mould placed under the hydraulic press.

6. The mould was compressed at about 7 tons

pressure for a minute before the pressure was slowly released.

7. The mould was carefully dismantled and the pellet removed, taking care not to touch the analytical surface of the pellet.

8. The pellet was identified by writing on one surface with a soft fibre pen before being placed analytical side uppermost in pellet trays.

9. All components of the mould were thoroughly washed in warm water and dried after each sample.

10. Prior to analysis all pellets were dried in an oven at 110 celsius for around 10 minutes.

A1.b Data collection and reduction techniques.

A1.b.i Major elements

At Durham the normal method for major element analysis was to use whole rock pressed powder pellets. However, as an experiment it was decided to use fused glass beads. Fusion beads are a preferred method over whole rock pellets because of their better homogeneity and, because of the lower concentration of elements in the bead, inter-elemental and mass absorbtion effects are reduced.

Twenty international standards (Table A1.1) were prepared as both fusion beads and pressed powder pellets using the methods outlined in section A1.a. Each set of standards was then run through the XRF spectrometer to obtain raw count data. The raw counts were then processed in two ways; using the MTS statistics package 'Midas', and a program written by C.R. Watson called 'XRF.QD'.

The MIDAS method

This involved plotting the raw count data for each of the ten analysed elements (See Introduction) against the known concentration of that element in the standard (from

Abbey 1983). From these simple linear regression curves it would be expected that if there were no inter-elemental and mass absorbtion effects then a straight line centred on the origin would be obtained, however, there is always some interference. Consequently these calibration plots produced 2 coefficients for each element; first the gradient of the best fit line, and also the intercept of the line with the 'x' axis. Such plots of count rates v known composition were also inspected to see if the count rate was dependant upon the concentration of any other element in the sample. Certainly for fused beads inter element effects were found to be insignificant (Table A1.2).

The regression coefficients obtained above were then entered into the XRF logging and analysis program attached to the XRF spectrometer (Plate A.1a). The same international standards were then run as 'unknowns'. The logging program, using the regression coefficients entered above, then calculated the weight % oxide of each of the ten elements analysed in the 'Unknown' standards. The values obtained were then compared to accepted values (from Abbey 1983).

The XRF.QD method.

The raw count data for the standards, weight % composition of the standards and the raw counts for standards run as 'unknowns' were carefully formatted into an input file. This input file was then run as the data set for the program XRF.QD.

The main difference between XRF.QD and 'Midas' is that instead of using a simple linear regression (applying an equation of the form $y = ax + c$) XRF.QD uses a quadratic fit (ie. applies an equation of the form $y = ax^2 + bx + c$). Also XRF.QD corrects for mass absorbtion (from Heinrich 1966) and all results are normalised to 100 %.

Both the Midas and XRF.QD methods were carried out on 20 international standards and on both fused beads and powder pellets.

Table A1.3 shows results for 10 of the international samples run as 'unknowns' and showing the variation in accepted values with those obtained using Midas and XRF.QD. These results in Table A1.3 were obtained using only fused glass beads. Table A1.4 however,is a comparison table of both fusion and neat powder pellets, with the results expressed as a percentage of the relative mean deviation from the accepted compositional value from Abbey (1983).

From table A1.4 it can be seen that using fusion beads and simple linear regression coefficients (Midas) gives superior results to neat pellets using either a quadratic fit (XRF.QD) or Midas. That is except for sodium analyses, the lightest major element analysed (At. No. 11, At. mass 23). Here concentration of sodium in the fused glass sample is adversely affected by volatilization of sodium during the heating phase of the production of the fused bead.

Using whole rock powder pellets the best major element analyses were obtained using XRF QD. (Table A1.4).

In this thesis all major element analysis of Rhum samples was carried out using fusion beads.

A1.b.ii Trace element analyses

The techniques used to analyse for trace elements is similar to that used for major elements, except that because of the generally low concentrations of these elements in a sample fused beads cannot be used and counting times are also increased.

All samples were analysed for 18 trace elements and calibration made using 12 international standards. The trace elements analysed were; Ba, Nb, Zr, Y, Sr, Rb, Zn, Cu, Ni, Pb, U, Th, Cr, Nd, La, Ce, Ga, V. and the results obtained were expressed in parts per million (ppm)

Data reduction was carried out using R.C.O. Gill's program 'Tratio'. This program uses a simple linear regression calibration (see section A1.b.i), although correction is made for mass absorbtion and inter-elemental effects including Kb line interference where necessary.

Table A1.5 shows a comparison of the accepted values for trace element concentrations in international standards against the same standards run as 'unknowns'.

Plate A.I Phillips PW I400 X-Ray fluorescence spectrometer, note the remote sample changer in the foreground.

<u>Plate A.Ia</u> Shows microcomputers for controlling the XRF spectrometer and the printer used for obtaining 'hard' copies of results produced by the internal 'Logging and Analysis Program' - either the raw count data or weight % composition if regression coefficients have been entered (see Section A.I.b).

Plate A.2 Apparatus used in the production of fused glass beads.

I) Platinum crucibles on silica tray ready to be put into 2)

2) Furnace - maintained at I050 celsius.

3) Hotplate - maintained at 220 celsius

4) Graphite moulds and stainless steel collar

5) Aluminium plunger

6) Freshly cast bead covered with silica dish

7) Meker burner

8) Cast beads on cooling block

9) Pt tipped tongs,and pliers used for trimming finished beads.

IO) Finished bagged and labled fusion beads.

Plate A.3 Equipment used in the production of neat powder pellets.

I) Beaker for mixing rock powder with 'Mowiol'

2) 'Mowiol' - a 2% aqueous solution of PVA

3) Stainless steel pellet mould

4) Hydraulic press

5) Oven maintained at II0 celsius for drying finished pellets prior to analysis.

Table A1.1

ACCEPTED INTERNATIONAL STANDARD COMPOSITIONS (wt % oxide)
(Abbey 1983)

	ELEMENT										
	SiO_2	Al_2O_3	Fe_2O_3	MgO	CaO	Na_2O	K_2O	TiO_2	MnO	P_2O_5	
AGV-1	59.61	17.19	6.79	1.52	4.94	4.32	2.92	1.06	0.10	0.51	AGV-1
BR	38.39	10.25	12.90	13.35	13.87	3.07	1.41	2.61	0.20	1.05	BR
G2	69.22	15.40	2.69	0.75	1.96	4.06	4.46	0.48	0.03	0.13	G2
PCC1	42.10	0.73	8.28	43.50	0.55	0.01	0.00	0.01	0.12	0.10	PCC1
MRG1	39.32	8.50	17.82	13.49	14.77	0.71	0.18	3.69	0.17	0.06	MRG1
DTS1	40.61	0.25	8.70	49.80	0.14	0.01	0.00	0.00	0.12	0.00	DTS1
GSP1	67.32	15.28	4.30	0.97	2.03	2.81	5.51	0.66	0.04	0.28	GSP1
SY2	60.10	12.12	6.30	2.70	7.98	4.34	4.48	0.14	0.32	0.43	SY2
SY3	59.68	11.80	6.41	2.67	8.26	4.15	4.20	0.15	0.32	0.54	SY3
SY1	59.50	9.60	8.22	4.20	10.20	3.30	2.67	0.49	0.40	0.22	SY1
GA	69.96	14.51	2.77	0.95	2.45	3.55	4.03	0.38	0.09	0.12	GA
G1	72.64	14.04	1.93	0.38	1.39	3.32	5.48	0.26	0.03	0.09	G1
BLANK	100	0.00	0.00	0.00	0.00	0.00	0.00	0.00	0.00	0.00	BLANK
DRN	52.85	17.52	9.69	4.40	7.05	2.99	1.70	1.09	0.22	0.25	DRN
GSN	65.8	14.67	3.77	2.30	2.50	3.77	4.63	0.68	0.056	0.28	GSN
UBN	39.43	2.90	8.45	35.28	1.20	0.10	0.02	0.11	0.12	0.04	UBN
NIM-P	51.10	4.18	12.77	25.33	2.66	0.37	0.09	0.20	0.22	0.02	NIM-P
NIM-S	63.63	17.34	1.40	0.46	0.68	0.43	15.35	0.04	0.01	0.12	NIM-S
NIM-D	68.96	0.30	16.95	43.51	0.28	0.04	0.01	0.02	0.22	0.02	NIM-D
NIM-L	52.40	13.64	9.99	0.28	3.22	8.37	5.51	0.48	0.77	0.06	NIM-L
NIM-N	52.64	16.50	8.90	7.50	11.50	2.46	0.00	0.20	0.18	0.03	NIM-N

Composition of international standards (from Abbey 1983) expressed in weight % oxide.

** Logging and analysis program for PU1400 **

J.M.L. August 1980

Do you want to enter regression coefficients(YES/NO)? YES

To leave coefficient unchanged just hit return

To jump to next element enter a slash (/)

REGRESSION COEFFICIENTS SHOWING INTER-ELEMENT CORRECTIONS

FUSED DISC. COEFFICIENTS SHOWING SIGNIFICANT INTER-ELEMENT CORRECTIONS

Coefficients for Si

Constant	:-4.3935	:? 4.8546 (CONSTANT)
Si	: .010625	:? .77447E-2 (SLOPE)
Al	: 0	:?
Fe	: 0	:?
Mg	: 0	:?
Ca	: 0	:?
Na	: 0	:?
K	: 0	:?
Ti	: 0	:?
Mn	: 0	:?
P	: 0	:?
S	: 0	:?
Si^2	:-2.2744E-07	:? 0

Coefficients for Al

Constant	: .18047	:? -.29712
Al	: 9.5386E-03	:? .97914E-2
Si	: 0	:?
Fe	: 0	:?
Mg	: 0	:?
Ca	: 0	:? .83467E-4
Na	: 0	:?
K	: 0	:?
Ti	: 0	:?
Mn	: 0	:?
P	: 0	:?
S	: 0	:?
Si^2	: 0	:?

.83467E-4 — INTER ELEMENTAL INTERACTION CORRECTION FACTOR (PRODUCED USING POLYNOMIAL REGRESSION)

Coefficients for Mg

Constant	:-.08168	:? 1.2891
Mg	: .064358	:? .63683E-1
Si	: 0	:? -.11065E-3
Al	: 0	:? -.81212E-3
Fe	: 0	:?
Ca	: 0	:?
Na	: 0	:?
K	:-2.9479E-04	:? 0
Ti	: 0	:?
Mn	: 0	:?
P	: 0	:?
S	: 0	:?
Si^2	: 0	:?

Coefficients for Ca

Constant	: .25196	:? .1775E-1
Ca	: 1.6799E-03	:? .162E-2
Si	: 0	:?
Al	: 0	:?
Fe	: 0	:?
Mg	: 0	:?
Na	: 0	:?
K	: 0	:? .5048E-4
Ti	:-9.7441E-05	:? -.30064E-4
Mn	:-6.3494E-04	:? 0
P	: 0	:?
S	: 0	:?
Si^2	: 0	:?

Coefficients for Na

Constant	: .86952	:? -.49478
Na	: .19844	:? .27974
Si	: 0	:?
Al	: 0	:?
Fe	: 0	:?
Mg	:-2.3108E-03	:? 0
Ca	: 0	:?
K	: 0	:?
Ti	: 0	:?
Mn	: 0	:?
P	: 0	:?
S	: 0	:?
Si^2	: 0	:?

Coefficients for K

Constant	:-.078233	:? -.2928E-1
K	: 1.6988E-03	:? .17131E-2
Si	: 0	:?
Al	: 0	:?
Fe	: 0	:?
Mg	: 0	:?
Ca	: 0	:?
Na	: 0	:?
Ti	: 0	:?
Mn	: 0	:?
P	: 0	:?
S	: 0	:?
Si^2	: 0	:?

Coefficients for Ti

Constant	:-.38468	:? -.3898
Ti	: 2.3838E-04	:? .28152E-3
Si	: 0	:?
Al	: 0	:?
Fe	: 0	:?
Mg	: 0	:?
Ca	: 7.0826E-05	:? .80214E-5
Na	: 0	:?
K	:-1.5697E-05	:? 0
Mn	:-5.1016E-04	:? 0
P	:-3.5083E-04	:? 0
S	: 0	:?
Si^2	: 0	:?

Coefficients for Mn

Constant	:-.029518	:? .136E-1
Mn	: 5.316E-04	:? .49993E-3
Si	: 0	:?
Al	: 4.4383E-05	:? 0
Fe	: 0	:?
Mg	: 4.891E-05	:? 0
Ca	: 0	:?
Na	:-1.7311E-03	:? 0
K	: 0	:?
Ti	: 0	:?
P	:-4.8176E-05	:? 0
S	: 0	:?
Si^2	: 0	:?

Coefficients for Fe

Constant	:-.91994	:? -.15449
Fe	: 4.3643E-04	:? .40633E-3
Si	: 0	:?
Al	: 4.5778E-04	:? 0
Mg	: 0	:?
Ca	: 0	:?
Na	: 0	:?
K	: 0	:?
Ti	: 0	:? .8111E-4
Mn	: 0	:?
P	: 0	:?
S	: 0	:?
Si^2	: 0	:?

Coefficients for P

Constant	:-.10494	:? -.9956E-1
P	: 5.8236E-03	:? .5808E-2
Si	: 0	:?
Al	: 0	:?
Fe	: 0	:?
Mg	: 0	:?
Ca	: 0	:?
Na	: 0	:?
K	: 0	:?
Ti	: 0	:?
Mn	: 0	:?
S	: 0	:?
Si^2	: 0	:?

Are all values correct (YES/NO)? YES

Readv to log ****

Table A1.3 Fusion Bead Standards - run as 'unknowns' - comparison of data reduction techniques.

Element SiO_2 (Wt. % oxide).

	Midas method		XRF.QD method	
	Value	Diff.	Value	Diff.
AGV1	60.27	+0.66	60.12	+0.51
BR	38.87	+0.48	38.75	+0.36
G2	68.19	-1.03	68.84	-0.38
PCC1	42.27	+0.17	43.27	+1.17
MRG1	39.69	+0.37	38.28	-1.04
DTS1	40.58	+0.03	40.12	-0.49
GSP1	66.50	-0.82	67.74	+0.42
SY2	60.40	+0.30	59.69	-0.41
SY3	59.10	-0.58	59.88	+0.20
SY1	59.05	-0.45	59.77	+0.27
GA	69.09	-0.87	70.66	+0.70
G1	72.14	-0.50	71.81	-0.83
Si BLNK.	100.61	+0.61	100.49	+0.49
		$\bar{X}$ 0.57		$\bar{X}$ 0.86
		* 0.95%		* 1.14%

$\bar{X}$ = MEAN DEVIATION OF ALL 21 STANDARDS

* = MEAN RELATIVE DEVIATION OF ALL 21 STANDARDS (AS %)
(See also Table A1.4).

Accepted standard compositions are given in Table A1.1

Table A1.3 continued.....

Table A1.3 Fusion bead Standards - run as 'unknowns' - comparison of data reduction techniques.

Element Al_2O_3 (Wt. % oxide).

	Midas method		XRF.QD method	
	Value	Diff.	Value	Diff.
AGV1	17.71	+0.52	16.95	-0.21
BR	10.30	+0.05	10.21	-0.04
G2	15.29	-0.11	14.95	-0.45
PCC1	0.87	+0.14	0.73	0.00
MRG1	8.76	+0.26	8.62	+0.12
DTS1	0.31	+0.06	0.13	-0.12
GSP1	15.01	-0.27	15.08	-0.20
SY2	12.63	+0.51	12.23	+0.11
SY3	11.88	+0.08	11.76	-0.04
SY1	9.56	+0.04	9.35	-0.25
GA	14.89	+0.38	14.74	+0.23
G1	14.33	+0.29	13.96	-0.08
Si BLNK.	0.00	0.00	0.00	0.00
		$\bar{X}$ 0.18		$\bar{X}$ 0.22
		* 1.6%		* 2.0%

$\bar{X}$ = MEAN DEVIATION OF ALL 21 STANDARDS

* = MEAN RELATIVE DEVIATION OF ALL 21 STANDARDS (AS %) (See also Table A1.4).

Accepted standard compositions are given in Table A1.1

Table A1.3 continued......

Table A1.3. Fusion bead Standards - run as 'unknowns' - comparison of data reduction techniques.

Element Fe2O3 (Wt. % oxide).

	Midas method		XRF.QD method	
	Value	Diff.	Value	Diff.
AGV1	6.79	0.00	6.79	0.00
BR	13.07	+0.17	13.69	+0.79
G2	2.61	-0.08	2.26	-0.43
PCC1	9.09	+0.81	8.10	-0.18
MRG1	17.88	+0.06	18.06	+0.24
DTS1	9.12	+0.42	7.80	-0.90
GSP1	4.23	-0.07	4.39	+0.09
SY2	6.28	-0.02	6.56	+0.26
SY3	6.39	-0.02	6.77	+0.36
SY1	8.24	+0.02	8.56	+0.34
GA	2.68	-0.09	2.76	-0.01
G1	1.95	+0.02	1.98	+0.05
Si BLNK.	0.01	+0.01	0.00	0.00
		$\bar{X}$ 0.20		$\bar{X}$ 0.30
		* 2.6%		* 3.9%

$\bar{X}$ = MEAN DEVIATION OF ALL 21 STANDARDS

* = MEAN RELATIVE DEVIATION OF ALL 21 STANDARDS (AS %) (See also Table A1.4).

Accepted standard compositions are given in Table A1.1

Table A1.3 continued.....

Table A1.3 Fusion bead Standards - run as 'unknowns' - comparison of data reduction techniques.

Element MgO (Wt. % oxide).

	Midas method		XRF.QD method	
	Value	Diff.	Value	Diff.
AGV1	1.79	+0.27	1.47	-0.05
BR	13.42	+0.07	13.10	-0.25
G2	0.43	-0.32	0.93	+0.18
PCC1	43.44	-0.06	43.68	+0.18
MRG1	13.69	+0.20	13.20	-0.29
DTS1	49.59	-0.21	48.65	-0.15
GSP1	0.82	-0.15	1.01	+0.04
SY2	3.22	+0.52	2.79	+0.09
SY3	3.13	+0.46	2.59	-0.08
SY1	4.09	-0.11	4.13	-0.07
GA	1.30	+0.35	0.92	-0.03
G1	0.23	-0.15	0.59	+0.21
Si BLNK.	-0.13	-0.13	0.23	+0.23
		$\bar{X}$ 0.28		$\bar{X}$ 0.14
		* 1.9%		* 0.9%

$\bar{X}$ = MEAN DEVIATION OF ALL 21 STANDARDS

* = MEAN RELATIVE DEVIATION OF ALL 21 STANDARDS (AS %) (See also Table A1.4).

Accepted standard compositions are given in Table A1.1

Table A1.3 continued.....

Table A1.3 Fusion bead Standards - run as 'unknowns' - comparison of data reduction techniques.

Element CaO (Wt. % oxide).

	Midas method		XRF.QD method	
	Value	Diff.	Value	Diff.
AGV1	5.06	+0.12	4.80	-0.14
BR	13.98	+0.11	13.74	-0.13
G2	2.09	+0.13	1.8	-0.16
PCC1	0.54	-0.01	0.50	-0.05
MRG1	14.88	+0.11	14.71	-0.06
DTS1	0.18	+0.04	0.07	-0.07
GSP1	1.96	-0.07	1.86	-0.17
SY2	8.17	+0.19	7.70	-0.28
SY3	8.32	+0.06	8.17	-0.09
SY1	10.08	-0.12	9.89	-0.31
GA	2.59	+0.14	2.36	-0.09
G1	1.40	+0.01	1.14	-0.35
Si BLNK.	0.03	+0.03	0.00	0.00
		$\bar{X}$ 0.11		$\bar{X}$ 0.17
		* 2.6%		* 4.0%

$\bar{X}$ = MEAN DEVIATION OF ALL 21 STANDARDS

* = MEAN RELATIVE DEVIATION OF ALL 21 STANDARDS (AS %) (See also Table A1.4).

Accepted standard compositions are given in Table A1.1

Table A1.3 continued.....

Table A1.3 Fusion bead Standards - run as 'unknowns' - comparison of data reduction techniques.

Element Na_2O (Wt. % oxide).

	Midas method		XRF.QD method	
	Value	Diff.	Value	Diff.
AGV1	4.60	+0.28	3.85	-0.47
BR	3.28	+0.21	2.71	-0.36
G2	3.87	-0.19	4.65	+0.61
PCC1	-0.09	-0.10	0.37	+0.36
MRG1	0.78	+0.07	0.28	-0.43
DTS1	0.16	+0.15	0.00	-0.01
GSP1	2.78	-0.03	2.52	-0.29
SY2	4.63	+0.29	4.18	-0.16
SY3	4.10	-0.05	4.16	+0.01
SY1	3.39	+0.09	3.15	-0.15
GA	3.70	+0.15	3.02	-0.53
G1	3.14	-0.18	3.93	+0.61
Si BLNK.	-0.43	-0.43	0.65	+0.65
		$\bar{X}$ 0.25		$\bar{X}$ 0.38
		* 6.3%		* 9.5%

$\bar{X}$ = MEAN DEVIATION OF ALL 21 STANDARDS

* = MEAN RELATIVE DEVIATION OF ALL 21 STANDARDS (AS %) (See also Table A1.4).

Accepted standard compositions are given in Table A1.1

Table A1.3 continued.....

Table A1.3 Fusion bead Standards - run as 'unknowns' - comparison of data reduction techniques.

Element K2O (Wt. % oxide).

	Midas method		XRF.QD method	
	Value	Diff.	Value	Diff.
AGV1	2.93	+0.01	2.93	+0.01
BR	1.37	-0.04	1.39	-0.02
G2	4.5	+0.04	4.37	-0.09
PCC1	0.01	+0.01	0.00	0.00
MRG1	0.18	0.00	0.15	-0.03
DTS1	0.00	0.00	0.00	0.00
GSP1	5.49	-0.02	5.45	-0.06
SY2	4.55	+0.07	4.46	-0.02
SY3	4.24	+0.04	4.22	+0.02
SY1	2.65	-0.02	2.61	-0.06
GA	4.07	+0.04	4.13	+0.10
G1	5.55	+0.07	5.45	-0.03
Si BLNK.	0.00	0.00	0.00	0.00
		$\bar{X}$ 0.03		$\bar{X}$ 0.04
		* 1.1%		* 1.3%

$\bar{X}$ = MEAN DEVIATION OF ALL 21 STANDARDS

* = MEAN RELATIVE DEVIATION OF ALL 21 STANDARDS (AS %)
(See also Table A1.4).

Accepted standard compositions are given in Table A1.1

Table A1.3 continued.....

Table A1.3 Fusion bead Standards - run as 'unknowns' - comparison of data reduction techniques.

Element MnO (Wt. % oxide).

	Midas method		XRF.QD method	
	Value	Diff.	Value	Diff.
AGV1	0.11	+0.01	0.11	+0.01
BR	0.2	0.00	0.22	+0.02
G2	0.04	+0.01	0.04	+0.01
PCC1	0.12	0.00	0.10	-0.02
MRG1	0.17	0.00	0.19	+0.02
DTS1	0.12	0.00	0.10	-0.02
GSP1	0.04	0.00	0.05	+0.01
SY2	0.32	0.00	0.31	-0.01
SY3	0.33	+0.01	0.33	+0.01
SY1	0.40	0.00	0.40	0.00
GA	0.08	-0.01	0.08	-0.01
G1	0.03	0.00	0.04	+0.01
Si BLNK.	0.00	0.00	0.00	0.00
	$\bar{X}$	0.005	$\bar{X}$	0.013
	*	2.5%	*	6.5%

$\bar{X}$ = MEAN DEVIATION OF ALL 21 STANDARDS

* = MEAN RELATIVE DEVIATION OF ALL 21 STANDARDS (AS %)
(See also Table A1.4).

Accepted standard compositions can be found on Table A1.1

Table A1.3 continued.....

Table A1.3 Fusion bead Standards - run as 'unknowns' - comparison of data reduction techniques.

Element TiO_2 (Wt. % oxide).

	Midas method		XRF.QD method	
	Value	Diff.	Value	Diff.
AGV1	1.05	-0.01	1.05	-0.01
BR	2.64	+0.03	2.70	+0.09
G2	0.47	-0.01	0.49	+0.01
PCC1	0.00	-0.01	0.00	-0.01
MRG1	3.66	-0.03	3.66	-0.03
DTS1	-0.02	-0.02	0.00	0.00
GSP1	0.66	0.00	0.68	+0.02
SY2	0.15	+0.01	0.16	+0.02
SY3	0.17	+0.02	0.17	+0.02
SY1	0.48	-0.01	0.50	+0.01
GA	0.34	-0.04	0.37	-0.01
G1	0.24	-0.02	0.27	+0.01
Si BLNK.	0.00	0.00	0.00	0.00
		$\bar{X}$ 0.017		$\bar{X}$ 0.016
		* 2.4%		* 2.3%

$\bar{X}$ = MEAN DEVIATION OF ALL 21 STANDARDS

* = MEAN RELATIVE DEVIATION OF ALL 21 STANDARDS (AS %) (See also Table A1.4).

Accepted standard compositions are shown on Table A1.1

Table A1.3 continued.....

Table A1.3 Fusion bead Standards - run as 'unknowns' - comparison of data reduction techniques.

Element P205 (Wt. % oxide).

	Midas method		XRF.QD method	
	Value	Diff.	Value	Diff.
AGV1	0.50	-0.01	0.49	-0.02
BR	1.07	+0.02	1.08	+0.03
G2	0.18	+0.05	0.18	+0.05
PCC1	---	---	---	---
MRG1	0.06	0.00	0.06	0.00
DTS1	0.04	+0.04	0.04	+0.04
GSP1	0.29	+0.01	0.29	+0.01
SY2	0.48	+0.05	0.46	+0.03
SY3	0.55	+0.01	0.54	0.00
SY1	0.24	+0.02	0.23	+0.01
GA	0.10	-0.02	0.10	-0.01
G1	0.05	-0.04	0.05	-0.04
Si BLNK.	0.00	0.00	0.00	0.00
		$\bar{X}$ 0.02		$\bar{X}$ 0.02
		* 8.7%		* 8.7%

$\bar{X}$ = MEAN DEVIATION OF ALL 21 STANDARDS

* = MEAN RELATIVE DEVIATION OF ALL 21 STANDARDS (AS %) (See also Table A1.4).

Accepted standard compositions can be found on Table A1.1

Table A1.4 - Comparison Table, Fusion Beads versus Powder Pellets - expressed as percentage mean relative deviation.

	Neat Pellets		Fusion Beads	
	Midas	XRF.QD	Midas	XRF.QD
SiO_2	0.88	0.98	0.95	0.71
Al_2O_3	1.8	4.2	1.6	2.0
Fe_2O_3	5.0	2.8	2.6	3.9
MgO	4.1	2.5	1.9	0.9
CaO	4.9	2.1	2.6	4.0
Na_2O	3.0	3.3	6.3	9.5
K_2O	2.0	2.7	1.1	1.3
TiO_2	3.5	3.9	2.4	2.3
MnO	8.5	2.4	2.5	6.5
P_2O_5	11.3	3.2	8.7	8.7
S	2.0	2.0	-	-

All values are expressed in percent.

Table A.1.5

Element	Standard																							
	SY-1		DR-N		UB-N		G-2		BR		BCR-1		PCC-1		DTS-1		GA		MRG-1		GSP-1		SY-2	
	Acc.	Cal.	Acc.	Cal.	Acc.	Cal.	Acc.	Cal	Acc.	Cal.	Acc.	Cal	Acc.	Cal.	Acc.	Cal.	Acc.	Cal.	Acc.	Cal.	Acc.	Cal.	Acc.	Cal.
Ba	282	289	385	408	30	22	1900	1886	1050	1129	250	313	4	0	5	0	850	827	50	36	1300	1289	460	473
Nb	—	—	6	7	0	0	13	9	0	0	19	13	1	0	0	0	10	12	20	20	23	10	23	—
Zr	—	—	125	133	8	4	300	298	250	313	185	182	7	1	12	0	150	136	105	105	500	396	280	160
Y	—	—	30	21	11	1	11	0	30	24	40	32	0	0	0	0	21	5	16	10	29	3	130	—
Sr	—	—	400	391	10	11	480	493	0	0	370	325	0	0	0	0	310	318	260	252	240	240	275	251
Rb	195	123	70	69	6	6	170	166	47	44	47	46	0	2	0	2	175	177	8	10	250	249	220	206
Zn	219	237	145	133	92	86	84	86	150	145	125	110	41	39	40	51	80	98	190	195	45	103	250	—
Cu	—	—	50	45	28	39	10	13	72	48	16	26	—	22	8	17	16	21	135	119	33	36	5	7
Ni	43	39	16	14	—	—	4	5	260	255	10	11	—	—	—	—	7	6	195	202	9	12	10	13
Pb	—	—	—	—	18	16	30	31	8	6	14	15	11	11	11	12	30	31	10	9	54	—	—	—
U	—	—	1	1	0	0	2	1	3	3	2	2	5	1	0	0	4	2	0	0	2	1	—	—
Th	—	—	5	8	0	4	25	28	12	9	6	5	10	4	0	4	17	16	1	0	105	—	—	—
V	89	62	225	228	75	57	36	55	235	234	420	412	30	22	—	—	38	59	520	485	54	85	52	46
Cr	56	49	42	42	—	—	8	6	380	370	15	26	—	—	—	—	12	18	450	458	12	7	12	17
Nd	—	—	22	28	—	—	58	54	60	60	26	28	0	4	—	—	25	30	19	8	190	—	71	70
Ga	20	20	22	19	5	4	23	24	20	16	22	21	1	2	—	—	16	17	18	15	23	22	28	29
La	233	187	21	25	0	3	92	133	80	83	27	36	0	17	0	13	38	58	10	4	195	—	88	97
Ce	—	—	46	40	0	0	160	164	0	101	53	33	0	2	0	5	70	69	25	16	360	—	210	125

Acc = Accepted international standard value

Calc = value obtained using program 'TRATIO' on standard run as 'unknown.

— = denotes concentration of element is outside the range of specified parameters.

ALL VALUES ARE FOR CONCENTRATION IN PARTS PER MILLION (PPM).

Appendix 2 - CIPW Norm calculations.

From the major element geochemistry determinations of basalts and hybrids from south-east Rhum, CIPW Norms and differentiation indices were calculated using the computer program 'NORMCAL' by R.C.O. Gill. This data was then used for plotting various graphs and tables in Chapter 4. An outline of how the program is used is given overleaf.

Table A2.1 shows an example of a summary norm table produced using 'NORMCAL'. The samples shown are predominantly sheared Tertiary basalts caught up in the MRF in south-east Rhum (see Chapter 4).

NORMCAL.

Language PL1

Author R.C.O.Gill.

Date September 1971.

Compile time

FUNCTION AND INTRODUCTION.

This program is a modified translation of an Atlas Autocode programme by R.F.Cheeney of Edinburgh University. It has been extended to offer normative data on a cation-equivalent basis as outlined by Barth,(Theoretical Petrology,1952); this scheme greatly simplifies hand recalculation, if this should prove necessary.A detailed account of the information produced appears in the tables at the end of these notes.

The program is stored on disc (MTS) in the NUMAC IBM 360/67 Computer at Newcastle-upon-Tyne, and may be accessed as GLT9:NORMPL1 from any users number.

Data to be run should be on punched cards, and chemical data can be in any order provided it is consistent throughout the batch and a specimen number appears at the beginning of each set, enclosed in single quotes, i.e. 'GILL456 ' . This string can contain 80 alphanumeric characters, although difficultycan be found if the string includes the single quotes used to encloseit.

There are no restrictions on format, except that it is advisable to leave the first column of every cardblank in case the last column of the previous card is filled and two numbers are thereby merged into one.

In its basic form, NORMCAL accepts internally consistent chemical analyses.The analytical process used in Durham does not, however, produce such analyses directly; each analysis consists of two parts. The elements determined by the X-R-F comprise one section in which the members have the correct proportions among themselves but (if the Holland and Brindleprocedure has been used) sum to 100 exclusive of the elements or groups determined by other methods. These separately determined elements make up the second group (for example, FeO, CO_2,Cl,H_2O) for which correction has to be made to all members of the first. A so-called ANRECAL option is avialable in NORCAL to make this and any other necessary corrections. If it is called, a corrected weight percent analysis appears at the head of each set of norm data. Note that no allowance is made for the mass absorption contribution of the separately determined components, which may be significant in some cases. Best results are obtained in such cases by introducing the separetly determined components into the X-R-F. correction procedure. The ANRECAL option need then only be used if correction for FeO is required.

INPUT ORDER AND PROGRAM DIRECTION.

There are a number of input orders in NORMCAL, and whichever one is used, and whether the ANRECAL option is called or not, the chemical data finally enters an array (1-30). The locations of the various elements in the array are fixed, whatever the sequence in which they are read in.The locations are as follows:

1. SiO_2
2. Al_2O_3
3. Fe_2O_3 (ferric or total iron,depending on Q. see later)
4. FeO
5. MgO
6. CaO
7. Na_2O
8. K_2O
9. H_2O^+
10. CO_2
11. TiO_2
12. P_2O_5
13. SO_3
14. S
15. Cl
16. F
17. MnO
18. ZrO_2
19. Cr_2O_3
20. Li_2O
21. BaO
22. Nb_2O_5

24.-30. Vacant. Not used for norm. May be used as sink for unwanted elements, e.g. CO_2 if the user wants a CO_2 free norm.

For directing data correctly into this array, either directly or through ANRECAL, a number of convienient input sequences are established in NORMCAL. Users may choose to conform to one of these in punching their data. A facility exists however for the user to set up his own input order in preference to one of the existing options. This facility will be refered to as "user directed input". Its use involves reference to the above table, (see later). Use of the user directed input is generally to be prefered.

Choice of the element sequence and control of the ANRECAL and user directed input options are effected by means of the interger Q, the first item in the input stream after the title. The options are listed below:

Q=1 or 2*	Established input orders, ANRECAL used.
Q=3 to 6	Established input orders, ANRECAL bypassed.
Q=9*	User directed input, ANRECAL used.
Q=10	User directed input, ANRECAL bypassed
Q=11	Controlled oxidation ratio option (user directed input, ANRECAL by-passed).

A special facility exists whereby, if Q= 50+ Q value as above, the user is able to determine for himself the conditions under which certain projections are printed out. Otherwise the projections are only calculated if the total of the components exceeds 75% of the wholenorm. For most purposes this facility may be ignored.

When a user directed input sequence is to be used (i.e. Q=9,10,11) the sequence must first be defined by a string of numbers following Q. The first is the number of the elements to be read in, N, and this is followed by N intergers: each interger represents an element, its position in the string is the same same as the position of the element in the input sequence and its value denotes the location of the element in the array, as defined by the table above.

* If ANRECAL is used, location 3 in the array initially contains total iron as Fe_2O_3, from which FeO is subtracted in the calculation. The same applies if Q=11, but in this case FeO is not given for each rock, (see below

Alternatively if a standard input sequence is to be used (Q=1,2,3,4,5,6,or11), the order of oxides and elements can be obtained by reference to the program listing. The sequence appear on the first and second pages, and are clearly labelled. For Q=1, the order can be read off at the point marked LAB(1), for Q=2, LAB(2), and so on. The order of oxide names is given in captions immediately preceeding these points.

Q=11 provides the facility for setting a constant value to Fe_2O_3/FeO. The value of this constant is given immediately after Q=11, and only total iron oxide is given for each analysis. FeO and Fe_2O_3 are calculated in the program.

The full data input sequence is as follows:

1. Batch title, up to 120 alphanumeric characters, enclosed in single quotes.

   e.g. 'DOLERITES FROM PASSION CREEK'

2. The value for Q (interger).

2a. If Q=9,10, or 11, the number of oxides N followed by numbers giving the order in which they are to be read in. All intergers.

2b. If Q=11, the value of Fe_2O_3/FeO (floating point).

3. Main data. Specimen identifier in single quotes, followed by N oxide values, repeated until data run finished.

Separate batches of data can be linked by placing a card bearing ' RESTART ' (the single quotes must be observed) between them. This returns the program to the very beginning, and items 1,2,2a(as appropriate) and 3 above must therefore be supplied afresh after each 'RESTART' card.

Treatment of Minor Elements

The following affinities are recognised:

MnO and NiO are added to FeO

BaO is added to CaO

Li_2O is added to K_2O

Negative Normative Minerals

The possibility of negative values arises for some normative minerals in cases of rock chemistry which are incompatible with the conventional CIPW normative scheme. This in general is not a failure of the scheme itself, but indicates an abnormal excess of some species, usually anionic, such that individual hand calculation is the only appropriate treatment. If one element persistently has a disruptuve effect in a set of data, the batch can probably be run without this element and the norms so obtained modified by hand to incorporate the element in question. This is the simplest using the equivalent norm, as advocated by Barth.

Summary Table

A summmary table giving the norms only in the form suitable for typing into a thesis or paper, is printed out when the input sequence or a 'RESTART' group within that sequence is completed.

Long jobs

With runs of more than 100 specimens, the following points should be observed:

(a) The storage available for the summary table facility is limited to 100 specimens (in order to keep Normcal jobs within Class C). Blocks greater than 50 should be broken down as necessary using 'RESTART' cards(introductory data must be given again after each of these cards). When a 'RESTART' card is met in the input sequence, the accumulated tabular data is printed out and the storage used is cleared for the next block

(b) For maximum turnaround with long jobs, it pays to calculate lines needed as accurately as possible. On average, salic rocks need 60 lines per specimen, mafic rocks 100 lines.

Over-riding preset limits for projections print-out

Each of the projections plag-qz-ol-diop, plag-ne-ol-diop and qz-ne-kp is only calculated if the sum of the constituents exceeds LIM(1), LIM(2) and LIM(3) respectively. In normal use, LIM defaults to 75% of the total norm. If the user wishes to apply other limits, the course of action is as follows.

1. Add 50 to the value of Q

2. Define the limit(s) to be applied, thus:

LIM(1) = 85; LIM(3) = 20;

This should appear on a card immediately preceding the first specimen card, i.e. after the other preliminary data. The semi-colons are essential but format is free.

It is not necessary to define all three numbers; those not defined default to 75. If Q = 50 and none are defined, a card bearing a semi-colon only must appear at this point in the deck.

Rhum norm calculations - data 24.5.85

NORMCAL .. R.C.O.GILL

SUMMARY NORM TABLE

	17-9	11-8	17-3	21-11	15-6	10-9	24-2	12-6	22-1	10-2	12-12	11-7
QUARTZ	0.0	3.8	0.0	0.0	0.0	13.2	0.0	47.2	37.0	0.0	0.0	11.8
ORTHOCLASE	0.4	6.4	4.1	1.3	12.7	19.7	5.8	27.8	14.2	5.2	1.7	9.8
ALBITE	28.1	22.0	21.0	31.8	36.9	47.1	24.2	19.5	32.5	8.2	15.4	19.2
ANORTHITE	33.0	25.4	39.2	30.0	13.4	2.7	30.8	0.0	4.4	32.2	41.4	22.9
NEPHELINE	0.0	0.0	0.0	0.0	0.8	0.0	0.7	0.0	0.0	5.1	5.9	0.0
ACMITE	0.0	0.0	0.0	0.0	0.0	0.0	0.0	0.2	0.0	0.0	0.0	0.0
DIOPSIDE	13.2	25.1	18.3	11.8	21.7	10.4	19.6	1.5	5.3	25.0	21.9	23.5
HYPERSTHENE	0.7	10.0	1.4	4.8	0.0	3.1	0.0	2.4	2.8	0.0	0.0	7.1
OLIVINE	12.2	0.0	10.5	7.9	7.0	0.0	12.6	0.0	0.0	14.0	8.1	0.0
MAGNETITE	6.5	3.8	3.5	6.3	4.0	2.0	4.7	0.6	1.6	3.9	3.3	3.3
ILMENITE	5.2	3.0	1.8	5.3	3.0	1.4	1.4	0.6	1.9	2.2	2.2	2.2
APATITE	0.6	0.4	0.2	0.7	0.4	0.5	0.2	0.1	0.3	0.2	0.2	0.2
DIFF. INDEX	28.6	32.2	25.1	33.1	50.5	80.0	30.7	94.5	83.6	21.4	23.0	40.8
NA/(NA+K)	0.99	0.79	0.84	0.96	0.76	0.72	0.52	0.43	0.71	0.83	0.94	0.67
(NA+K)/AL	0.31	0.37	0.25	0.37	0.67	0.93	0.35	1.01	0.85	0.32	0.25	0.40
F3/(F2+F3)	0.26	0.26	0.26	0.26	0.26	0.26	0.26	0.26	0.26	0.26	0.26	0.26

Rhum norm calculations - data 24.5.85

NORMCAL .. R.C.O.GILL

SUMMARY NORM TABLE

	21-10	16-9	21-3	g-1	pcc-1
QUARTZ	0.0	0.0	0.0	28.1	0.0
CORUNDUM	0.0	0.0	0.0	0.6	0.0
ORTHOCLASE	2.1	1.4	2.8	32.4	0.1
ALBITE	24.7	24.7	14.7	29.2	4.1
ANORTHITE	24.9	33.9	37.6	6.3	0.1
NEPHELINE	8.4	0.0	3.7	0.0	0.0
DIOPSIDE	12.2	11.7	23.8	0.0	2.1
HYPERSTHENE	0.0	10.9	0.0	2.1	8.6
OLIVINE	15.5	5.2	11.7	0.0	61.5
MAGNETITE	6.1	6.4	3.7	0.7	3.4
ILMENITE	5.3	5.2	1.8	0.5	0.0
APATITE	0.6	0.6	0.2	0.1	0.0
DIFF. INDEX	35.3	26.1	21.1	89.6	4.2
NA/(NA+K)	0.95	0.95	0.89	0.49	0.97
(NA+K)/AL	0.47	0.29	0.25	0.80	0.94
F3/(F2+F3)	0.26	0.25	0.26	0.26	0.26

Summary Norm Table; Produced using 'Normcal'

Appendix 3

Geol. Mag. 122 (5), 1985, pp. 439–445. Printed in Great Britain

The age and structural setting of limestones and basalts on the Main Ring Fault in southeast Rhum

N. J. SMITH

Department of Geological Sciences, University of Durham,
South Road, Durham, DH1 3LE, U.K.

(*Received* 31 October 1984; *accepted* 14 January 1985)

Abstract – In southeast Rhum, a Mesozoic/Tertiary sequence is preserved as a fault-bounded and rotated wedge. This is juxtaposed between Precambrian rocks (Torridonian sediments and Lewisian gneiss) and caught up in the complex structure of the Tertiary Main Ring Fault (MRF), which shows three distinct phases of movement. The Mesozoic rocks comprise fossiliferous limestone, sandstone and shale, which show differing degrees of thermal metamorphism depending on their relationships to the Layered Complex. On the basis of faunal and lithological evidence the Mesozoic sediments have been correlated with the Lower Liassic Broadford Beds. The Rhum sediments are overlain by sheared Tertiary basalts, the contact between them probably representing the original landscape unconformity. The presence of these younger strata caught up along the MRF provides crucial evidence for a major phase of central subsidence in the early history of the Rhum Tertiary volcanic centre.

1. Introduction

Geikie (1897) recorded the presence of a 'much altered grey and white limestone or marble' on the northern slopes of Glen Dibidil but, in the subsequent Memoir, Harker (1908) fails to mention any occurrence of limestone or marble in southeast Rhum. Many years later, Hughes (1960*b*) rediscovered limestone near Allt nam Bà. Two small areas were mapped; both were found to be metamorphosed and the more northerly (Hughes 1960*b*, fig. 1) to contain a high temperature calc-silicate mineral assemblage including tilleyite. Hughes also noted that the structural position of the limestones was similar to a wedge of Lewisian gneisses preserved along the Rhum ring fault some 450 m to the south and he tentatively assigned a Lewisian age to the limestones, noting that pure calcite limestones had previously been recorded from Lewisian paragneisses (Peach *et al.* 1907). Following the discovery by Dr G. Farrow of loose boulders of fossiliferous metamorphosed limestone, the southern limestone area (of Hughes, 1960*b*) was found to be fossiliferous, containing ill-preserved remains of bivalves and a possible belemnite. On this basis the rocks were tentatively assigned to the Jurassic (Dunham & Emeleus, 1967).

As part of a reinvestigation of southeast Rhum, the writer is at present engaged in a detailed examination of the structure of the Main Ring Fault (MRF; Bailey, 1945) between Allt nam Bà and Dibidil. Several new discoveries have been made. The most significant of these are the following.

(i) The limestones extend much further south than previously established.

(ii) They are intimately associated with fairly pure sandstones (locally metamorphosed to quartzites) and quite highly fossiliferous sandy limestones and shales, with faunas indicating a Lower Liassic age.

(iii) These sediments are closely associated with Tertiary basaltic lavas (the 'crushed basaltic rocks' of Emeleus & Forster, 1979).

The purpose of this account is to describe the lithologies and to suggest how these rocks were emplaced within the complicated structural setting of the MRF in southeast Rhum.

2. The Mesozoic strata

The Mesozoic rocks in southeast Rhum consist of a succession of highly inclined, westerly dipping beds of sandstone, limestone, sandy limestone and shale. There appears to be some lateral variation in the thickness of individual units within the mapped area, but poor exposure makes precise measurement difficult. On the lower northeast slopes of Beinn nan Stac (some 100 m south of the Allt nam Bà valley) an estimated thickness of Mesozoic strata totals *c.* 35 m. The sequence (now inverted) can be divided up as shown in Table 1.

The quartzites dip at around 50° to the west, with the limestones and shales dipping somewhat more steeply (*c.* 70°). This variation in dip would seem to be due to localized rotation and collapse within the faulted wedge, possibly caused by dissolution of the adjacent limestone.

On the lower southern slopes of Beinn nan Stac (NM 405 938), the quartzite is thicker (19 m) although the succession appears thinner, with the limestone cut

Table 1. Mesozoic strata of southeast Rhum

Lithology	Locality in outcrop	Thickness (metres)
Basalt (unconformity)	East	60 (minimum)
Quartzite		7.4
Limestone		14.5
(No exposure – limestone and sandy limestone inferred)		10.5
Shale	West	c. 2

out against the Torridonian strata at the Inner Ring Fault (see Fig. 1, and Section 4 below). Dissolution of limestone along this interface has caused localized slumping, and a prominent undercut cliff feature has formed. Many deep sink holes at the base of this cliff suggest that the limestone continues under the reverse-faulted Torridonian rocks. The Jurassic rocks are steeply dipping (60° W) and the reverse-faulted junction with the Torridonian dips 45° SW.

2.a. Sandstone

Originally thought of as basal Torridonian, this sandstone is unlike any Torridonian sediments in the area. It consists of rounded to sub-rounded quartz grains with a bimodal size distribution (2–3 mm and 0.2–0.5 mm). Dusty rims of ferruginous minerals are common and grain-to-grain contacts are low, the grains being supported by a siliceous cement. The rock has been metamorphosed by the ultrabasic complex producing a highly indurated quartzitic sandstone. Feldspar is very rarely present, in marked contrast to the common, and frequently abundant, occurrence of this mineral in the Torridonian sandstones.

Calcareous sandstones and sandy limestones also occur. The predominant constituents are matrix-supported sub-rounded quartz grains, 0.2–0.5 mm in diameter. Thermal metamorphism of these rocks has occasionally resulted in the formation of calc-silicate minerals. A section of this calcareous sandstone was found to contain a single poorly preserved coral cross section (?*Thecosmilia* sp.).

2.b. Limestone

The limestone varies from a calc-silicate mineral assemblage through pure calcite marble to a partially recrystallized, fairly fossiliferous limestone. Hughes (1960*b*) described calc-silicate rocks about 250 m south of Allt nam Bà, and they are also found in the valley itself, in a wall-like outcrop just below the waterfall at 200 m altitude (NM 4060 9436; Emeleus & Forster, 1979, fig. 5, locality IIb). This outcrop is within the marginal suite of the Layered Complex – hence its highly metamorphosed condition. It is thought that the calc-silicate rocks were originally impure (slightly siliceous) limestones that during movement on the MRF became detached from the main faulted wedge and subsequently engulfed the hot marginal members of the layered complex.

A short distance to the north of Allt nam Bà (Fig. 1), small nodules of calc-silicate rocks (which contain diopside and idocrase) are included in Unit 2 peridotites. These nodules may also represent fragments of limestone caught up along the fault and incorporated into the Layered Complex. These particular inclusions, however, were taken beyond the marginal suite and incorporated into part of the layered ultrabasic series, thus implying a fair degree of fluidity in the Unit 2 material at the time of emplacement.

Limestones not directly incorporated in, but in contact with, marginal rocks of the Layered Complex are also substantially metamorphosed. Limestone in a small easterly-facing cliff 50 m south of Allt nam Bà is totally recrystallized to a typical sugary-textured marble obliterating all remnants of fossils and other structures. Small idocrase crystals (*c*. 1–2 mm) are also present, while harkerite has been tentatively identified in an adjoining calc-silicate rock (specimen SR 199b). Further south, the limestones are progressively less affected by thermal metamorphism. Recognizable fragments of bivalves and possible corals are observed, but poor preservation precludes precise identifications.

The limestones form relatively few surface outcrops, but it has been possible to delimit their real extent by the distribution of sink holes, often clearly visible on aerial photographs. To date, the best fossils recovered from the area were found in one of the newly discovered outcrops – an area of impure limestone contained reasonably well-preserved cast-and-mould pectinid bivalves and a number of casts of belemnites of Jurassic affinities. Their genera have not yet been identified, but the faunal assemblage and general character of the rocks closely resemble lithologies of Lower Lias age (see Section 2.d below).

2.c. Shale

In the Allt nam Bà–Beinn nan Stac area, all shales have hitherto been assigned to the Torridonian Bagh na h-Uamha Shale member (Black & Welsh, 1961). However, in one small area *c*. 250 m south-southeast of the Allt nam Bà waterfall the shale has been found to contain a well-preserved belemnite guard and other indeterminate pyritized fossil fragments. Some of the shale at least, therefore, must be Mesozoic. Like the Torridonian, this Mesozoic (Jurassic) shale is highly indurated but contains 6–10% of angular quartz grains and up to 5% opaque grains (generally pyrite) in a fine-grained 'mud'. It is fault-bounded to the west, and tapers southwards where it is lost beneath overthrust Torridonian sediments.

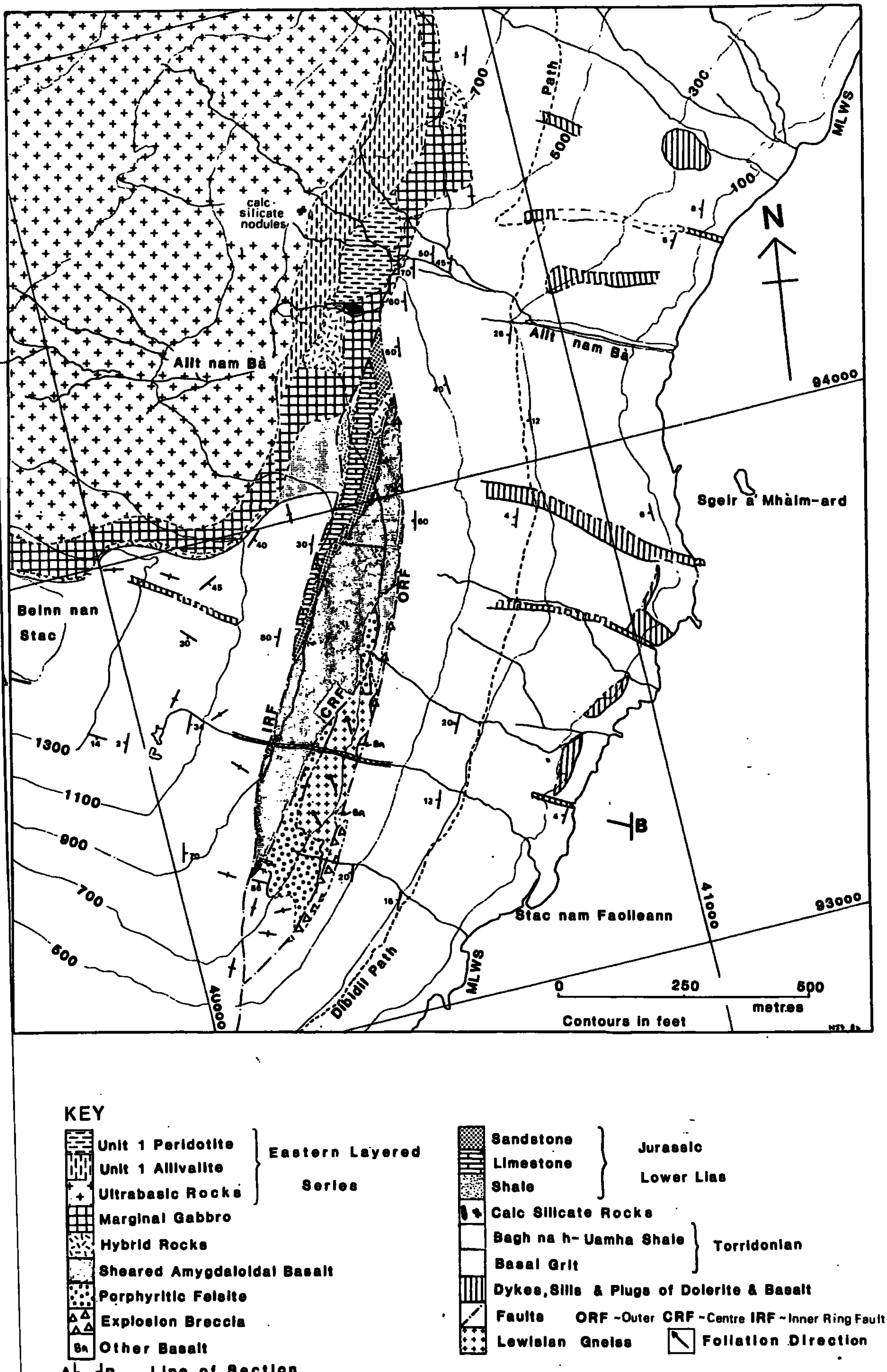

Figure 1. Sketch map of the geology of southeast Rhum.

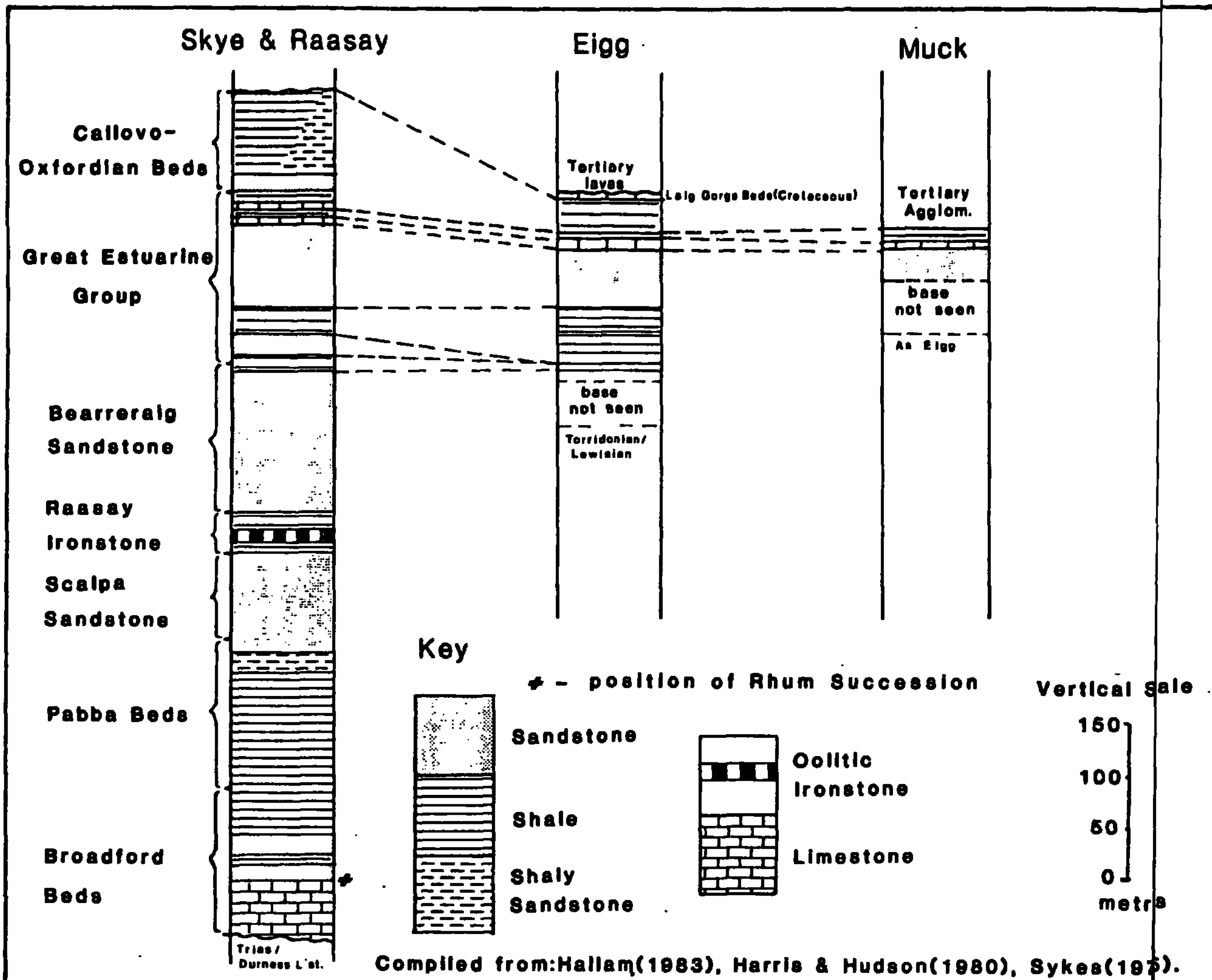

Figure 2. Comparative Mesozoic sections in the Inner Hebrides.

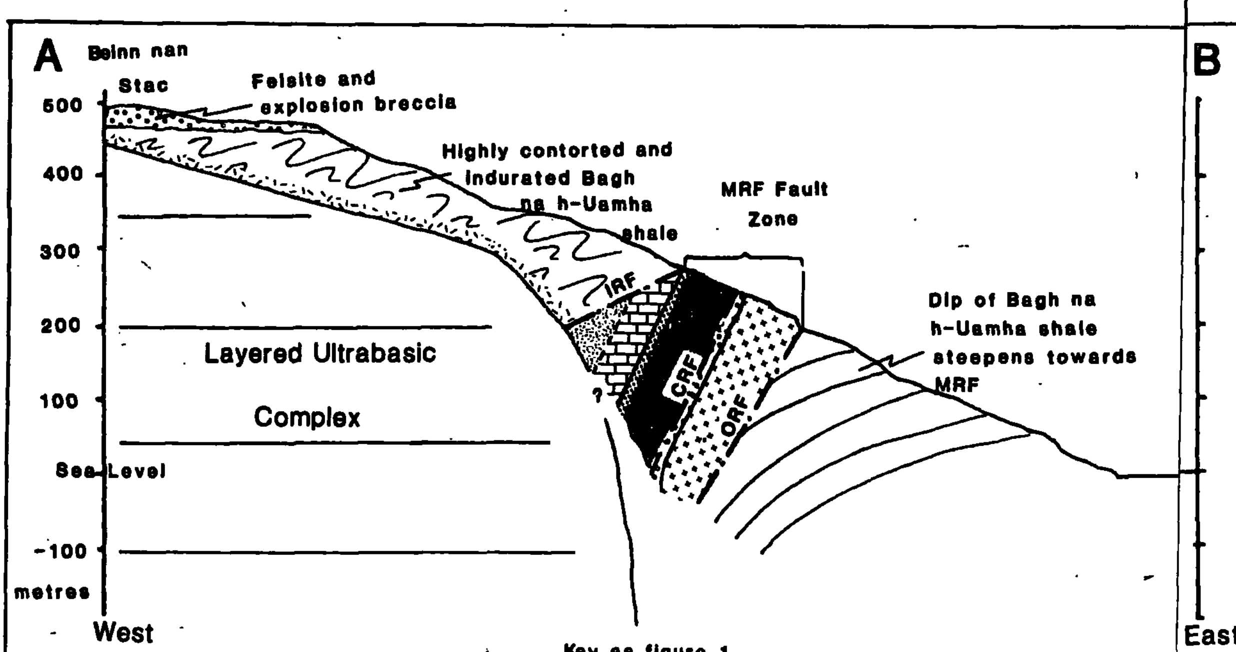

Figure 3. Sketch section across the MRF in southeast Rhum.

2. Comparison of Rhum Mesozoics with neighbouring areas

Several of the Hebridean islands adjacent to Rhum contain well-developed Mesozoic successions – those of Eigg, Muck and Skye are summarized in Figure 2. However, the successions of Eigg and Muck do not match the Rhum Mesozoic sediments.

On Skye, an almost continuous sequence from the Lower Lias (Broadford Beds) through Middle and Upper Lias into the Corallian is preserved (Peach *et al.* 1910; Hallam, 1959). Here, the Lower Lias comprises sandy limestones, limestones and thin shales, all with abundant bivalves, brachiopods and local concentrations of corals. The Rhum sequence bears a strong resemblance to the Lower Liassic rocks near Broadford, Skye. In particular, the limestone is similar to the Ob Breakish coral bed (Hallam, 1959, fig. 9), even in weathering characteristics.

The Rhum rocks therefore, are considered to represent a remnant of Lower Liassic strata to the west of the Camasunary–Skerryvore Fault (Binns, McQuillin & Kenolty, 1974). The Jurassic rocks of Eigg and Muck, to the east of the fault, are appreciably younger and the relationship of these rocks, at the start of the Tertiary, to the Rhum succession was similar to that now seen at Strathaird, Skye (Peach *et al.* 1910, fig. 3).

3. The sheared Tertiary basalts

The basalts outcrop wholly within the MRF, and are more extensive than previously established (cf. Fig. 1; Emeleus & Forster, 1979, fig. 5, locality II.3; Emeleus, 1980). The basalt is fault-bounded to the east and southeast by the ORF and CRF respectively (see Figs. 1 and 3). To the north, the basalts are adjacent to the Mesozoic rocks and no faulting was observed. Consequently the contact probably represents the unconformity between subaerial plateau lavas and Mesozoic strata, as occurs elsewhere in the British Tertiary Igneous Province (BTIP), although nowhere else on Rhum. Unlike the lavas of northwest Rhum (Emeleus, 1982, 1985), which post-date the Central Complex, the lavas in southeast Rhum developed before emplacement of the complex had begun. These basalts are regarded as a remnant of a much more extensive lava field, probably an extension of that of Eigg and Muck.

The lavas are typically ophitic to sub-ophitic basalts with a matrix of plagioclase laths (An_{67}–An_{60}) enclosed by augite. They are often feldspar-phyric with phenocrysts predominantly of plagioclase but occasionally of augite. However, alteration (chloritization and saussuritization of mafic minerals and plagioclase) obscures much of the original mineralogy. Opaque oxides (magnetite and haematite) are common (up to 10% modally). Small-scale fractures have channelled alteration, with the fracture planes also exhibiting signs of shearing – the scale of the shearing demonstrated by a plagioclase phenocryst which has been broken into two parts and displaced by some 5 mm. Amygdales, which are abundant in some rocks, often show signs of elongation due to shearing. Epidote, with some zeolite, occupies the cavities, and concentric infilling structures are occasionally observed.

4. Structural history of the Main Ring Fault

The structure of southeast Rhum is dominated by the MRF, which comprises several distinct faults. For the purposes of clarification the following nomenclature is proposed (see also Figs. 1 and 3).

Outer Ring Fault (ORF), the easternmost arcuate fault;
Centre Ring Fault (CRF), the fault separating the sheared Tertiary basalts from felsites and gneisses;
Inner Ring Fault (IRF), the westernmost fault, which brought stratigraphically low-level Torridonian against Jurassic sediments and sheared Tertiary basalts.

These three components of the MRF are related to different phases of movement in Stage 1 of the early Tertiary history of Rhum (Emeleus, Wadsworth & Smith, 1985). The sequence of movement was: (i) uplift within the ORF caused by diapiric uprise of acid magma; (ii) subsidence within the CRF caused by relaxation of diapiric pressure; (iii) renewed uplift on the westward-dipping IRF, pre-dating, or possibly related to, the emplacement of the Layered Complex.

In the Allt nam Bà area, initial movement in Stage 1 is represented by highly thermally altered but recognizable Lewisian gneiss in direct contact with the ORF. The fault is marked by extensive mylonitization, and the foliation in the gneiss (normally trending *c.* 340°) becomes bent around to become coincident with the line of faulting which trends *c.* 025°. This would seem to suggest that lateral movement, plus a fair degree of heating, must have accompanied the faulting. North of the gneiss a small tract of lower Torridonian (?Basal Grit) occurs, within the same faulted wedge as the Lewisian gneiss. The Lewisian/basal Torridonian fault-slice wedges out northwards where the ORF now comes into contact with the Tertiary lavas. Thus the MRF is seen to bifurcate leaving Tertiary against Torridonian in the north, but Lewisian and basal Torridonian abutting younger Torridonian to the south, thus indicating that the northern portion of this fault was active on at least two occasions, initially for major upward movement, and subsequently during subsidence of the 'piston block' (Emeleus, Wadsworth & Smith, 1985). From the point of bifurcation southwards, the easternmost fault trace (ORF) was exclusively involved in early upward movement, while movement on the more westerly

CRF was exclusively downwards. Here basalt was brought down against Lewisian gneiss.

Where lavas are against the ORF, the fault plane is perfectly defined and dips 65° westwards. Slickensides on the fault plane are steep and indicative of downward movement to the west. There is also intense mylonitization, which extends for a number of metres on either side of the fault plane, plus scattered evidence of explosive brecciation. This brecciation is in the form of highly comminuted, angular, basaltic and Torridonian fragments in a matrix of very fine rock powder. Similar breccias are found elsewhere within the MRF, as in Coire Dubh (Dunham, 1968) and the Southern Mountains Complex (Hughes, 1960*a*). These breccias probably represent fragmentation during volatile escape from degassing acid magma brought close to the surface, with the gas forcibly escaping along the pre-existing zone of structural weakness of the MRF. Indeed, the fact that the ORF is exploited by explosion breccia indicates that both the ORF and CRF were present at the time of degassing.

The CRF dips 65° westwards, with parts of the fault plane having been intruded by felsite. This felsite shows no indication of faulting, shearing or deformation. Consequently, the downward faulting must have been totally completed before solidification of the acidic magma. The felsite magma has obscured the trace of the CRF, though it is included on Figs. 1 and 3 for the sake of clarity. The junction between basalt and felsite, and that between felsite and Lewisian gneiss, is extremely sharp and is well exposed in gully walls margining a deeply eroded, later cross-cutting dyke (NM 4030 9357).

The IRF dips at an angle of 45° to the southwest and brings highly indurated and contorted Bagh na h-Uamha shales into contact with the wedge of Jurassic sediments and Tertiary lavas. This junction is well preserved on the lower shoulder of Beinn nan Stac (NM 4051 9385), where the contact is with limestone. The limestones adjacent to the fault have been heavily dissolved, leaving deep sink holes at the base of the small cliff feature formed by the contorted Bagh na h-Uamha shales. This dissolution has undercut much of the cliff, producing localized collapse of the hanging wall. Further south, where the fault is in contact with the more resistant basalt (Fig. 1), the rocks on both sides of the fault are intensely sheared with steep slickensides and mylonitization.

On the southeast slopes of Beinn nan Stac (NM 4030 9358), basalt is in contact with a small outcrop of pale-weathering sandstone similar to that found further north. This outcrop represents the southernmost visible extension of the Mesozoic strata. A short way to the south, overthrust Torridonian rocks cut out both lavas and the sandstones although a deep sink hole, present on the fault plane 20 m to the south, provides evidence that calcareous rocks are still present hereabouts.

Movement on the IRF and elsewhere along MRF represents the last phase of Stage 1. T renewed uplift of the 'piston block' is somew reminiscent of the development of 'resurgent ca drons' (Smith & Bailey, 1968). Uplift of about 2 km required in order to bring the stratigraphically low-le Torridonian to the structural levels it now occup within the MRF. The cause of this uplift is uncerta but it may be linked to emplacement of the adjoin Ultrabasic Complex at the onset of Stage 2.

5. Conclusions

The limestones, and other new sedimentary litholo of southeast Rhum, are seen to contain a Mesoz fossil assemblage and, on the basis of comparison w other Mesozoic strata in the Hebridean area, probably an extension of the Lower Liassic Broadf Beds. The sediments are intimately associated w Tertiary lavas, the contact probably representing original landscape unconformity. Originally Mesozoic sediments and Tertiary lavas would h rested on a basement of Lewisian gneiss Torridonian sediments, but on Rhum, due movements along the MRF and adjacent faults, t are now limited to overturned and fault-bounded re (see Fig. 3). It is the presence of the small fault-boun sliver, lying as it does between stratigraphically ol rocks, that provides the crucial evidence for ma subsidence in the early Tertiary history of the Rh volcanic centre.

Acknowledgements. The author would like to thank all th who have assisted in the production of this paper, especi Dr C. H. Emeleus. The comments of the two anonym referees were also of considerable benefit. Thanks are due to the Nature Conservancy Council for permissio work on Rhum and for facilities provided. Lastly, I sho like to gratefully acknowledge the receipt of a scholars from St Chad's College, Durham.

References

Bailey, E. B. 1945. Tertiary Igneous Tectonics of Rh Inner Hebrides. *Quarterly Journal of the Geolog Society of London* **100**, 165–91.

Binns, P. E., McQuillin, R. & Kenolty, K. 1974. *Geo of the Sea of the Hebrides.* Report of the Institut Geological Sciences no. 73/14, 43 pp.

Black, G. P. & Welsh, W. 1961. The Torridon succession of the Isle of Rhum. *Geological Magazin* 8, 265–76.

Dunham, A. C. 1968. The felsites, granophyre, explo Breccia and tuffisites of the north-eastern margin of Tertiary Igneous Complex of Rhum, Inverness-sh *Quarterly Journal of the Geological Society of Lon* **123**, 327–52.

Dunham, A. C. & Emeleus, C. H. 1967. The Tertiary geol of Rhum, Inner Hebrides. *Proceedings of the Geolog Association* **78**, 391–418.

Emeleus, C. H. 1980. *Rhum, Solid Geology Map, 1:20,0*

Newbury: Nature Conservancy Council. Aberdeen University Press.

ELEUS, C. H. 1982. The Central Complexes. In *The Igneous Rocks of the British Isles* (ed. D. S. Sutherland), pp. 369–414. Chichester: Wiley-Interscience.

ELEUS, C. H. 1985. The Tertiary lavas and sediments of northwest Rhum, Inner Hebrides *Geological Magazine* **122**, 419–37.

ELEUS, C. H. & FORSTER, R. M. 1979. *Tertiary Igneous Rocks of Rhum – Field Guide.* Newbury: Nature Conservancy Council.

ELEUS, C. H., WADSWORTH, W. J. & SMITH, N. J. 1985. The early igneous and tectonic history of the Rhum Tertiary Volcanic Centre. *Geological Magazine* **122**, 451–7.

GIE, SIR A. 1897. *The Ancient Volcanoes of Great Britain*, Vol. 2. London: Macmillan.

HLAM, A. 1959. Stratigraphy of the Broadford Beds of Skye, Raasay, and Applecross. *Proceedings of the Yorkshire Geological Society* **32**, pt. 2, no. 9, 165–84.

HLAM, A. 1983. Jurassic, Cretaceous and Tertiary sediments. In *The Geology of Scotland* (ed. G. Y. Craig), pp. 343–56. Edinburgh: Scottish Academic Press.

HKER, A. 1908. *Geology of the Small Isles of Inverness-shire.* Memoir. Geological Survey of Scotland. 210 pp.

HARRIS, J. P. & HUDSON, J. D. 1980. Lithostratigraphy of the Great Estuarine Group (Middle Jurassic), Inner Hebrides. *Scottish Journal of Geology* **16**, 230–50.

HUGHES, C. J. 1960*a*. The Southern Mountains Igneous Complex, Isle of Rhum. *Quarterly Journal of the Geological Society of London* **116**, 111–38.

HUGHES, C. J. 1960*b*. An occurrence of tilleyite-bearing limestone in the Isle of Rhum. *Geological Magazine* **97**, 384–8.

PEACH, B. N., HORNE, J., GUNN, W., CLOUGH, C. T., HINXMAN, L. W. & TEALL, J. J. H. 1907. *The Geological Structure of the North-west Highlands of Scotland.* Memoir. Geological Survey of Great Britain.

PEACH, B. N., HORNE, J., WOODWARD, H. B., CLOUGH, C. T., HARKER, A. & WEDD, C. D.. 1910. *The Geology of Glenelg, Lochalsh, and the South-east Part of Skye.* Memoir. Geological Survey of Scotland. 206 pp.

SMITH, B. L. & BAILEY, R. A. 1968. Resurgent Cauldrons. *Geological Society of America, Memoir.* no. 116, 613–62.

SYKES, R. M. 1975. Stratigraphy of the Callovian and Oxfordian stages (Middle–Upper Jurassic) in Northern Scotland. *Scottish Journal of Geology* **2**(1), 51–78.

Appendix 4

Geol. Mag. 122 (5), 1985, pp. 451–457. Printed in Great Britain

The early igneous and tectonic history of the Rhum Tertiary Volcanic Centre

C. H. EMELEUS*, W. J. WADSWORTH† & N. J. SMITH*

* Department of Geological Sciences, University of Durham, South Road, Durham DH1 3LE, U.K.
† Department of Geology, University of Manchester, Manchester M13 9PL, U.K.

(*Received* 31 October 1984; *accepted* 14 January 1985)

Abstract – Early Tertiary igneous activity on Rhum was preceded by doming and the formation of a major arcuate fault system, the Main Ring Fault (MRF), within which Lewisian gneisses, Torridonian sediments and younger rocks were uplifted by as much as 2 km. Doming and uplift are attributed to the diapiric rise of acid magma which ultimately formed the granophyres and felsites of Rhum. Felsite emplacement was accompanied and immediately preceded by the formation of explosion breccias and tuffisites. This phase involves massive gas escape along the MRF fractures; it marked a period of major subsidence within the MRF during which fossiliferous Jurassic sediments and relics of Tertiary lava flows were brought to low structural levels within the MRF. Finally, a further period of uplift, again of about 2 km, took place once more bringing gneisses and basal Torridonian sediments within the MRF to high structural levels. The driving force for this last phase of uplift may have been provided by a further uprise of acid magma or, more realistically, may have been directly connected with emplacement of layered ultrabasic rocks which now form the core of the Rhum centre.

1. Introduction

Although the main geological components of the Isle of Rhum had been clearly defined soon after the turn of the century by Harker (1908), it is to E. B. Bailey that we owe the first modern, integrated account of the Tertiary tectonics and igneous history of the area. In a classic paper, Bailey (1945) demonstrated that the Tertiary igneous rocks largely occurred within a major arcuate fault, termed the Main Ring Fault (MRF), and, furthermore, he showed beyond doubt that major uplift of the order of 2000 m had occurred within the ring fault. Crucial evidence for this uplift came from the occurrence of Lewisian gneisses, which were only found within the area bounded by the MRF. Similarly, the lowermost Torridonian units (the Basal Grit, and the lower part of the Bagh na h-Uamha Shale) were also confined within the MRF, and were clearly in juxtaposition with higher members of the Torridonian succession across the fault. Bailey also recognized that there had been considerable structural disturbance of the Torridonian adjacent to the MRF; in particular, the strata immediately outside the fault showed marked departures from the regional dip and strike (Fig. 1).

In addition, Bailey discussed the possible significance of the acid complexes (felsite–explosion breccia associations) around Sgurr nan Gillean in the south, and Meall Breac in the northeast. He regarded these (especially Sgurr nan Gillean) as minor ring systems within the MRF, and suggested that the upheaval on the MRF was due to the upward intrusion of the felsite magma. The close spatial connection between Tertiary acid magmatism and the movement on the MRF was subsequently confirmed by more detailed studies of the two areas, now termed the Southern Mountains Complex (SMC) and the Northern Marginal Complex (NMC), described by Hughes (1960) and Dunham (1968) respectively. This theme was further developed by Walker (1975) in connection with his proposal that acid diapirism was a significant early event in the history of all the British Tertiary intrusive centres.

Three main stages may be recognized in the growth and decline of the Rhum centre (Dunham & Emeleus, 1967; Emeleus & Forster, 1979; Emeleus, 1982, 1983). Stage 1 was dominated by acid magmatism, although the initial activity seems to have been basaltic, giving rise to minor gabbro plugs in the NMC (Dunham & Emeleus, 1967). The acid magma is represented by the large Western Granite (Black, 1954) and by the granophyre–felsite–explosion breccia associations of the SMC (Hughes, 1960) and the NMC (Dunham, 1968). Basaltic activity appears to have recurred towards the end of Stage 1, when numerous minor intrusions (inclined sheets accompanied and followed by dykes) were emplaced. The majority of the dykes trend approximately northwest–southeast but a significant number form a subsidiary swarm in a northeast–southwest direction (Forster, unpub. Ph.D. thesis, Univ. Durham, 1980; Speight *et al.* 1982). Stage 1 is considered to have been terminated by movement on the MRF (Dunham & Emeleus, 1967).

Stage 2 involved formation of the extensive bodies of ultrabasic rocks and associated gabbros which together form the high, rugged ground in central southern Rhum, and mostly lie within the MRF. It has been postulated that emplacement of the ultrabasic

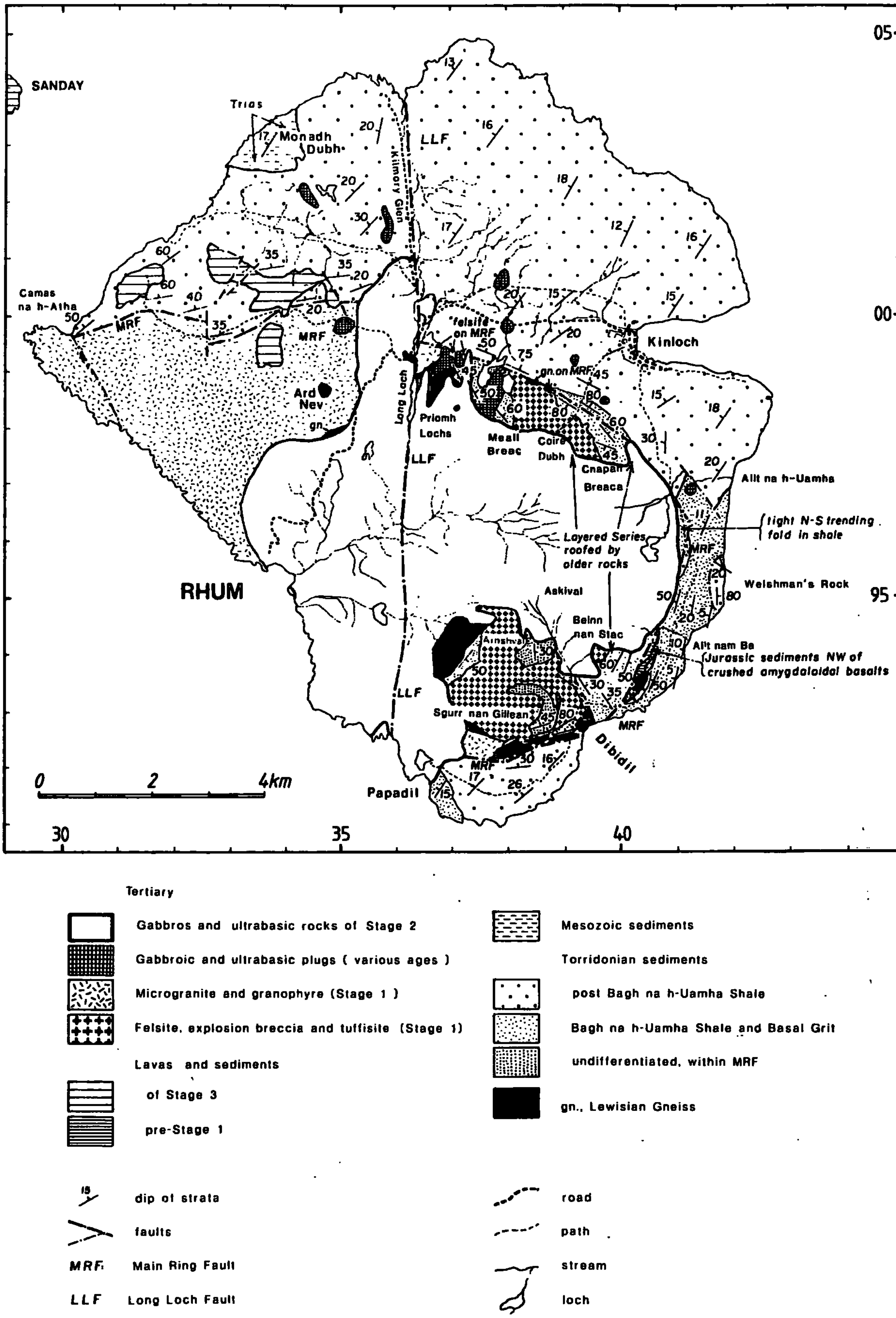

Figure 1. Geological sketch map of the Isle of Rhum.

been affected by much more extensive faulting and fracturing than the Tertiary igneous rocks, suggesting that there was significant pre-Tertiary movement on the Long Loch Fault, as is known from the Camasunary–Skerryvore Fault.

3. Detailed evidence of Stage 1 igneous and tectonic activity

As a starting point in this discussion, it is assumed, following Walker (1975), that the initial high-level manifestation of Tertiary intrusive activity on Rhum was the doming of the country rock cover in response to the diapiric uprise of acid magma. Evidence of such doming is provided in the area outside the MRF by the local distortion of the regional dip and strike of the Torridonian rocks (Fig. 1). In particular, along the northern part of the MRF, between Camas na h-Atha in the extreme west, and Cnapan Breaca in the east, the Torridonian rocks have been strongly uptilted in the vicinity of the fault. In a belt approximately 1 km wide, the strike is broadly parallel with the curvature of the MRF, and the outward dips increase progressively in steepness as the fault is approached, locally reaching 85°. This effect is less marked in southeast Rhum, partly because the regional strike must have been roughly parallel to the margin of the dome. In this case the Torridonian rocks have not been simply uptilted, but appear to have been thrown into a series of minor fold structures, which now parallel the margin of the intrusive complex, from Cnapan Breaca to south of Allt nam Ba. In fact, much of the Torridonian immediately outside the MRF in this area dips relatively steeply towards the west. It is possible that the tight small-scale folds found in Torridonian shales near the MRF at Allt na h-Uamha (NM 411 965) were also developed at this stage. The peripheral folding may also account for the unusually gentle dips in the Torridonian west of Welshman's Rock and for the relative steepness of the small thrust plane identified in this area (Emeleus, 1981).

There is also some evidence of a possible early doming event *within* the area now bounded by the MRF, in terms of the distribution and relative attitude of Lewisian and Torridonian material. If the occurrences immediately adjacent to the MRF are disregarded for the moment, the principal outcrops of Lewisian gneiss, which generally appear to cap acid intrusive rocks, are found in a more westerly situation than the Torridonian Basal Grit and Bagh na h-Uamha Shale (Fig. 1; Emeleus, 1980). Further, the contact between the Lewisian gneisses and the Basal Grit is found to dip towards the northeast in the northern part of the area, near the Priomh Lochs (NM 372 986), and towards the southeast in the Ainshval area (NM 374 938), closer to the southern margin of the proposed dome. Other indications of early deformation are found in Coire Dubh, where WNW-trending minor folds in Torridonian rocks (Dunham, 19[illegible]) could be the result of peripheral folding around a dome (see also Dunham & Emeleus, 1967). However, it must be emphasized that because of the emplacement of the main ultrabasic/basic complex in Stage 2, the evidence of earlier events within the central area is rather fragmentary, although it is at least consistent with the idea of initial (pre-MRF) doming. There has also been a considerable amount of later faulting (especially in the southeast, between Dibidil and Papadil) which further complicates the situation.

It is proposed that continued upward movement of acid magma, and accentuated doming, eventually culminated in the development of an arcuate fracture (MRF), within which the central block moved upwards like a piston, carrying Lewisian gneiss and immediately overlying Torridonian material to high structural levels. Corresponding elevation of the upper part of the country rock cover (Mesozoic sedimentary rocks overlain by Tertiary plateau lavas) to even higher levels would presumably have resulted in substantial surface erosion, and probably removal of much or all of these components from the centre of the updomed, proto-volcanic area.

The exact sequence of the immediately ensuing events is uncertain, but central subsidence took place, presumably on relaxation of diapiric pressure. Subsidence was largely guided by the fractures of the initial MRF but in places the actual movement occurred along new fractures situated a short distance (from tens to hundreds of metres) inside the original MRF. Thus, when the central piston block subsided, fault-bounded pieces of Lewisian gneiss together with basal Torridonian were left stranded at high structural levels along the MRF. The gneiss relics now occur to the north of Meall Breac (NM 386 987), on the southeast side of Beinn nan Stac (NM 404 935), and in considerable numbers west of Dibidil on the lower southern slopes of Sgurr nan Gillean (Fig. 1). Interestingly, the gneiss relics sometimes provide evidence suggesting an *early* period of intense thermal metamorphism. Leucocratic gneisses on the southeast side of Beinn nan Stac show clear signs of partial melting with felsic rims between quartz and feldspar. Similar textures occur in a gneiss block in otherwise little metamorphosed explosion breccias in Coire Dubh (C. Ellis, personal communication). Thermally metamorphosed Lewisian gneisses are well known elsewhere on Rhum (e.g. near the Priomh Lochs and to the West of Ainshval), but at these localities the gneisses are adjacent to mafic intrusives of Stage 2.

Clear evidence for major central subsidence is obtained from the exposures on the southeast slopes of Beinn nan Stac. Fossiliferous Jurassic strata and basaltic rocks, probably lavas of Tertiary age, occur along the MRF but they are generally separated from the outermost part of the fault system by Lewisian gneiss and Torridonian sediments. Where this is not ks occurred along another ring fracture largely hin, but partly coincident with, the MRF. This also ears to have involved central uplift, possibly ociated with the formation of a marginal ring-dyke abbro (Brown, 1956). A relatively small number of es was intruded towards the end of this stage, and of interest that several of these aphyric intrusions of ultrabasic composition (Forster, unpub. Ph.D. sis, Univ. Durham, 1980; McClurg, unpub. Ph.D. sis, Univ. Edinburgh, 1982). Emplacement of the bros and ultrabasic rocks frequently caused severe mal metamorphism of earlier rocks, sometimes minating in rheomorphism (Hughes, 1960; Wads- th, 1961; Dunham, 1964). Although the emplace- t of the ultrabasic rocks and associated gabbros clearly later than the acid magmatism of Stage 1, it likely that the concentration of basaltic magma at d th, and the fractional crystallization which led to t development of the Rhum layered complex, o rlapped with Stage 1, and may even have been v lly connected with it in terms of providing the t mal energy needed to initiate and sustain the early a magmatism.

tage 3 involved severe subaerial erosion, when c r of the order of 1 km in thickness was removed fr n the top of the Rhum volcano (cf. Brown, 1963), ex osing part of its infrastructure. Detritus was swept d n the flanks of the volcano, accumulating in st -sided valleys which became filled with water- de osited conglomeratic debris, as well as basalt and ba ltic andesite lava flows, probably originating ou ide the Rhum centre (Emeleus, 1982, 1983). Ig ous activity terminated with the intrusion of a few ba lt dykes, including possible far-flung members of th Skye swarms (Forster, unpub. Ph.D. thesis, Univ. Du ham, 1980).

is account is largely concerned with Stage 1, but pa of the problem associated with any attempt to de her the early history of the Rhum volcanic co plex is the fact that later events have considerably mo ified, or even obliterated, the evidence of the early sta s of development. However, enough information is n w available to show that, although the dominant mo ment of the MRF-bounded central block had bee upwards during Stage 1 (and probably in Stage 2 as well), there are certain facts which are difficult to rec ncile with the relatively simple 'uplift' model. The e may be summarized as follows.

(1 The occurrence of stratigraphically high-level roc (fossiliferous Jurassic sediments and amygdaloi- dal asalts resembling Tertiary lava flows) associated with he lower members of the Torridonian succession in t fault zone of the MRF.

(2 The distribution of Lewisian gneiss within the area ounded by the MRF.

(3 The high-level character of the porphyritic felsit and associated explosion breccias.

In short, evidence for central uplift is clear, but discoveries since Bailey's re-appraisal of Rhum tectonics make it plain that there is equally compelling evidence for central subsidence. In fact, Bailey (1945, p. 180) suggested that 'upheaval was punctuated by collapse and explosion'. The problem is to reconcile the apparently conflicting evidence and to produce a model capable of accommodating both aspects. This is attempted by first of all discussing the nature of the immediately pre-Tertiary geology in the vicinity of Rhum, followed by reconstruction of the possible sequence of tectonic and magmatic events during Stage 1, in the light of detailed field evidence from the relevant areas within (and adjacent to) the MRF.

2. The regional setting of the Rhum Tertiary centre

The Rhum centre lies astride a NNE-trending ridge of Precambrian rocks (Lewisian gneisses overlain by a thick succession of Torridonian sediments) and is flanked by Mesozoic basins to the west and east. The Minch basin on the west just laps on to northwest Rhum at Monadh Dubh, where Triassic sediments cap the higher members of the Torridoniam succession (Fig. 1). To the east, the Mesozoic basin extending from south-central Skye, southwards under Eigg and Muck, to western Mull, is separated from Rhum by the major Camasunary–Skerryvore Fault (Binns, McQuillin & Kenolty, 1974). By analogy with southern Skye (cf. Wedd, 1910, fig. 3) it is suggested that a thin succession of Lower Jurassic sediments (possibly equivalent to the Broadford Beds; see Smith, this issue) covered Rhum. These were probably capped by Tertiary lavas, possibly representing a western extension of the basalt flows found on Eigg and Muck which pre-date central igneous activity on Rhum (Emeleus & Forster, 1979).

Major faults, trending approximately north–south, were important in controlling development of the Mesozoic basins and may also have influenced subsequent lava effusion and accumulation in the Eocene (Walker, 1975). One of these is the Long Loch Fault, which forms a prominent feature extending across Rhum from Kilmory in the north to Papadil in the south (Fig. 1). Movement on the fault post-dates emplacement of the youngest ultrabasic rocks and the associated gabbros. The actual measurable displacement is limited to about 800 m in a horizontal right-lateral sense. However, investigations into the ultrabasic rocks of central Rhum have led McClurg (unpub. Ph.D. thesis, Univ. Edinburgh, 1982) and Volker (unpub. Ph.D. thesis, Univ. Edinburgh, 1983) to suggest that this structure may have played a significant part in the emplacement of the younger ultrabasic rocks (termed the Central Series). The 3 km long, 150–200 m wide, flat floor of Kilmory Glen contrasts with the narrow trench eroded along the Long Loch Fault where it transects the layered ultrabasic complex. The Torridonian rocks may have the case, as slightly further north, the basalt in contact with the MRF shows signs of mylonitization with associated explosive brecciation, indicative of collapse. The boundary between the gneiss and basalt is a steep fault (*c.* 65°WNW) although in part this fault has been exploited by later acid magma in the form of felsite (see Smith, this issue).

This postulated episode of central subsidence is attributed to a reduction in magma pressure in the diapir as a result of magma escaping along the system of fractures forming the MRF (as on southeast Beinn nan Stac, see above) accompanied by deflation consequent on gas release. The formation of ring fractures eventually weakened the roof of the acid diapir to such an extent that gases from the crystallizing magma were explosively released, shattering the country rocks along the ring fracture and at the same time penetrating along lines of weakness within the central block. These lines of weakness were principally faults, but bedding planes within the Torridonian may also have been exploited, as indicated by the flat-lying breccias within bedded Torridonian rocks on the eastern slopes of Sgurr nan Gillean (Hughes, 1960). Explosive shattering of the rocks along the faults permitted the now viscous, degassed acid magma from the top of the diapir to intrude to even higher levels, forming the porphyritic felsite masses which appear steep-sided and dyke-like near the MRF, but pass into sheet-like masses further into the central block. Some features described from the felsites resemble those from pyroclastic flows (e.g. fiamme, cf. Williams, this issue) and current investigations aim to determine whether the porphyritic felsite–explosion breccia assemblage is essentially subaerial, formed on or close to the floor of a caldera structure and brought to lower levels as the caldera developed, or whether it represents material formed fairly near the surface but still under some cover as is suggested by the Dibidil exposures. It is possible that the Rhum felsites and related rocks could have close similarities to the sub-surface welded acid rocks described from the Sabaloka Cauldron in the northern Sudan (Almond, 1977). Whatever the true situation, the felsite–explosion breccia assemblage appears to be closely linked with the subsidence stage and with the ring faulting. Explosion breccia, with small felsite intrusions, occurs along the MRF immediately east of the Long Loch Fault (Dunham, 1968), and both are present along the faulted boundary between basalt lavas, gneiss and country rock on the southeast side of Beinn nan Stac. The tuffisites (intrusive tuffs) of Rhum are largely, although not exclusively, found along or close to the MRF. Significantly, felsites and explosion breccias appear to have escaped the effects of crushing associated with MRF movements, although it can be difficult to distinguish between crush breccias and explosion breccias (cf. the 'pseudotachylytes' of the Vredefort Dome (Bailey, 1926)). The fundamental question is whether the felsite masses of Cnapan Breaca and Meall Breac (NMC), and those forming the Ainshval-Sgurr nan Gillean ridge (SMC), represent the remains of domes of acid magma which formed on a caldera floor, perhaps covered by a blanket of explosion breccia, or whether they are entirely intrusive. Whatever their precise mode of formation the association is considered to be essentially of high level origin, developed during a period of central subsidence when they were brought to relatively low structural levels.

The final major event in the Stage 1 activity is believed to have been a further period of central uplift within the MRF. This seems to be the only satisfactory way of explaining the present distribution of the rocks involved. Thus, at Allt nam Ba, and on the southeast side of Beinn nan Stac, the Mesozoic/Tertiary supracrustal rocks lie between Torridonian and Lewisian outcrops. The Torridonian on the *inner* side of the Mesozoic/Tertiary material is from *lower* stratigraphic levels than the main Torridonian immediately outside the MRF. In other words, it is necessary to invoke a late episode of uplift to more than compensate for the preceding period of subsidence, in terms of the Torridonian stratigraphy; on this basis final uplift may have been of the order of 2 km. It seems plausible to suggest that the MRF system was again utilized during this episode, but that once more there were minor divergences, with the development of new fracture lines locally. In particular, along the eastern part of the MRF system, the latest movements seem to have been concentrated some 100–200 m inside the original fault line, with the results that the Jurassic sediments and Tertiary lavas were preserved as thin, highly inclined and fault-bounded slivers, which managed to survive the final uplift and to record the intermediate stage of substantial subsidence. If the present erosion level had been a few hundred metres higher, this episode of subsidence would not have been suspected. The crucial exposures are 900 m southeast of the summit of Beinn nan Stac, where Torridonian and Jurassic sediments are in reverse-faulted contact, with the fault plane dipping at around 45° towards the northwest. This fault may be traced many hundreds of metres both to the southwest and north-northeast, over the shoulder of the hill. Thus it is clear that the mass of contorted and indurated Bagh na h-Uamha Shale, covering southeast Beinn nan Stac, has been pushed over the Jurassic sediments and Tertiary basaltic rocks and, to the south, over the original outer part of the MRF (Smith, this issue).

4. Discussion and conclusions

While the motive power for the early phase of uplift appears to have been provided by diapiric movement of acid magma, the force causing the late uplift is uncertain. It might have involved further upward movement of acid magma, in a manner analogous to the development of resurgent cauldrons (Smith & Bailey, 1968) or, alternatively, it could have been caused by the emplacement of the layered ultrabasic rocks and associated gabbros of Stage 2. There is no clear evidence of the participation of acid magma(s) in the later phase of uplift, but it has been strongly advocated that the layered ultrabasic rocks were emplaced upwards by as much as 1600 m to their present level in the Rhum centre as a hot, but essentially solid, cylindrical body lubricated by basaltic magma (Brown, 1956; Wager & Brown, 1968). With this proposal in mind, it is instructive to look at the contacts between the Eastern Layered Series ultrabasic rocks and gabbros, and earlier rocks within the MRF. On Beinn nan Stac these earlier rocks (Torridonian sediments, explosion breccias and felsites) appear to overlie the mafic rocks, with the contact dipping gently to the southeast, while in the NMC, particularly in the upper part of Coire Dubh and in the area about 1 km east of Cnapan Breaca, the contact between mafic rocks and members of the NMC dips fairly gently to the north-northeast. Thus, at these localities the earlier rocks appear to be in roof-like relationships to the mafic rocks which in turn may extend under them as far as the (sub-surface) course of the MRF. Furthermore, the layering in the ultrabasic rocks also appears to extend under the roof of earlier rocks, with the result that successively lower layers approach more closely to the MRF. An implication of this observation is that these roof-like contacts are original igneous contacts and that layering in the ultrabasic rocks was capable of developing to within a few tens of metres (or less) of the margins of the body of mafic magma. These observations are not proof that the last phase of uplift was the consequence of movement of the layered ultrabasic rocks but this interpretation does remain a distinct possibility. If upward movement of the mafic rocks did occur, pushing ahead almost all the earlier rocks within the MRF, then it is necessary to find a force capable of uplifting the very large mass of dense rocks involved, now comprising at least the Eastern Layered Series; furthermore, it is necessary to envisage a certain amount of (? thermal) erosion along the course of the MRF, to judge from the somewhat transgressive course of the eastern margin of the mafic rocks towards the original trace of the fault between Cnapan Breaca and Allt nam Ba.

It is concluded that in the early part of Stage 1 of the Rhum centre there was a diapiric uprise of acid magma which initially caused doming leading to ring fracturing with formations of the MRF. Uplift of the piston-like MRF-bounded block amounted to as much as 2 km but terminated when degassing and escape of acid magma along the MRF resulted in deflation, subsidence of the piston block and possible caldera formation. At this stage explosion breccias, felsites and tuffisites were formed. In addition, Mesozoic sediments and Tertiary lavas were brought into juxtaposition with fragments of Lewisian gneiss and basal Torridonian sediments which had been elevated in the initial uplift but were effectively left stranded along the MRF on collapse of the central piston block. Subsequently, further uplift of the piston block occurred, either powered by a new uprise of acid magma or, possibly more realistically, connected with the upward movement of mafic rocks and/or magmas at the start of Stage 2 in the development of the Rhum centre. Further investigations are in progress in southern Rhum which, it is hoped, will help in the solution of this major, unresolved problem.

References

ALMOND, D. C. 1977. The Sabaloka igneous complex, Sudan. *Philosophical Transactions of the Royal Society of London* **287** A, 595–633.

BAILEY, E. B. 1926. Domes in Scotland and South Africa: Arran and Vredefort. *Geological Magazine* **63**, 481–95.

BAILEY E. B. 1945. Tertiary igneous tectonics of Rhum (Inner Hebrides). *Quarterly Journal of the Geological Society of London* **100**, 165–188.

BINNS, P. E., MCQUILLIN, R. & KENOLTY, N. 1974. *The Geology of the Sea of the Hebrides*. Institute of Geological Sciences Report No. 73/14, 43 pp.

BLACK, G. P. 1954. The acid rocks of Western Rhum. *Geological Magazine* **91**, 257–72.

BROWN, G. M. 1956. The layered ultrabasic rocks of Rhum, Inner Hebrides. *Philosophical Transactions of the Royal Society of London* **240** B, 1–53.

BROWN, G. M. 1963. Melting relations of Tertiary granitic rocks in Skye and Rhum. *Mineralogical Magazine* **33**, 533–62.

DUNHAM, A. C. 1964. A petrographic and geochemical study of back-veining and hydridization at a gabbro–felsite contact in Coire Dubh, Rhum, Inverness-shire. *Mineralogical Magazine* **33**, 887–902.

DUNHAM, A. C. 1968. The felsites, granophyre, explosion breccias and tuffisites of the north-eastern margin of the Tertiary igneous complex of Rhum, Inverness-shire. *Quarterly Journal of the Geological Society of London* **123**, 327–52.

DUNHAM, A. C. & EMELEUS, C. H. 1967. The Tertiary geology of Rhum, Inner Hebrides. *Proceedings of the Geologists' Association* **78**, 391–456.

EMELEUS, C. H. 1980. *Rhum: Solid Geology Map, 1:20000*. Edinburgh: Nature Conservancy Council.

EMELEUS, C. H. 1981. A thrust at Welshman's Rock, Isle of Rhum. *Scottish Journal of Geology* **17**, 1–6.

EMELEUS, C. H. 1982. The central complexes. In *Igneous Rocks of the British Isles, Part 7, The Tertiary* (ed. D. S. Sutherland) pp. 369–414. Chichester: John Wiley.

EMELEUS, C. H. 1983. Tertiary igneous activity. In *Geology of Scotland*, 2nd edn. (ed. G. Y. Craig), pp. 357–98. Edinburgh: Scottish Academic Press.

EMELEUS, C. H. & FORSTER, R. M. 1979. *Field Guide to the Tertiary Igneous Rocks of Rhum*. London: Nature Conservancy Council, 44 pp.

HARKER, A. 1908. *The Geology of the Small Isles of Inverness-shire (Rhum, Canna, Eigg, Muck, etc.)*.

Memoir. Geological Survey of Scotland. Edinburgh: H.M.S.O. 210 pp.

HUGHES, C. J. 1960. The Southern Mountains igneous complex, Isle of Rhum. *Quarterly Journal of the Geological Society of London* **114**, 111–38.

SMITH, N. J. 1985. The age and structural setting of limestones and basalts on the Main Ring Fault in Southeast Rhum. *Geological Magazine* **122**, 439–45.

SMITH, R. L. & BAILEY, R. A. 1968. Resurgent cauldrons. In *Studies in Volcanology – a Memoir in Honor of Howell Williams* (ed. R. R. Coats, R. A. Hay and C. A. Anderson), pp. 613–22. Memoir Geological Society of America no. 116.

SPEIGHT, J. M., SKELHORN, R. R., SLOAN, T. & KNAPP, R. J. 1982. The dyke swarms of Scotland. In *Igneous Rocks of the British Isles, Part 7, The Tertiary* (ed. D. S. Sutherland), pp. 449–59. Chichester: John Wiley.

WADSWORTH, W. J. 1961. The layered ultrabasic rocks of South-West Rhum, Inner Hebrides. *Philosophical Transactions of the Royal Society of London* **244B**, 21–64.

WAGER, L. R. & BROWN, G. M. 1968. *Layered Igneous Rocks*. Edinburgh: Oliver and Boyd. 588 pp.

WEDD, C. B. 1910. In *The Geology and Glenelg, Lochalsh and the South-east Part of Skye*, pp. 116–21. Memoir. Geological Survey of Scotland. Edinburgh: H.M.S.O.

WALKER, G. P. L. 1975. A new concept in the evolution of the British Tertiary intrusive centres. *Journal of the Geological Society of London* **131**, 121–41.

WILLIAMS, P. J. 1985. Pyroclastic rocks in the Cnapan Breaca felsite, Rhum. *Geological Magazine* **122**, 447–50.

Titles of unpublished Ph.D. theses referred to in the text:

FORSTER, R. M. 1980. A geochemical and petrological study of the Tertiary minor intrusions of Rhum, Northwest Scotland. Unpublished Ph.D. thesis, University of Durham.

MCCLURG, J. 1982. Geology and structure of the northern part of the Rhum ultrabasic complex. Unpublished Ph.D. thesis, University of Edinburgh.

VOLKER, J. A. 1983. The geology of the Trallval area, Rhum, Inner Hebrides. Unpublished Ph.D. thesis, University of Edinburgh.

References

References

Abbey S. 1983. Studies in 'standard samples' of silcate rocks and minerals. Canadian Geological Survey. Paper 83-15.

Allwright E.A. 1980. The Structure and Petrology of the Tertiary Volcanic Rocks of Eigg, Muck and Canna, NW Scotland. Unpubs. M.Sc. Thesis University of Durham.

Almond D.C. 1977. The Sabolka Igneous Complex. Sudan. Philosophical Transactions of the Royal Society of London. V. 27a p 595-633.

Anderson E.M. 1936. Dynamics of formation of cone sheets, ring dykes and cauldron subsidences. Proceedings of the Royal Society of Edinburgh. V. 1.vi pp128.

Bailey E.B. 1945 Tertiary igneous tectonics of Rhum, (Inner Hebrides). Quarterly Journal of the Geological Society of London. V. 100 p 165-188

Bell J.D. 1966. Granites and associated rocks of the eastern part of the Western Redhills Complex Isle of Skye. Transactions of the Royal Society of Edinburgh. V. 66 p307-343.

Bell J.D. 1976. The Tertiary Intrusive Complex on the Isle of Skye. Proceedings of the Geologists' Association. v. 87 p 247-271.

Binns P.E. McQuillin R. & Kenolty N. 1974. The Geology of the Sea of the Hebrides. Special report of the Institute of Geological Sciences. No. 73/14. 43pp.

Black G.P. 1954. The Significance of Tridymite in Igneous and Metamorphic Processes. Mineralogical Magazine. V. 30. p518

Black G.P. & Welsh. W. 1961. The Torridonian Sucession of the Isle of the Isle of Rhum. Geological Magazine V.98. p265 - 276.

Blake D.M, Elwell R.W.D, Gibson I.1, Skelhorn R.R, Walker G.P.L. 1965. Some relationships resulting from the intimate associations of acid and basic magmas. Quarterly Journal of the Geological Society of London. V. 121 p 31-50.

Bott M.H.P. and Tantrigoda D.A. 1987. Interpretation of the Gravity and Magnetic anomalies over the Mull Tertiary Intrusion Complex, NW Scotland. Journal of the Geological Society V. 144 p17-28.

Brown G.M. 1956 The Layered Ultrabasic Rocks of Rhum. Philosophical Transactions of the Royal Society of London V. 240(B) p1-53.

Brown G.M. 1963 Melting Relations of Tertiary Granitic Rocks in Skye and Rhum. Mineralogical Magazine. V.33 No. 262. p553-562

Butcher A.R. 1985 Channeled Metasomatism in Rhum layered Cumulates - Evidence from Late Stage Veins. Geological Magazine. V. 122 No. 5.

Byers F.M, Carr W.J, Oakild P.P, Quinlivan W.D, Sargent K.A. 1976. Volcanic suites and related cauldrons of the Timber Mountain - Oasis Valley Complex, Southern Nevada. United

States Geological Survey Prof. Paper 919. 70pp.

Christiansen R.L, Lipman P.W, Carr W.J, Byers F.M, Orkild P.P, Sargent K.A. 1977. Timber Mountain - Oasis Valley Complex of Southern Nevada. Geological Society of America Bulletin No. 88. p943-959.

Cox K.G. 1980. A Model for Flood Basalt Vulcanism. Journal of Petrology. V. 21. p629-650.

Cox K.G. Bell J.D. Pankhurst R.J. 1979. The Interpretation of Igneous Rocks. London:George, Allen and Unwin.

Dagley P, Musset A.E. 1986. Palaeomagnetic and radiometric dating of the BTIP, Eigg and Muck. Geophysical Journal of the Royal Astronomical Society. V. 85 p221-242.

Dunham A.C. 1962 The Petrology and Structure of the Northern Edge of the Tertiary Igneous Complex of Rhum. Unpubs. D.Phil Thesis University of Oxford.

Dunham A.C. 1965 The Nature and Origin of the Groundmass Textures in Felsites and Granophyres from Rhum, Inverness-shire. Geological Magazine. V. 102. p 8-23.

Dunham A.C. 1968 The Felsites, Granophyre, Explosion Breccia, and Tuffisites of the NE Margin of the Tertiary Igneous Complex of Rhum. Quarterly Journal of the Geological Society of London. V.123 p 327-352.

Dunham A.C. 1980. The emplacement of the Tertiary Igneous Complex of Rhum. In 'Mechanisms of Igneous Intrusion' Editors - G.Newall and

N.Rast. Geological Journal Special Issue No. 2. Gallery Press, Liverpool.

Dunham A.C. and Emeleus C.H. 1967. The Tertiary Geology of Rhum, Inner Hebrides. Proceedings of the Geologists Association. V. 78. p391-418

Durant G.P. Dobson M.R. Kokelaar B.P. Macintyre R.M. and Rea W.J. 1976. Preliminary Report on the Nature and Age of the Blackstones Bank Igneous Centre, Western Scotland. Journal of the Geological Society of London. V. 132. p319-326.

Emeleus C.H. 1980 Rhum, solid geology map (1:20,000) Newbury, Nature Conservancy Council. Aberdeen University Press.

Emeleus C.H. 1985. Tertiary Lavas and Sediments of NW Rhum Inner Hebrides. Geological Magazine V. 122. No.5. p419-437.

Emeleus C.H. 1987. The Rhum Layered Complex, Inner Hebrides, Scotland. In: Origins of Igneous Layering. Ed. I. Parsons. 263-286. Reidel.

Emeleus C.H. and Forster R.M. 1979. Field Guide to the Tertiary Igneous Rocks of Rhum. London. Nature Conservancy Council. 44pp.

Emeleus C.H. Wadsworth W.J. and Smith N.J. 1985. The Early Igneous and Tectonic History of the Rhum Tertiary Volcanic Centre. Geological Magazine. V. 122 No.5. p451-457.

Fitton J.G, James D.E, Thirlwall M.F. 1984. A users guide to XRF analysis of rock samples. Grant Institute of Geology. Unpublished report.

Faithfull J.W. 1985 The Lower Eastern Layered Series of Rhum. Geological Magazine V.122 No. 5.

Geikie Sir A. 1897. The Ancient Volcanoes of Great Britain. Volume 2. London. Macmillan.

Hallam A. 1959. Stratigraphy of the Broadford Beds of Skye, Raasay and Applecross. Proceedings of the Yorkshire Geological Society. V.32 pt.2 No.9.

Hallam A. 1983. Jurassic, Cretaceous, and Tertiary Sediments. In: The Geology of Scotland (ed. G.Y. Craig) p 343-356. Edinburgh: Scottish Academic Press.

Harker A. 1908. Geology of the Small Isles of Inverness-shire. Memoir of the Geological Survey of Scotland. 210pp

Harris J.P. and Hudson J.D. 1980. Lithostratigraphy of the Great Estuarine Group (Middle Jurassic) Inner Hebrides. Scottish Journal of Geology. V. 16 (pt. 2-3) p 230-250.

Heinrich K.F.J. 1966. X-ray absorbtion uncertainty. In: McInley T.D, Heinrich K.F.J, and Whittry D.B. (Editors), The Electron microprobe. New York, Wiley and Sons. p296-377.

Hughes C.J. 1960a The Southern Mountains Complex, Isle of Rhum. Quarterly Journal of the Geologcal Society of London. V.116 p111-138.

Hughes C.J. 1960b. An Occurence of Tillyite Bearing Limestone in the Isle of Rhum. Geological Magazine V. 97. p384-388.

Jenkins R. and De Vries J.L. 1967. Practical x-ray spectrometry. Macmillan, London.

King B.C. 1954. The Ard Bheinn area of the Central Igneous Complex of Arran. Quarterly Journal of the Geological Society of London V.110 p323-355.

Lipman P.W. 1976. Caldera collapse breccias in the western San Juan mountains. Geological Society of America Bulletin V. 87 p1397-1410.

Lipman P.W. 1984. The roots of ash flow calderas in western North America: windows into the tops of granite batholiths. Journal of Geophysical Research. V. 89 No.10 p8801-8841.

Marsh B.D. 1984. The Mechanics of Caldera Resurgence. Journal of Geophysical Research V. 89 No. 10 p8245-8251.

Marshall L.A, Sparks R.S.J. 1984. Origin of some mixed magma and net-veined ring intrusions. Journal of the Geological Society. V. 141 p171-182.

Mc Clurg J.E. 1982. The Geology and Structure of the Northern Part of the Rhum Ultrabasic Complex. Unpublished Ph.D Thesis, University of Edinburgh.

Mc Quillin R. Tuson J. 1963. Gravity Measurements over the Rhum Tertiary Plutonic Complex. Nature (London) V. 199. p1276.

Norrish K. and Chappell B.W. 1977. X-ray fluorescence spectrometry. In: Physical Methods in Determinative Mineralogy (J. Zussman ed.) Academic Press, London.

Norrish K. Hutton J.T. 1969. An accurate x-ray spectrographic method for the analysis of a wide range of geological samples. Geochemica Cosmochemica acta. V.33 p431-453.

Oates M.J. 1978. A Revised Stratigraphy for the Western Scottish Lower Lias. Proceedings of the Yorkshire Geological Society. V.42 p143-156.

Palacz Z.A. Tait S.R. 1985 Isotopic and Geochemical Investigation of Unit 10 from the Eastern layered Series of the Rhum Intrusion, NW Scotland. Geological Magazine. V.122 No. 5.

Peach B.N. Horne J. Woodward H.B. Clough C.T. Harker A. Wedd C.D. 1910. The Geology of Glenelg, Lochalsh and the SE Part of Skye. Memoir of the Geological Survey of Scotland. pp206.

Smith N.J. 1985. The Age and Structural Setting of Limestones and Basalts on the MRF in South-east Rhum. Geological Magazine V. 122 No.5 p439-445.

Smith R.L. 1960 Zones and Zonal Variations in Welded Ash Flows. United States Geological Survey Professional Paper No. 354-F.

Smith R.L. Bailey R.A. 1968. Resurgent Cauldrons. Memoir of the Geological Society of America. V. 116 p613-662

Smith R.L, Bailey R.A, Ross C.S. 1961. Structural evolution of the Valles Caldera, New Mexico, and its bearing on the emplacement of ring dykes. United States Geological Survey Prof. Paper. V. 242d p145-149.

Sparks R.S.J, Sigurdson H, Wilson L. 1977. Magma mixing: A mechanism for triggering acid explosive eruptions. Nature V. 267 p315-318.

Stewart A.D. 1966 On the Correlation of the Torridonian Between Rhum and Skye. Geological Magazine. V.103 p432-439.

Sykes R.M. 1975. Stratigraphy of the Callovian and Oxfordian Stages (Middle - Upper Jurassic) in NW Scotland. Scottish Journal of Geology. V. 2(1) p51-78.

Tait S.R. 1985 Fluid Dynamic and Geochemical Evolution of Cyclic Unit 10 of the Rhum Eastern Layered Series. Geological Magazine. V.122 No. 5.

Thompson R.N. 1980. Askja 1875, Skye 56MA: basalt triggered, plinian, mixed magma eruptions during emplacement of the Western Redhills granite, Isle of Skye, Scotland. Geol. Rundschau. V. 69 p245-262.

Thompson R.N. 1982. Magmatism of the British Tertiary Province. Scottish Journal of Geology. V.18 p49-107.

Thompson R.N, Morrison M.A, Dicken A.P, Gibson I.L, Harman R.S. 1986. Two contrasting styles of interaction between basic magmas and continental crust in the BTVP. Journal of Geophysical Research. V. 91 p5985-5997.

Thompon R.N. Esson J. and Dunham A.C. 1972. Major Element Chemical Variation in the Eocene Lavas of the Isle of Skye, Scotland. Journal of Petrology. V. 13. p219-254.

Tilley C.E. 1931. The Gabbro Limestone Contact Zone of Camas Mor, Muck, Invernesss-shire.

Mineralogical Magazine. V.22 p 439-468.

Tilley C.E. 1938. Aluminous Pyroxenes in Metamorphosed Limestones. Geological Magazine. V.75 No.884.

Tilley C.E. 1944 A Note on the Gneisses of Rhum. Geological Magazine. V. 81 p129-131.

Tilley C.E. 1947 The Gabbro - Limestone Contact of Camas Mor Muck, Inverness-shire. Extrait Comptes Rendus de la Societe Geologique de Finlande. No.20.

Tilley C.E. 1948. Dolomite Contact Skarns of the Broadford area of Skye: a Preliminary Note. Geological Magazine. 75. p 213-218.

Tilley C.E. 1951. The Zoned Skarns of the Broadford area of Skye: a Study of Boron - Fluorine Metasomatism in Dolomites. Mineralogical Magazine V.29 p621-666

Wadsworth W.J. 1961 The Layered Ultrabasic rocks of SW Rhum, Inner Hebrides. Philosophical Transactions of the Royal Society of London. V.244(B) p21-64.

* Wager L.R. and Brown G.M. 1968 - See below

Wager L.R. Weedon D.S. Vincent E.A. 1953. A Granophyre from Coire Uaigneich Isle of Skye Containing Quartz Paramorphs after Tridymite. Mineralogical Magazine. V.30 p263-276.

Walker G.P.L. 1975. A new concept in the evolution of the British Tertiary Intrusive Centres. Journal of the Geological Society of London. V. 131 p121-141.

Walker G.P.L. 1984. Downsag Calderas, ring faults, caldera sizes and incremental caldera growth. Journal of Geophysical Research. V. 89 No.10. p8407-8416.

* Wager L.R and Brown G.M. 1968. 'The Layered Igneous Rocks'. Oliver and Boyd. Edinburgh. 587pp

Williams P.J. 1985 Pyroclastic Rocks from the Cnapan Breaca Felsite, Rhum. Geological Magazine. V.122 No.5.

Volker J.A. 1983. The Geology of the Trallval Area Rhum, Inner Hebrides, Scotland. Unpublished Ph.D Thesis University of Edinburgh.

Tailpiece

One of the (only ?) benefits of catching the 5 am. ferry to Rhum......

'Night and Day...... Sunrise over Canna.

Figure 2 Sketch Map of the Geology of South - east Rhum

Nicholas J. Smith 1987

Figure 6.1 Stylised Development of the Rhum Volcanic Centre

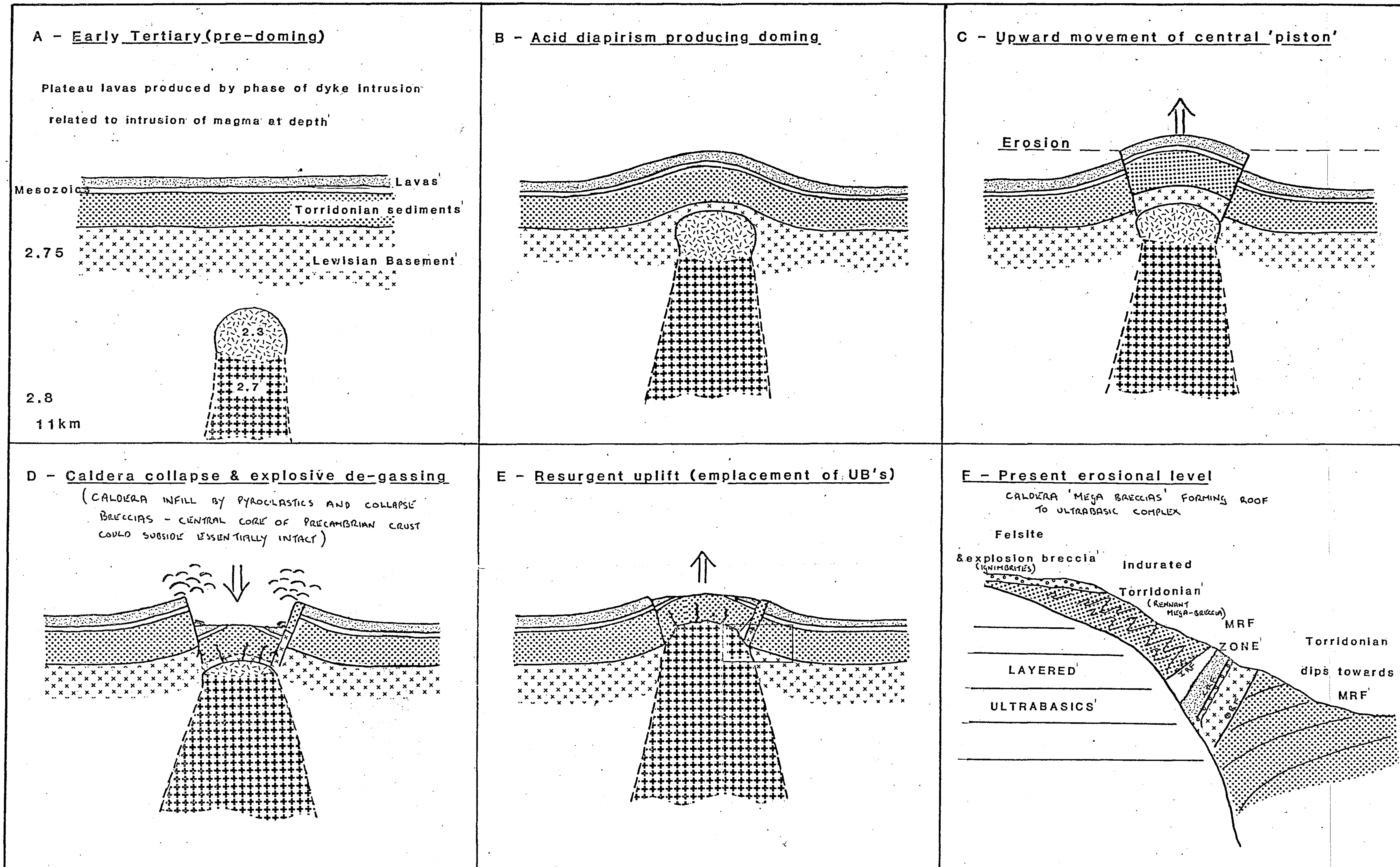

Figure 6.1